ABSTRACT

Title of Thesis: BEHAVIOR AND PERFORMANCE OF HIGH PERFORMANCE CONCRETE FOR PAVEMENTS

Degree candidate: Haejin Kim

Degree and year: Master of Science, 2003

Thesis directed by: Professor Dimitrios G. Goulias
Department of Civil and Environmental Engineering

Under TE –30, High Performance Concrete Pavement program, several states are undertaking a variety of innovative research in high performance concrete pavement materials and innovative design/construction features. This project addressed the needs of Maryland State Highway Authority in exploring the use of fiber reinforced and low shrinkage concrete in pavements. Past experience with these materials have indicated i) potential benefits in flexural fatigue resistance and reduction in crack development, and ii) potential reduction in slab warping effects with implications on pavement slab longevity. The objective of this study was to examine the design and lab performance of these materials for Maryland conditions, monitor their lab and field performance, and quantify potential benefits. Extensive fatique modeling was undertaken for developing the fatigue relationships and SN curves for these mixtures. In addition, finite element analysis (FEM) was used to

model the behavior of these materials in field conditions and developing the base analytical model to be used in comparing future behavior and performance of the pavement test sections with these mixtures.

BEHAVIOR AND PERFORMANCE OF HIGH PERFORMANCE CONCRETE FOR PAVEMENTS

by

Haejin Kim

Thesis submitted to the Faculty of the Graduate School of the
University of Maryland, College Park in partial fulfillment
of the requirements of the degree of
Master of Science
2003

Advisory Committee:

Professor Dimitrios G. Goulias, Chair
Professor Charles W. Schwartz
Professor M. Sherif Aggour

DEDICATION

This thesis is dedicated to my wonderful father, Do-Ha Kim. I completed my Masters thesis with the key verse, Matthew 6:33.

"But seek first his kingdom and his righteousness, and

all these things will be given to you as well."

Matthew 6:33

ACKNOWLEDGEMENTS

I wish to acknowledge the following individuals whose enormous contributions led to the successful completion of this thesis:

- Dr. Dimitrios G. Goulias, thanks for giving me the opportunity to do the Masters under your instruction and advice I appreciate your tremendous patience during my challenging moments. I am very glad to have been associated with you.
- Dr. Charles W. Schwartz, thanks for his excellent instruction to write up the backcalcuation chapter.
- Dr. M. Sherif Aggour, thanks for taking time off your busy schedule to serve on my committee.
- Thanks to Stewart Bennie who was my lab partner and a good friend. I appreciate his hard working spirit that I learned from him.
- Thanks to Linda Bennie who took care of my wife and my daughter, Monica during my busy time of research work.
- Thanks to my wife, Seonmi who fed me and took care of me. I love you and I'm very thankful for your silent support.
- Thanks to my brothers and sisters in my church for their prayer and support.
- Thanks to my collogues, Kapil Gupta, Sunil Arora, Nelson Gibson, Regis Carvalho, Emin Kutay for their friendship.

TABLE OF CONTENTS

LIST OF TABLES

LIST OF FIGURES

CHAPTER 1

1.1 Introduction

Pavement structures undergo repeated load application during their life span which causes strength and stiffness deterioration of concrete due to fatigue. The fracture of concrete as a result of fatigue is the most predominant cause of structural failure due to its low tensile strength. In an attempt to control the low tensile strength, the incorporation of fibers in concrete has been considered. In fiber reinforced concrete, millions of fibers are introduced into the concrete as it is mixed. These fibers are dispersed randomly throughout the concrete and thus improve concrete properties in all directions. The main advantage of fiber reinforced in concrete is the improvement of flexural strength against both static and cyclic loading.

Several fiber materials in various sizes and shapes have been developed for use in FRC. Among these fibers, the fibrillated polypropylene has been one of the most successful commercial applications. The common forms of these fibers are smooth-monofilament, twisted, fibrillated and tridimensional mat. Collated fibrillated polypropylene fibers have some unique properties that make them suitable for reinforcement in concrete. The fibers have a low density, are chemically inert and non corrosive, and have chemical resistance to mineral acids and inorganic salts. These fibers have high tensile strength and high elongation. The high elongation of polypropylene fibers enables large energy absorption and improves ductility and fatigue strength.

Past experience with these materials in pavements have indicated potential benefits in flexural fatigue resistance and reduction in crack development, and

potential reduction in slab warping effects with implications for pavement slab longevity. This research is part of a nationwide effort (TE - 30) on using high performance concrete materials and design features for pavements. In this research, the benefits of fiber reinforced concrete and low shrinkage concrete in pavements were investigated with lab and filed experimentation.

1.2 Background

Conventional concrete has two major weaknesses, low tensile strength and a destructive and brittle failure. In an attempt to increase concrete ductility and energy absorption, fiber reinforced concrete (FRC) has been introduced. In fiber reinforced concrete, millions of fibers are introduced into the concrete as it is mixed. These fibers are dispersed randomly throughout the concrete and thus improve concrete properties in all directions. Thus properties such flexural strength, tesile strength, plastic energy absorption, and fatigue may significantly be enhanced when proper fiber type and content is used.

Another important parameter of concrete is shrinkage and its impact on cracking due to curing and drying. If concrete is restrained from shrinking, tensile stresses may develop and concrete may crack. In flat structures, such as highway pavements and bridge decks, shrinkage cracking is a major concern. In recent years, short, randomly distributed fibers such as polypropylene fiber, steel fiber, etc. have been used to reduce shrinkage cracking.

1.3 Research Objectives

The primary objectives of this investigation were to determine the benefits of using fiber reinforced concrete and low shrinkage concrete in Maryland paving conditions. Thus, the investigation explored the fatigue and energy absorption performance of fibrillated polypropylene fiber reinforced concrete when subjected to fatigue loading, and the shrinkage properties of fiber and low shrinkage mixtures. In addition, finite element analysis (FEM) was used to model the behavior these materials in field conditions. The models were calibrated using stress and deflection measurements from filed instrumentation.

The specific objectives of this investigation were;

1. to determine the properties of the fresh concrete mixtures using fiber and low shrinkage mix designs;
2. to determine the properties of hardened concrete such as compressive strength, flexural strength, shrinkage, and toughness;
3. to compare the flexural fatigue performance of plain and fiber reinforced concrete mixtures;
4. to develop fatigue models for these mixtures and relate fatique to mixture properties;
5. to compare field behavior and performance with these materials using FEM analysis and field data
6. to develop a base analytical model for future use in monitoring the behavior of the mixtures with monitoring field data. To this end appropriate FEM mesh characteristics and conditions reflecting the

material properties and field conditions were selected for determining the appropriate moduly and modulus of subgrade reaction.

1.4 Organization of The Report

The first chapter presents the introduction, research objectives and the organization of this report. Chapter 2 presents an extensive literature review of existing research on polypropylene fiber reinforced concrete and concrete shrinkage. Chapter 3 presents the materials and testing plan. Chapter 4 presents the experiment results from the laboratory and field testing. Chapter 5 presents the fatigue analysis including fatigue modeling of plain concrete and fiber concrete with 0.1%, 0.2%, 0.3%, and 0.4% fiber content. Chapter 6 presents the finite element (FM) analysis in which the subgrade modulus of k value was back-calculated with deflection and strain data from the field. Finally Chapter 7 presents the summary, conclusions and recommendations.

CHAPTER 2 LITERATURE REVIEW

2.1 Introduction

Over the years, in order to increase concrete's flexural behavior, ductility and energy absorption, fiber reinforced concrete (FRC) has been introduced. In fiber reinforced concrete, fibers are introduced into the concrete as it is mixed. These fibers are dispersed randomly throughout the concrete and thus improve concrete properties. Other advantages include the increase in tensile strength, fatigue strength, and impact strength.

Several fibers in various sizes and shapes have been developed for use in FRC to enhance the fatigue behavior and shrinkage cracking behavior. Fibrillated polypropylene fibers have been one of the most successful due to some unique properties that make them suitable for reinforcement in concrete, such as high tensile strength and elongation. The high elongation enhances energy absorption and improves ductility, fatigue strength, and impact resistance of concrete.

The objective of the literature review was to review past research on the behavior of polypropylene fiber reinforced concrete while focusing on two important aspects which are fatigue behavior and shrinkage cracking.

2.2 Properties and Fatigue Behavior of Polypropylene Fiber Reinforced Concrete

Several projects have investigated the use of fiber reinforced concrete. Nagabhushanam et al. (1989) investigated the flexural fatigue strength of fibrillated polypropylene fiber reinforced concrete with three different concentrations of fibrillated polypropylene fibers. The test program included the evaluation of flexural

fatigue strength and endurance limit. The test results indicated an appreciable increase in post-crack energy absorption capacity and ductility due to the addition of fibers. When compared with corresponding plain concrete, the flexural fatigue strength and the endurance limit (for 2 million cycles) were significantly increased.

Johnston and Zemp (1991) investigated the flexural performance under static loads for nine mixtures. The results indicated that increasing the fiber content from 0.5% to 1.5% had a significant beneficial effect on the first crack strength despite the required increase in water/cement ratio (w/c) to meet workability requirements.

Bayasi and Celik (1993) investigated the effect of silica fume on the flexural strength of synthetic fiber reinforced concrete. Two fiber types such as fibrillated polypropylene fibers and polyester fibers were used with the amount of fibers ranged from 0 to 0.6% by volume. Silica fume was used as partial replacement of Portland cement at 0, 5, 10 and 25%. The results indicated that polyester fiber and polypropylene fibers have an inconsistent effect on the flexural strength but significantly increased the flexural toughness and the post-peak resistance of concrete.

Ozyildirim et. al. (1997) investigated the effect of different fiber types and volumes on Hydraulic cement concrete (HCC). The concrete contained fibers of steel (hooked-end and in percentages of 0.4 and 0.6 % by volume), fibrillated polypropylene (0.2 % by volume), monofilament polypropylene (0.1 and 0.3 % by volume), and polyolefin (1.3 and 1.6 % by volume). The results indicated that the impact resistance and toughness of the fiber reinforced concrete is greatly improved with the increase in fiber volume and length.

MATERIALS AND MIXTURES

Some of the results from previous studies using polypropylene fibers are presented next. Ozyildirim, et. al, (1997) examined the use of Fiber-Reinforced Concrete for Use in Transportation Structures. The fiber characteristics used in that study are reported in Table 2.1. All the concrete batches prepared in that study, Table 2.2, contained 377 kg/m^3 (635 lb/yd^3) of cementitious material consisting of 60 percent Type I/II cement and 40 percent ground granulated blast furnace slag by weight. The coarse aggregate was a granite gneiss with a nominal maximum size of 13 mm (0.5 in.). The fine aggregate was siliceous sand. A commercially available air-entraining admixture, water-reducing admixture, and naphthalene-based high range water-reducing admixture (HRWRA) were used for all batches.

TABLE 2.1 Fiber Characteristics

Fiber	Length MM (IN)	Diameter MM (IN)	Aspect Ratio (l/d)	Yield Strength Mpa (ksi)	Elastic Modulus Mpa (ksi)	Specific Gravity
Polypropylene (Fibrillated)	19 (0.75)	N/A	N/A	550-750 (80-110)	3450 (500)	0.91

(Source, Ozyildirim, 1997)

Similarly, Nagabhushanam, et. al (1989) examined the fatigue behavior of fiber reinforced concrete using the mix characteristics shown in Table 2.3. In both cases the batches had a ratio of water to cementitious material of 0.45, 0.40, respectively, with varying amounts of HRWRA added to obtain workable concretes. The properties of the fresh concrete from the first case are shown in Table 2.4. The

fresh concrete was mixed in accordance with ASTM C 192. Polypropylene Fibers were added as the last ingredient.

TABLE 2.2 Mixture Proportions

Mix	Fiber Content, %	Coarse Aggregate Kg/m3	Fine Aggregate Kg/m3	Cement Kg/m3	Slag Kg/m3	W/C Ratio	HRWRA oz	AEA ML
SPL	0	890	839	226	151	0.45	0	67
SP1	0.2	890	839	226	151	0.45	46	67
SP2	0.3	890	839	226	151	0.45	46	67
SP3	0.5	890	839	226	151	0.45	46	67
SP4	0.7	890	839	226	151	0.45	65	67

* HRWRA = High Range Water Reducer Admixture, AEA = Air Entrainment Admixture
(Source, Ozyildirim, et. al, 1997)

TABLE 2.3 Mix Quantities and Designation

Mix	Fiber Content, %	Coarse Aggregate lbs	Fine Aggregate lbs	Cement lbs	W/C Ratio	SPD cc	AEA cc
NP4	0	187.8	187.8	79.2	0.40	180	25
NF1	0.1	187.8	187.8	79.2	0.40	240	25
NF7	0.1	187.8	187.8	79.2	0.40	240	25
NF3	0.5	187.8	187.8	79.2	0.40	330	25
NF5	0.5	187.8	187.8	79.2	0.40	330	25
NF2	1.0	187.8	187.8	79.2	0.40	380	25
NF1	1.0	187.8	187.8	79.2	0.40	550	30

* SPD = Superplasticizer Dosage, AEA = Air Entrainment Admixture
(Source: Nagabhushanam, et. al, 1989)

TABLE 2.4 Properties of Fresh Concrete

Fiber	Fiber Content		Slump	Inverted	HRWRA	Air	Unit Weight		Temp
	Kg/m3	% Vol	MM(In)	Slump(s)	ML/m3	%	Kg/m3	(lb/ft3)	C
Polyprop.	1.8	0.2	30 (1.3)	5	1760	5.3	2340	(146)	24
Fibrillated	2.7	0.3	25 (1.0)	4	1760	6.3	2280	(142)	24
	4.6	0.5	15 (0.5)	10	1760	5.7	2280	(142)	23
	6.4	0.7	15 (0.5)	6	2515	7.5	2250	(140)	24

* HRWRA = High Range Water Reducer Admixture
(Source: Ozyildirim, et. al, 1997)

For the compression and static modulus tests, three to five 6 x12 in. cylinders were cast for each mix. For both the static flexural and flexural fatigue tests, twelve to fifteen 4 x 4 x 14 in. beams were cast using plastic molds immediately after mixing. The samples were and then covered with plastic sheet and cured for 24 hours at room temperature. The samples were then de-molded and immersed in water bath at 72 F°. The specimens for the compression, static flexural, and toughness tests remained in the water until tested at 28 days.

PROPERTIES OF FRESH CONCRETE

Satisfactory workability was obtained with all fiber contents, although the fibers decreased the workability of the concrete. To obtain sufficient workability, variable amounts of high range water reducer admixture (HRWRA) were added as shown in Table 2.4. Even with the HRWRA, slump values were low and indicate poor workability. Inverted slump test values provided a more accurate assessment of FRC workability (ACI 544.2R). In general, inverted slump values in the range of 3 to 30 sec are appropriate for placement and consolidation by vibration.

The air content of the concrete ranged from 3 to 7.5 percent. The variability of the air content and unit weight among batches indicated that considerable care must be used in preparing fiber reinforced concretes.

COMPRESSIVE STRENGTH

In general, the properties of all the hardened fiber reinforced concrete were better than those of the conventional concrete. As concluded by the investigators it is likely that the addition of HRWRA the addition of fibers might be partially responsible for such effect.

Three concrete cylinders were tested for compressive strength at 28 days. The test results, as an average of three specimens for the batches are shown in Table 2.5.

The compressive strength slightly increased at some fiber addition. However, at higher fiber volumes the strength of fiber reinforced concrete decreased. Such effect is believed to be related to difficulty in sample consolidation and eventually high concentration of fibers within the regions of the mixtures.

Other studies have indicated that adding fibers has only minor effect on compressive strength. The effects observed in this study may be due to between batch variability, the use of HRWRA and the decreased air content.

TABLE 2.5 Hardened Concrete Properties

Mix	Fiber Content		f_c	MOR
	Kg/m3	% Vol	Mpa (psi)	Mpa (psi)
NP4	0	0	40.7 (5905)	5.44 (790)
NF1	0.9	0.1	40.9 (5940)	4.55 (660)
NF7	0.9	0.1	46.3 (6720)	6.13 (890)
NF3	4.6	0.5	48.0 (6975)	5.82 (845)
NF5	4.6	0.5	46.7 (6780)	5.58 (810)
NF2	8.9	1.0	44.2 (6415)	5.20 (755)
NF1	8.9	1.0	38.4 (5570)	4.82 (700)

* f c = Compressive Strength, MOR = Modulus of Rupture
(Source, Nagabhushanam, et. al, 1989)

STATIC FLEXURAL TEST, FIRST-CRACK STRENGTH, AND FLEXURAL TOUGHNESS

The concrete beams were tested for the static flexural strength (Modulus of Rupture; MOR) by applying third point loading according to ASTM C78. The test results, as an average of three specimens for the batches are shown in Table 2.5.

To determine the first-crack strength and toughness values in accordance with ASTM C1018 the load-deflection data recorded was used to calculate the toughness indices and to investigate the ductility of concrete. Two LVDTs were placed under the beam at the centerline to measure the deflection. The rate of deflection was kept in the 0.002 to 0.004 in./min. range according to ASTM C1018.

As can be seen in Table 2.6, the first crack strength of the control concrete was 4.95 Mpa (720 psi). After the first crack, fiber reinforced concrete does not lose its load-carrying capability but instead transfer the load to the fibers spanning the cracked region. Toughness is defined as a measure of the concrete's ability to absorb energy during fracture. It is measured by a series of indices that are determined from

the area under the load-deflection curve. This index is given in Table 2.6. The results indicate increased toughness with increased fiber volume.

In addition to the toughness indices, the residual strength factors were calculated. The residual strength factors represent the average post-crack load over a specific deflection interval as a percentage of the load at first crack.

TABLE 2.6 First Crack Strength and Flexural Toughness

Mix	Fiber Content		First Crack	Toughness Index			Residual Factors	
	Kg/m3	% Vol	MPa (psi)	I_5	I_{10}	I_{20}	$R_{5,10}$	$R_{10,20}$
SPL	0	0.0	4.95 (720)	1	1	1	0	0
SP1	1.8	0.2	5.40 (785)	1.7	2.4	3.9	14.9	14.8
SP2	2.7	0.3	4.25 (615)	2.4	4.1	7.3	33.8	31.7
SP3	4.6	0.5	5.05 (730)	2.8	5.0	9.2	44.3	42.5
SP4	6.4	0.7	5.15 (745)	3.8	6.9	13.0	61.0	61.1

(Source, Ozyildirim, et. al, 1997)

FATIGUE STRENGTH AND ENDURANCE LIMITS

Ramakrishnan, V., Wu, G.Y., and Hosalli, G. (1989) investigated the endurance limits for the fiber reinforced concrete. Endurance limit in fatigue strength is defined as the maximum flexural fatigue stress at which the beam can withstand 2 million cycles of fatigue loading. The 2 million cycle limit is chosen to approximate the life span of a structure that may typically be subjected to fatigue loading, such as bridge deck or a highway pavement.

In their work, the frequency of loading used was 20 cycles/sec (Hz) for all tests. The machine used for these tests was Material Test System (MTS). The machine could be operated in any of three modes: load control (force applied to the

specimen), strain control (strain induced in the specimen), or deflection control (distance traveled by the ram or deflection of the specimen). Since this test was concerned with stress levels, load control was used for the fatigue testing. In their study the max fatigue stress of concrete corresponding to the endurance limits was found to increase substantially with the addition of fibers (Ramakrishnan, V., Wu, G.Y., and Hosalli, G., 1989).

FATIGUE LIFE MODELING

Flexural fatigue strength of concrete is an important parameter in the design of concrete pavements for roads, air-fields, and heavy-duty industrial yards. Many researchers have carried out laboratory fatigue experiments to look into the fatigue behavior of plain and fiber reinforced concrete since Feret's pioneer test. Most researchers adopted a relationship between stress level S, which is the ratio of the maximum loading stress to the modulus of rupture, σ_{max}/MR (MOR), and the number of load repetitions N, which causes fatigue failure. The relationship established is known as the Wholer equation.

$$S = \sigma_{max}/MR = a - b \text{ Log } (N)$$

where *a* and *b* are experimental coefficients that vary with loading conditions, compression, tension, or flexure.

The second form of the fatigue equation is a modification to the Wholer equation. It expresses the Wholer curves in terms of survival probabilities and

incorporates stress ratio R, which is the ratio of the minimum stress to the maximum stress $\sigma_{min}/\sigma_{max}$, into the Wholer equation. The R-term included simulates the loading condition in actual structures. The modified equation is shown as follows.

$$S = \sigma_{max}/MR = 1 - b\,(1 - R)\,\mathrm{Log}\,(N),$$

$$R = \sigma_{min}/\sigma_{max},\ 0 \le R \le 1$$

According to a study by Grzybowski and Meyer (Damage Accumulation in Concrete with and without Fiber Reinforcement, ACI Materials Journal, Vol. 90, pp. 594-604, 1993), S-N curves obtain in similar concrete mixtures are presented in Figure 2.1, 2.2. Based on the S-N curves, fatigue life for the plain and 0.25 % polypropylene fiber reinforced concretes was formulated into the following equation.

$$S = 1 - 0.072\,\mathrm{Log}\,(N)$$

where N = Number of cycles at failure for plain concrete
S = Stress Ratio (Maximum loading stress/Modulus of rupture) in Plain Concrete

And the fatigue life for 0.25% polypropylene fiber reinforced concretes can be formulated into the following equation.

$$S = 1 - 0.052\,\mathrm{Log}\,(N)$$

where N = Number of cycles at failure for polypropylene fiber concrete
S = Stress Ratio (Maximum loading stress/Modulus of rupture) in Polypropylene fiber concrete.

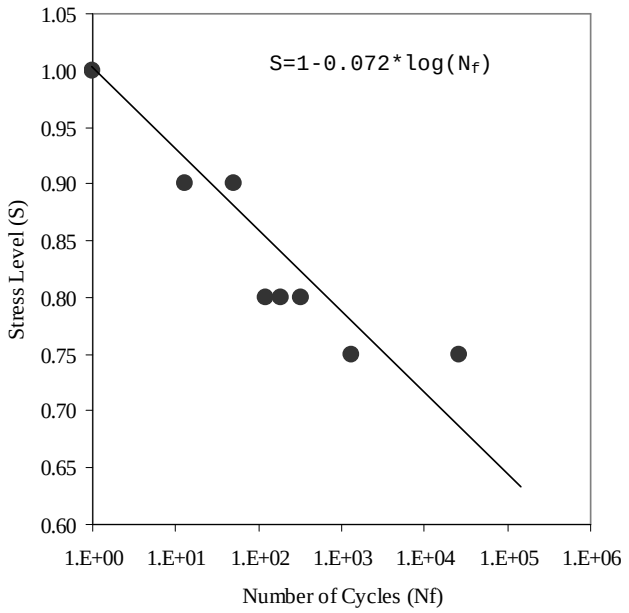

Figure 2.1 S-N Curve for the plain concrete
(Source. Grzybowski et. al. 1993)

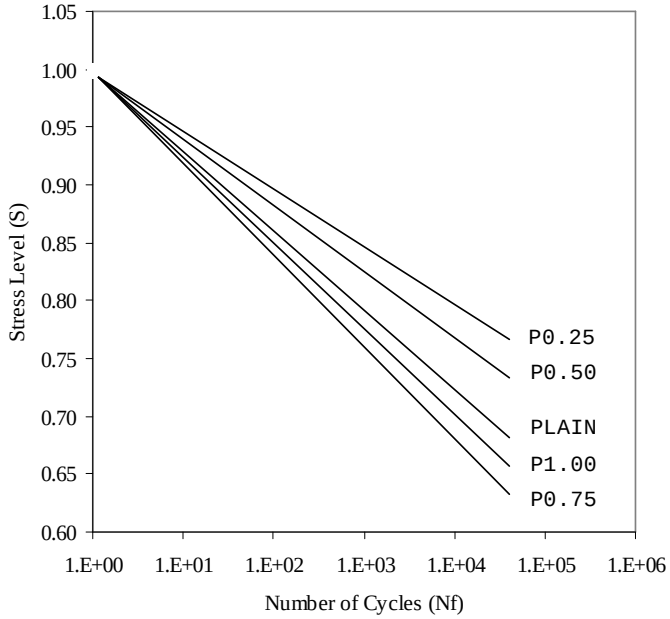

Figure 2.2 S-N Curve for the plain and fiber reinforced concrete
(Source Grzybowski et al. 1993)

CONCLUSIONS

From these selected past studies and additional literature review on fiber reinforced concrete the following conclusions are obtained:

- The use of fibers reduces the workability of concrete. However with the addition of HRWRA, workability can be achieved.
- The toughness of concrete improves with increasing fiber content. All concrete specimens reinforced with fibrillated polypropylene fibers exhibited an improved ductile behavior when compared with plain concrete.
- The addition of fibrillated polypropylene fibers has no significant influence on the static modulus of concrete.
- Good workability can be maintained in polypropylene fiber reinforced concrete by adding an appropriate quantity of super-plasticizer. No balling or tangling of fibers occurred during mixing and placing up to 1 percent by volume of polypropylene fibers.
- When using high volumes (0.5 – 1.0 percent) of fibrillated polypropylene fibers, fiber factor adjustments are necessary for the mix proportions to balance the mix for workability, placeability, appearance, and strength.

2.3 Shrinkage Cracking of Fiber Reinforced Concrete

Concrete shrinks when it is subjected to drying. The amount of shrinkage depends on many factors including the material properties, mixture composition, temperature and relative humidity of the environment, the age of the concrete, and the size of the structure. If concrete is restrained from shrinking, tensile stresses may develop and if tensile stresses go beyond the tensile strength concrete may start to crack. Cracking is a major concern in flat structures such as highway pavements, slabs for parking garages, and bridge decks. One way to reduce the shrinkage cracking is to reinforce concrete with short, randomly distributed fibers.

Several projects have investigated on the shrinkage cracking of fiber reinforced concrete. Miroslaw Grzybowski and Surendra P. Shah (1990) investigated the shrinkage cracking of fiber reinforced concrete using a ring-type specimen to simulate restrained shrinkage cracking. Two types of fibers (steel and polypropylene) with the amount of fibers ranged from 0.1 to 1.5 % by volume were used. The results indicated that the addition of small amount of steel fibers (0.25% by volume) reduced the average crack widths by about 20% and the maximum crack width by about 50% in comparison with plain concrete. Polypropylene fibers showed much less effective in reducing crack widths than steel fibers.

Balaguru (1994) investigated the contribution of fibers to crack reduction of cement composites during the initial and final setting period. Polypropylene fibers were evaluated both in the pulp form and in relatively longer lengths of 0.75. (19 mm). The longer polypropylene fibers were fibrillated. The results indicated that both

steel and synthetic fibers make a significant contribution to shrinkage crack reduction during the initial and final setting periods.

Shah, Weiss, and Yang (1998) investigated the shrinkage cracking of the fiber reinforced concrete. Fibers are added to concrete in low volume (less than 1 percent). The results showed that fibers typically do not significantly alter free shrinkage of concrete, however at high enough dosages they can increase the resistance to cracking and decrease crack width.

In a study conducted by Grzybowski, et. al. (1990) the mix proportions by weight for the matrix were: 1:2:2:0.5 (cement: sand: coarse aggregate: water). The maximum size of the aggregate was 9 mm (3/8 in.). Two types of fibers used were polypropylene and steel. The polypropylene fibers were collated and fibrillated, measuring 19 mm (3/4 in.) long; the steel fibers were 25 mm (1 in.) long and 0.4 mm (0.015 in.) in diameter. The following fiber contents were used – steel fiber: 0.25, 0.5, 1.0 and 1.5 percent, and polypropylene fibers: 0.1, 0.25, 0.5 and 1.0 percent.

A special microscope setup was designed to measure crack width as shown in Figure 2.3.

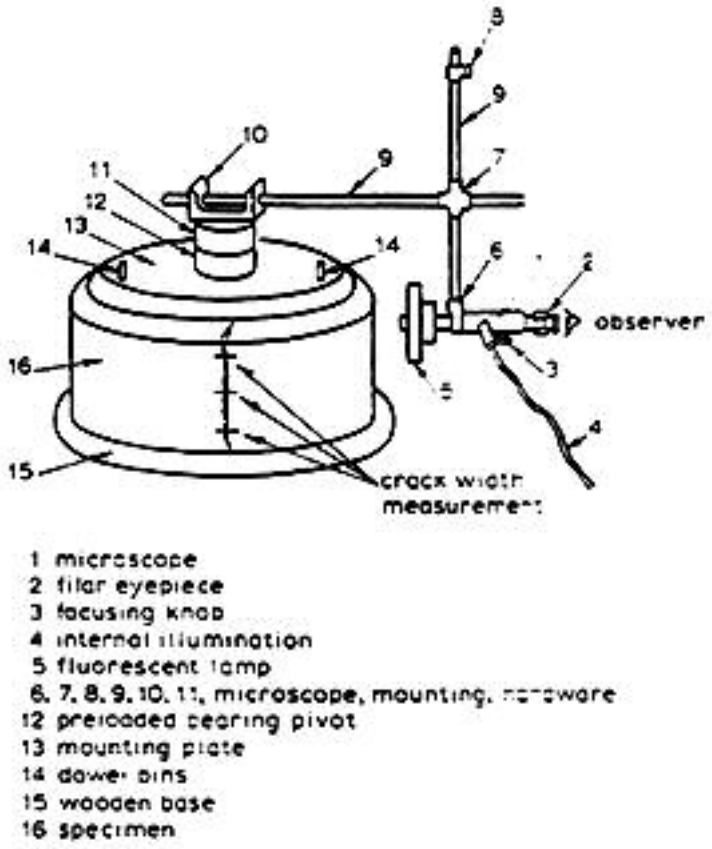

Figure 2.3 Special Microscope Setup
(Source, Grzybowski et. al. 1990)

FREE SHRINKAGE

The free shrinkage measurements are shown in Figure 2.4. The addition of fibers does not substantially alter the drying shrinkage, as can be seen in Figure 2.4, which gives the results of specimens made with 1 percent by volume of steel and polypropylene fibers. Similar results have been obtained by Malmberg and Skarendahl (1978).

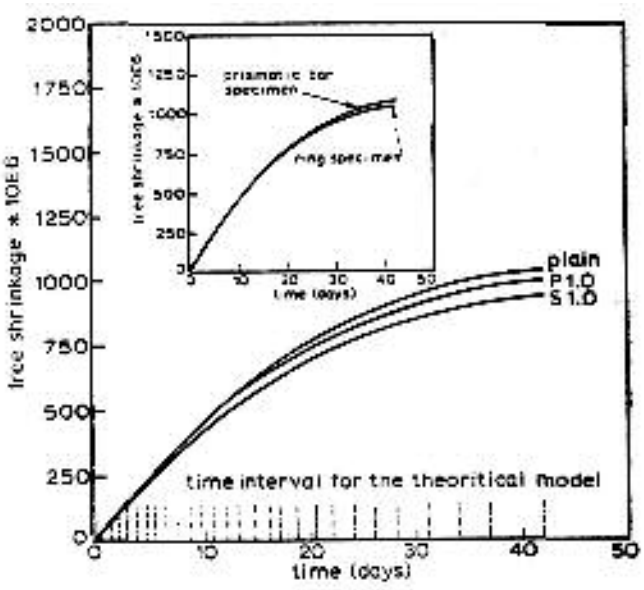

Figure 2.4 Free Shrinkage Tests Results
(Source, Grzybowski et. al., 1990)

RESTRAINED SHRINKAGE

The development of restrained shrinkage strain and cracking for plain concrete is shown in Figure 2.5. The specimen does not show any strain initially (up to about 3days). The value of free shrinkage strain at 3 days was about 150 micro-strains. However, as a result of restraint provided by the steel ring, the concrete ring did not shrink. When the cumulative tensile stress due to restraint by the steel ring reaches the current tensile strength of material, a crack will start. After cracking, the uncracked portion of the specimen will shrink, whereas the crack will continue to widen as is illustrated in Figure 2.5. With fiber reinforced concrete, fibers bridging the crack will provide resistance to crack widening, which will create a tensile stress in the uncracked portion. As a result, the measured strain values may exhibit a

reversal in trend as indicated in Figure 2.6, which plots the results for a specimen reinforced with 0.25 percent steel fibers.

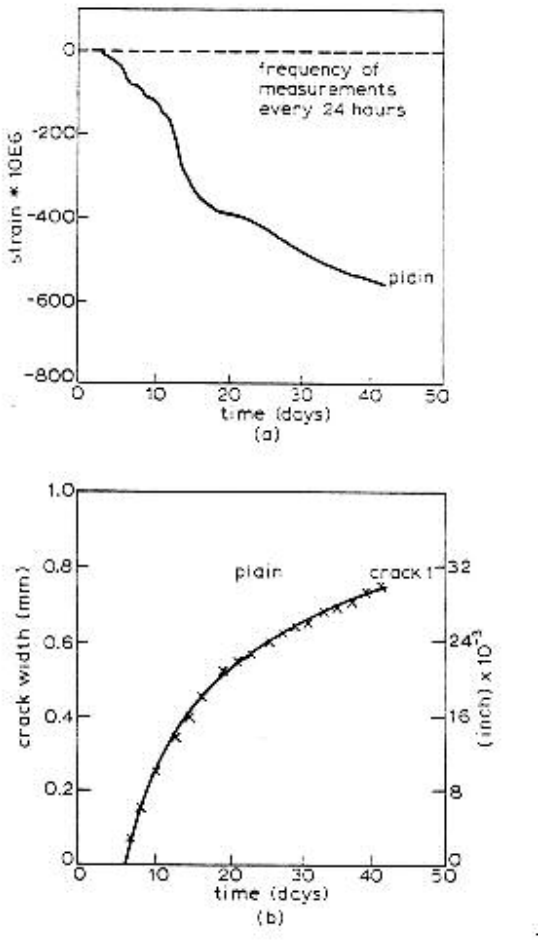

Figure 2.5 Strain and crack-width measurements for plain concrete specimen.
(Source, Grzybowski et. al., 1990)

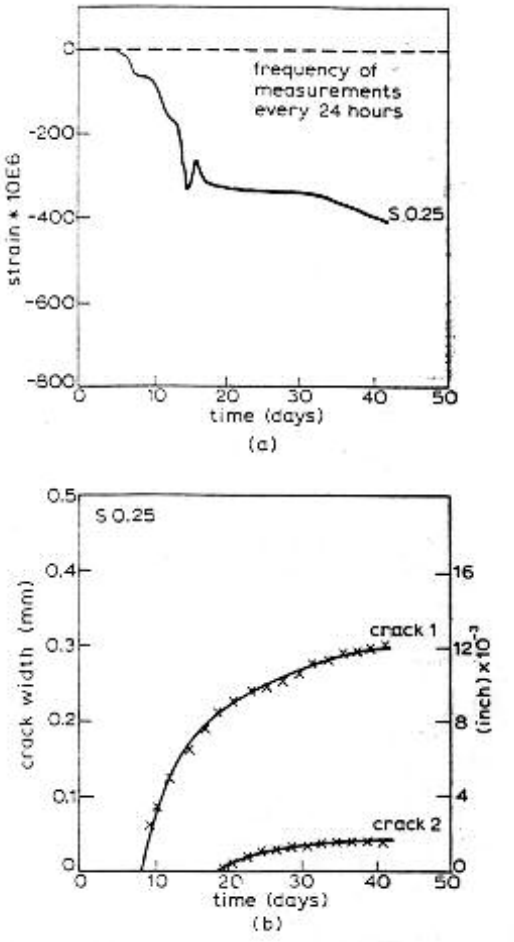

Figure 2.6 Strain and crack-width measurements for specimen reinforced with 0.25 % volume of steel fibers.
(Source, Grzybowski et. al., 1990)

The influence of fibers on shrinkage cracking can be seen from Table 2.7 and Figures 2.7 and 2.8. The widths of the crack at the end of 6 weeks are tabulated in Table 2.7. It can be seen that addition of a small amount of fibers (0.25 percent) can substantially reduce the width of the cracks.

TABLE 2.7 Experimental results and comparison with computational results

Specimen	Number of cracks, mm	Crack 1 (widest crack)		Crack 2		Crack 3		Total crack width, mm	Theoretical total crack width, mm
		Crack width, mm	Circumferential position,* mm	Crack width, mm	Circumferential position, mm	Crack width, mm	Circumferential position, mm		
Plain	1	0.900	875	—	—	—	—	0.900	1.050
S0.25	2	0.300	890	0.045	190	—	—	0.345	0.410
S0.5	3	0.100	800	0.065	0	0.050	420	0.215	0.252
S1.0	1	0.075	87	—	—	—	—	0.075	0.145
S1.5	3	0.011	210	0.010	395	0.009	690	0.03	0.080
P0.1	1	0.875	0	—	—	—	—	0.875	1.030
P0.25	1	0.480	900	—	—	—	—	0.480	0.610
P0.5	1	0.230	1110	—	—	—	—	0.230	0.400
P1.0	2	0.150	720	0.065	110	—	—	0.215	0.250

*Total circumferential length = 1170 mm.
1 mm = 0.0394 in.

(Source, Grzybowski et. al., 1990)

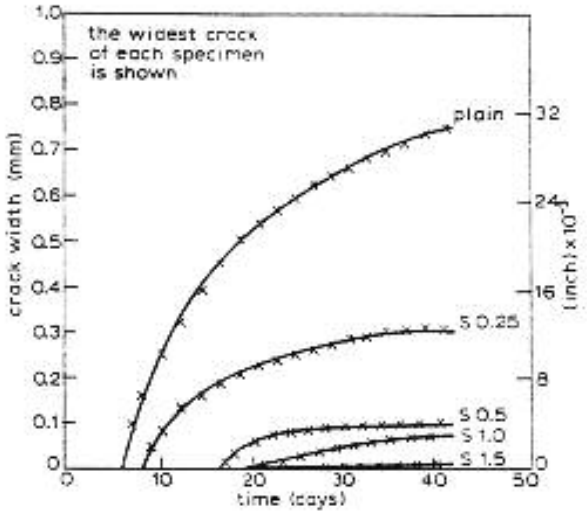

Figure 2.7 Crack width vs. time for various volume percentages of steel fibers
(Source, Grzybowski et. al., 1990)

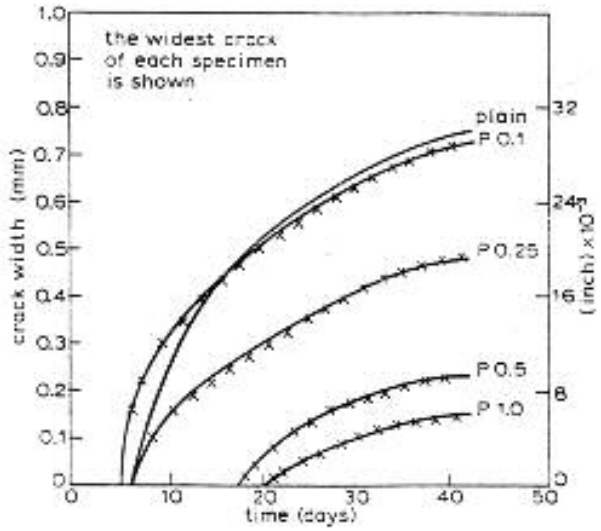

Figure 2.8 Crack width vs. time for various volume percentages of polypropylene fibers (Source, Grzybowski et. al., 1990)

CONCLUSIONS

The free shrinkage test results showed that shrinkage is independent of the specimen geometry. The results of tests investigated here showed that the amount of fibers as small as 0.25 percent by volume can substantially reduce crack widths resulting from restrained drying shrinkage. In terms of polypropylene fibers there was no influence of the addition of fibers for fiber content equal to 0.1 percent by volume.

Overall, the ring type specimen seems to be an appropriate to simulate restrained shrinkage cracking in concrete. However, the experimental results and conclusions are varying in function of the testing setup geometry, testing conditions and mixture characteristics. As it discovered in this study, specimens prepared with concrete rings have shown no cracks for extended periods of time, probably due to

the strength characteristics of the concrete mixtures considered herein. In any case the results from previous studies were reported herein for a better understanding of the implications of fibers in concrete shrinkage.

CHAPTER 3 MATERIALS & TESTING PLAN

3.1. Materials and Mix Design

In this study, local materials were used to produce the conventional concrete mixture meeting the MSHA MD7 mix, with a #57 aggregate, as well as the fiber reinforced and low shrinkage mixtures. A second large-size aggregate gradation was used with a #357 aggregate, to produce a large stone aggregate for the second low shrinkage mixture. The gradation of the aggregate (crushed stone) is shown in Figures 3.1 and 3.2. Specifically, in Figure 3.1 the preliminary gradation for the #57 aggregate used in standard pavement operation by MSHA obtained from the quarry/supplier during the 2000 production is shown. The gradation for the aggregate delivered to UMD by the supplier in 2001 is also shown in this Figure. Similarly, Figure 3.2 shows the aggregate gradation for the #357 aggregate.

The mixtures were prepared by using a Type I Portland cement and NewCem provided by Blue Circle. The sand was provided by Kaye Construction, Inc. The properties of the aggregate are shown in Table 3.1. Tables 3.1 and 3.2 present the mix design characteristics for the control and low shrinkage mixture with the large aggregate. The remaining mixtures used the mix design of the control concrete by adding different fiber contents, 0.1%, 0.2%, 0.3% and 0.4%, and by modifying the w/c ratio for the first low shrinkage mixture. Two admixtures were used, one for air entrainment, the second as water reducer, Table 3.3. The seven mixtures producing with their characteristics are shown in Table 3.3 . The properties of the ¾-inch fiber used are shown in Table 3.4

Table 3.1 Mix Design for #57

Cement	377 lb./cy
New Cement	203 lb./cy
Stone	1898 lb./cy
Sand	1176 lb./cy
Water	255 lb./cy
Fineness Modulus	2.57
Unit Weight $_{dry}$ (#57)	101.4
Gs of Stone (#57)	2.79
Gs of Sand	2.79
Gs of Cement	3.15
Gs of Newcem	2.93

* 1 lb/y3 = 0.593 kg/m3
Cement (Type I/II)
Newcem (Ground Blast Furnace Slag)
Stone (#57, Provided by Havre De Grace Quarry)
Sand (Provided by Kaye Construction, Inc.)
Gs = Specific Gravity

Table 3.2 Mix Design for #357

Cement	377 lb./cy
New Cement	203 lb./cy
Stone (#57)	1207 lb./cy
Stone (#357)	911 lb./cy
Sand	980 lb./cy
Water	255 lb./cy
Fineness Modulus	2.57
Unit Weight $_{dry}$ (#57)	101.4
Unit Weight $_{dry}$ (#357)	102.8
Gs of Stone (#57)	2.79
Gs of Stone (#357)	2.80
Gs of Sand	2.79
Gs of Cement	3.15
Gs of Newcem	2.93

* 1 lb/y3 = 0.593 kg/m3
Cement (Type I/II)
Newcem (Ground Blast Furnace Slag)
Stone (#57, #3, Provided by Havre De Grace Quarry)
Sand (Provided by Kaye Construction, Inc.)
Gs = Specific Gravity

Table 3.3 Mixtures' Properties

Aggregate Type	#57	#57	#57	#57	#57	#357 LS	#57 LS
W/C Ratio	0.44	0.44	0.44	0.44	0.44	0.44	0.40
Air Content (%)	6.6%	4.6%	6.6%	7.0%	5.8%	5.0%	6.0%
Slump (in./sec.)	1.5	1.5 / 17	1.125 / 15	1 / 21	0.625 / 29	1	1.5
Fiber Content	0.0%	0.1%	0.2%	0.3%	0.4%	0.0%	0.0%
Air Entrainment	1.7 oz./ 100 lbs.	1.9 oz./ 100 lbs.	1.9 oz./ 100 lbs.	1.9 oz./ 100 lbs.	1.9 oz./ 100 lbs.	2.0 oz./ 100 lbs.	2.0 oz./ 100 lbs.
Water Reducer	(M) 5 oz./ 100 lbs.	(M) 5oz./ 100 lbs.	(M) 5oz./ 100 lbs.	(M) 5.5oz./ 100 lbs.	(M) 6oz./ 100 lbs.	(M) 5.5oz./ 100 lbs.	(H) 2.7oz./ 100 lbs.

* (M) = Middle Range Water Reducing Admixture (Daracem 55, Provided by Grace Construction Products)
(H) = High Range Water Reducing Admixture (ADVA Flow, Provided by Grace Construction Products)
Air Entrainment Admixture (Daravair 1000, Provided by Grace Construction Products)
Target Air Content 6.5%

Table 3.4 Fiber Characteristics

Fiber	Length MM (IN)	Diameter MM (IN)	Aspect Ratio (l/d)	Yield Strength Mpa (ksi)	Elastic Modulus Mpa (ksi)	Specific Gravity
Polypropylene (Fibrillated)	19 (0.75)	N/A	N/A	550-750 (80-110)	3450 (500)	0.91

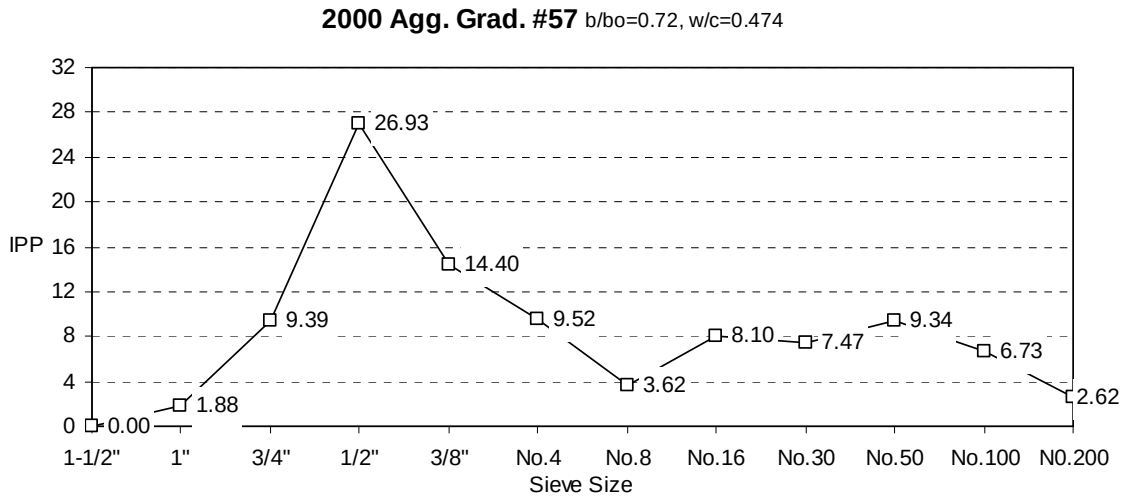

#57 Aggregate Gradation 2000 by Master Builders, Inc.

* IPP = Individual Percent Passing
* Source of Aggregate (Havre de Grace Quarry in Maryland)

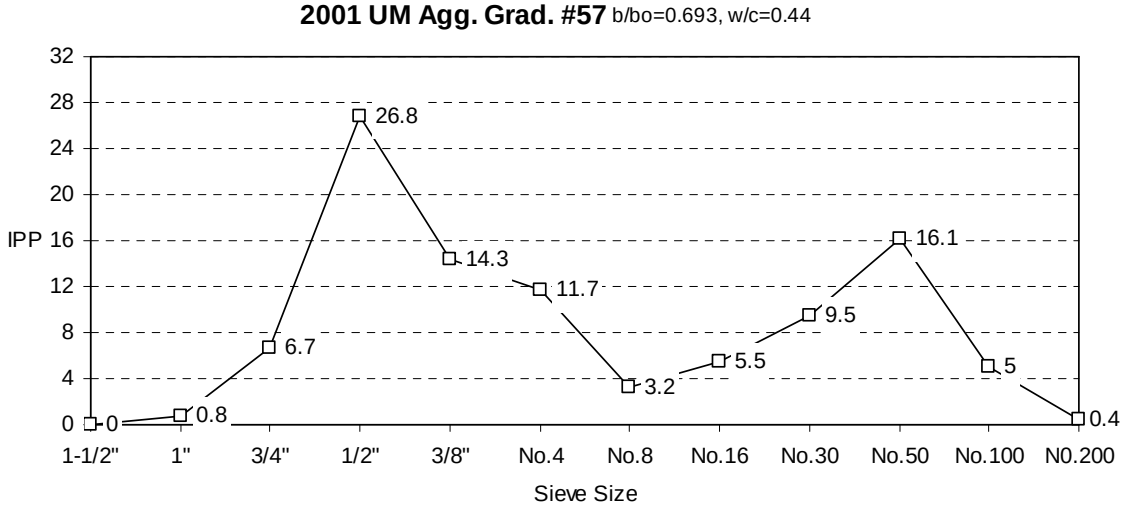

#57 Aggregate Gradation 2001 by University of Maryland Research Team

* IPP = Individual Percent Passing
* Source of Aggregate (Havre de Grace Quarry in Maryland)

Figure 3.1 Aggregate Gradation for #57

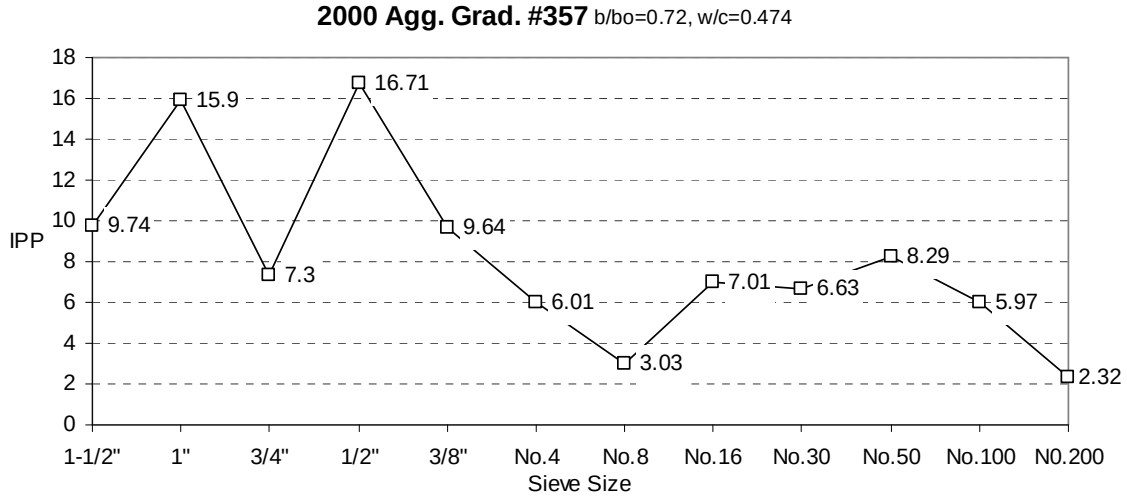

#357 Aggregate Gradation 2000 by Master Builders, Inc.

* IPP = Individual Percent Passing
* Source of Aggregate (Havre de Grace Quarry in Maryland)

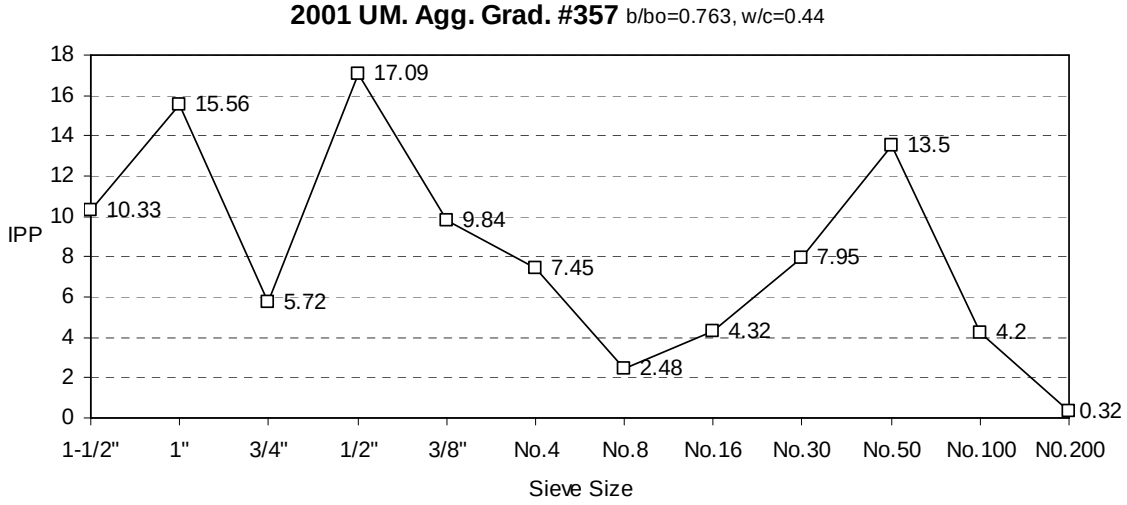

#357 Aggregate Gradation 2001 by University of Maryland Research Team

* IPP = Individual Percent Passing
* Source of Aggregate (Havre de Grace Quarry in Maryland)

Figure 3.2 Aggregate Gradation for #357

3.2 Testing Plan

The following testing was undertaken in the laboratory investigation for these mixtures.

3.2.1 Compressive Strength

3.2.1.1 Standards

1) ASTM C 39; Compressive Strength of Cylindrical Concrete Specimens determines the compressive strength of 6 inch x 12 inch concrete cylinders by applying a continuously increasing axial load to the specimen until failure occurs.
2) ASTM C 192; Making and Curing Concrete Test Specimens in the Laboratory. Three specimens were made for each test age and test condition. Specimen diameter should be three times the fiber length or maximum aggregate size.

3.2.1.2 Aging Period.

Tests were conducted at 28(14) days after casting the concrete.

3.2.1.3 Aging Temperature.

Mixing and Curing temperature (21 ± 3°C, 70 ± 5°F).

3.2.1.4 Polypropylene Fiber Content.

0.0%, 0.1%, 0.2%, 0.3%, 0.4%

3.2.1.5 Aggregate Gradations.

#57, #357

3.2.1.6 Slump (ASTM C 143)

Slump of Hydraulic Cement Concrete. However, FRC samples were also tested by (ASTM C 995) Time of flow through Inverted Cone test.

3.2.1.7 Air Content (ASTM C 138)

However, FRC samples were consolidated using external vibration.

3.2.1.8 Number of Samples : 21

3.2.2 Unrestrained Shrinkage of Hardened Concrete

3.2.2.1 Standards

1) ASTM C 157; Length Change of Hardened hydraulic-Cement Mortar and Concrete.
2) ASTM C 192; Making and Curing Concrete Test Specimens in the Laboratory.

Three specimens were used with 6 in. square cross-section by 21 in. length.

3.2.2.2 Aging Period

For air storage, measured length change at 24 hours, 4, 7,14 and 28 days.

3.2.2.3 Aging Temperature

Mixing and Curing temperature (21 ± 3°C, 70 ± 5°F).

3.2.2.4 Polypropylene Fiber Content

0.0%, 0.1%, 0.2%, 0.3%, 0.4%

3.2.2.5 Aggregate Gradations

#57, #357

3.2.2.6 Slump (ASTM C 143)

Slump of Hydraulic Cement Concrete. However, FRC samples were also tested by (ASTM C 995) Time of flow through Inverted Cone test.

3.2.2.7 Air Content. (ASTM C 138)

However, FRC samples were consolidated using external vibration.

3.2.2.8 Number of Samples : 21

3.2.3 Restrained Shrinkage of Plastic Concrete

3.2.3.1 Standards

1) ACI has not declared a standard test for restrained plastic shrinkage evaluation of FRC. As such, listed below are the tests recommended to evaluate shrinkage.
2) Restrained Shrinkage of Hardened Concrete, The steel ring test was used to monitor plastic shrinkage and associated cracking that may occur within a few hours of placement.

3.2.3.2 Aging Period & Temperature

The outer mold was stripped off 1day after casting. Then the specimen was cured for 6 days at 23 C, 100 percent relative humidity. After that the specimen was exposed to drying at 23 C, 39 percent relative humidity.

3.2.3.3 Polypropylene Fiber Content

0.0%, 0.1%, 0.2%, 0.3%, 0.4%

3.2.3.4 Aggregate Gradations

#57, #357

3.2.3.5 Slump (ASTM C 143)

Slump of Hydraulic Cement Concrete. However, FRC samples were also tested by (ASTM C 995) Time of flow through Inverted Cone test.

3.2.3.6 Air Content (ASTM C 138)

However, FRC samples were consolidated using external vibration.

3.2.3.7 Number of Samples : 21

3.2.4 Flexural Strength & Toughness

3.2.4.1 Standards

1) ASTM C-78; Flexural Strength of Concrete(using Simple Beam with Third-Point Loading).
2) ASTM C1018; Flexural Toughness and First-Crack Strength of Fiber-Reinforced Concrete(using Beam with Third-Point Loading).
3) ASTM C 192; Making and Curing Concrete Test Specimens in the Laboratory.

   Three specimens were made for each test age and test condition.

   Specimen width and depth should be three times the fiber length or maximum aggregate size.

3.2.4.2 Aging Period

Tests were conducted at 28(14) days after casting the concrete.

3.2.4.3 Aging Temperature

Mixing and Curing temperature(73.4°).

3.2.4.4 Polypropylene Fiber Content

0.0%, 0.1%, 0.2%, 0.3%, 0.4%

3.2.4.5 Aggregate Gradations

#57, #357

3.2.4.6 Slump (ASTM C 143)

Slump of Hydraulic Cement Concrete. However, FRC samples were also tested by (ASTM C 995) Time of flow through Inverted Cone test.

3.2.4.7 Air Content (ASTM C 138)

However, FRC samples were consolidated using external vibration.

3.2.4.8 Number of Samples : 21

3.2.5 Fatigue Endurance

3.2.5.1 Standard

1) ASTM C 192; Making and Curing Concrete Test Specimens in the Laboratory.

   Three specimens were made for each test age and test condition.

   Specimen width and depth should be three times the fiber length or maximum aggregate size.

2) Cyclic Load Testing; 5.5 kips MTS machine.

3.2.5.2 Aging Period

Tests were conducted at 28 days after casting the concrete.

3.2.5.3 Aging Temperature

Mixing and Curing temperature(73.4°F).

3.2.5.4 Polypropylene Fiber Content

0%, 0.1%, 0.2%, 0.3%, 0.4%

3.2.5.5 Aggregate Gradations

#57, #357

3.2.5.6 Stress Ratio

0.49, 0.59, 0.69

3.2.5.7 Endurance Limit

2 million cycles at 20 cycle per second loading.

3.2.5.8 Number of Samples : 45

CHAPTER 4 EXPERIMENTAL RESULTS

Based on the testing shown in Chapter 3, the following experimental results were obtained.

4.1 Compressive Strength

The compressive strength results are shown in Table 4.1. The presence of fiber had no conclusive effects on this concrete characteristic.

Table 4.1 Compressive Strength

Specimen	Aggregate Type	Fiber (%)	Age (days)	Compressive Strength (PSI)	Description
0-1	#57	0.0	28	5,377	
0-2			28	4,215	
0-3			28	5,624	
1-1	#57	0.1	28	6,296	
1-2			28	5,854	
1-3			28	6,402	
2-1	#57	0.2	28	5,341	
2-2			28	5,235	
2-3			33	5,607	
3-1	#57	0.3	33	4,584	
3-2			33	4,439	
3-3			33	4,606	
4-1	#57	0.4	33	5,320	
4-2			33	5,041	
4-3			33	4,245	
5-1	#357 LS	0.0	28	5,129	Low shrinkage
5-2			28	5,391	
5-3			-	-	
6-1	#57 LS	0.0	28	4,984	Low shrinkage
6-2			28	5,801	
6-3			37	3,785	

* 1 Psi = 6.89 kPa

4.2 Flexural Strength

The flexural strength testing results are shown in Table 4.2 For the fiber reinforced concrete strength increased with fiber concrete up to 0.3% fiber content. The low shrinkage mixture presented higher strength than the control mix.

Table 4.2 Flexural Strength

Specimen	Aggregate Type	Fiber (%)	Age (days)	Flexural Strength (PSI)	Average Flexural Strength	Size (IN)
0-1	#57	0	35	792	780	6x6x21
0-2				769		
0-3				779		
1-1	#57	0.1	37	695	650	6x6x21
1-2				647		
1-3				609		
2-1	#57	0.2	37	928	870	6x6x21
2-2				876		
2-3				805		
3-1	#57	0.3	37	835	898	6x6x21
3-2				881		
3-3				978		
4-1	#57	0.4	37	839	867	6x6x21
4-2				876		
4-3				885		
5-1	#357 LS	0	33	757	827	6x6x21
5-2				828		
5-3				895		
6-1	#57 LS	0	35	876	901	6x6x21
6-2				963		
6-3				864		

* 1 Psi = 6.89 kPa

4.3 Shrinkage

4.3.1 UNRESTRAINED SHRINKAGE

The concrete samples were cured in air storage with 70^{o}F temperature and 50% relative humidity. The testing results are shown in Table 4.3. As it can be see from the Table and Figures 4.1 and 4.2.

The Low Shrinkage mixture with reduced w/c ratio had low shrinkage than the one with large size aggregate. Shrinkage of the control concrete was very close to the one of the low shrinkage mixtures, while the fiber mixtures has higher shrinkage.

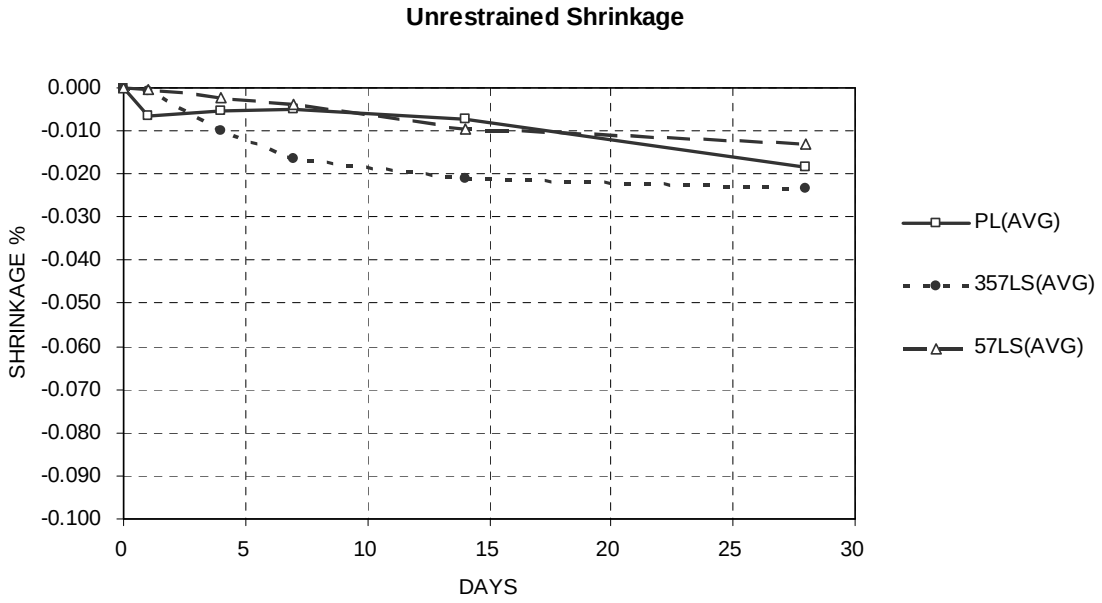

Figure 4.1 Plain Unrestrained Shrinkage Test Results

* 357LS = #357 Low Shrinkage Concrete, 57LS = #57 Low Shrinkage Concrete

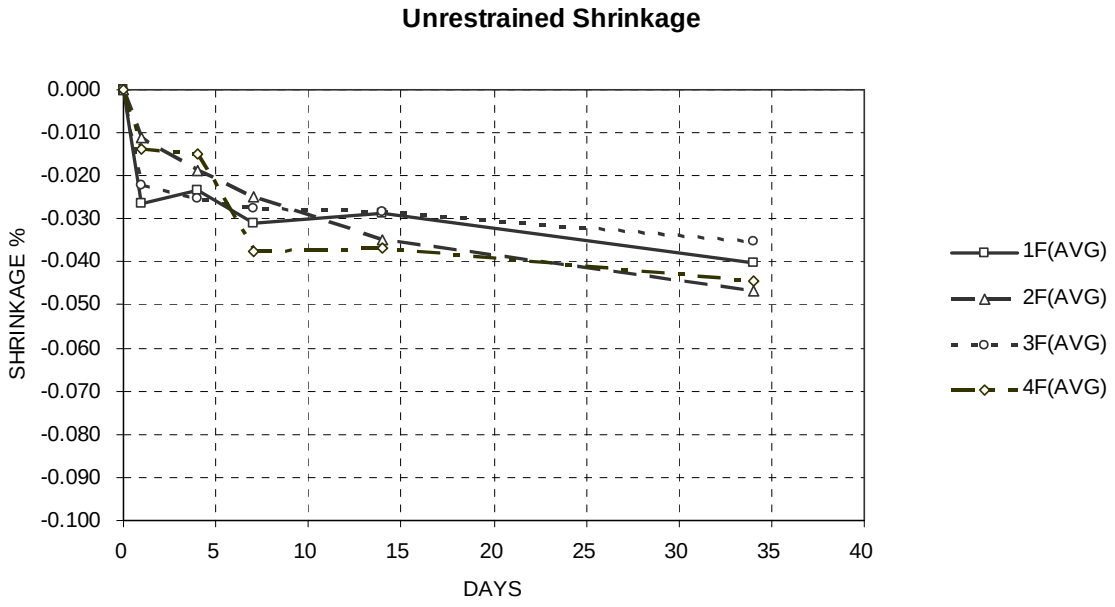

Figure 4.2 Fiber Reinforced Concrete Unrestrained Shrinkage Test Results

* 1F = 0.1% Fiber Reinforced Concrete, 2F = 0.2% Fiber Reinforced Concrete

Table 4.3 Unrestrained shrinkage

Specimen	Agg. Type	Fiber (%)	Age (After 28 days)	Initial Dial Reading	Dial Reading	Length Change (%)	Length Change Average (%)
0-1	#57	0.0	24 hours	0.17550	0.17485	-0.0065	-0.006
0-2				0.17800	0.17740	-0.0060	
0-3				0.07100	0.07030	-0.0070	
1-1	#57	0.1	24 hours	0.16450	0.16246	-0.0204	-0.026
1-2				0.17300	0.17030	-0.0270	
1-3				0.09800	0.09485	-0.0315	
2-1	#57	0.2	24 hours	0.08100	0.08014	-0.0086	-0.011
2-2				0.11890	0.11730	-0.0160	
2-3				0.16440	0.16348	-0.0092	
3-1	#57	0.3	24 hours	0.05780	0.05540	-0.0240	-0.022
3-2				0.19662	0.19450	-0.0212	
3-3				0.19000	0.18780	-0.0220	
4-1	#57	0.4	24 hours	0.09680	0.09440	-0.0240	-0.014
4-2				0.08200	0.08140	-0.0060	
4-3				0.16700	0.16590	-0.0110	
5-1	#357 LS	0.0	24 hours	0.10200	0.10195	-0.0005	-0.001
5-2				0.01285	0.01280	-0.0005	
5-3				0.15230	0.15217	-0.0013	

6-1	#57 LS	0.0	24 hours	0.11050	0.11045	-0.0005	-0.001
6-2				0.13400	0.13396	-0.0004	
6-3				0.16850	0.16843	-0.0007	
0-1	#57	0.0	4 days	0.17550	0.17496	-0.0054	-0.005
0-2				0.17800	0.17747	-0.0053	
0-3				0.07100	0.07050	-0.0050	
1-1	#57	0.1	4 days	0.16450	0.16240	-0.0210	-0.023
1-2				0.17300	0.17090	-0.0210	
1-3				0.09800	0.09520	-0.0280	
2-1	#57	0.2	4 days	0.08100	0.07864	-0.0236	-0.019
2-2				0.11890	0.11760	-0.0130	
2-3				0.16440	0.16239	-0.0201	
3-1	#57	0.3	4 days	0.05780	0.05520	-0.0260	-0.025
3-2				0.19662	0.19400	-0.0262	
3-3				0.19000	0.18758	-0.0242	
4-1	#57	0.4	4 days	0.09680	0.09490	-0.0190	-0.015
4-2				0.08200	0.08060	-0.0140	
4-3				0.16700	0.16580	-0.0120	
5-1	#357 LS	0.0	4 days	0.10200	0.10120	-0.0080	-0.010
5-2				0.01285	0.01170	-0.0115	
5-3				0.15230	0.15130	-0.0100	
6-1	#57 LS	0.0	4 days	0.11050	0.11031	-0.0019	-0.002
6-2				0.13400	0.13383	-0.0017	
6-3				0.16850	0.16820	-0.0030	
0-1	#57	0.0	7 days	0.17550	0.17498	-0.0052	-0.005
0-2				0.17800	0.17750	-0.0050	
0-3				0.07100	0.07050	-0.0050	
1-1	#57	0.1	7 days	0.16450	0.16188	-0.0262	-0.031
1-2				0.17300	0.16970	-0.0330	
1-3				0.09800	0.09464	-0.0336	
2-1	#57	0.2	7 days	0.08100	0.07824	-0.0276	-0.025
2-2				0.11890	0.11640	-0.0250	
2-3				0.16440	0.16215	-0.0225	
3-1	#57	0.3	7 days	0.05780	0.05490	-0.0290	-0.028
3-2				0.19662	0.19330	-0.0332	
3-3				0.19000	0.18790	-0.0210	
4-1	#57	0.4	7 days	0.09680	0.09264	-0.0416	-0.038
4-2				0.08200	0.07785	-0.0415	
4-3				0.16700	0.16400	-0.0300	
5-1	#357 LS	0.0	7 days	0.10200	0.10063	-0.0137	-0.016
5-2				0.01285	0.01100	-0.0185	
5-3				0.15230	0.15061	-0.0169	
6-1	#57 LS	0.0	7 days	0.11050	0.11020	-0.0030	-0.004
6-2				0.13400	0.13370	-0.0030	
6-3				0.16850	0.16796	-0.0054	
0-1	#57	0.0	14 days	0.17550	0.17480	-0.0070	-0.007
0-2				0.17800	0.17712	-0.0088	
0-3				0.07100	0.07035	-0.0065	
1-1	#57	0.1	14 days	0.16450	0.16203	-0.0247	-0.029
1-2				0.17300	0.16980	-0.0320	

1-3				0.09800	0.09501	-0.0299	
2-1	#57	0.2	14 days	0.08100	0.07731	-0.0369	-0.035
2-2				0.11890	0.11530	-0.0360	
2-3				0.16440	0.16126	-0.0314	
3-1	#57	0.3	14 days	0.05780	0.05550	-0.0230	-0.028
3-2				0.19662	0.19328	-0.0334	
3-3				0.19000	0.18710	-0.0290	
4-1	#57	0.4	14 days	0.09680	0.09293	-0.0387	-0.037
4-2				0.08200	0.07748	-0.0452	
4-3				0.16700	0.16440	-0.0260	
5-1	#357 LS	0.0	14 days	0.10200	0.10010	-0.0190	-0.021
5-2				0.01285	0.01075	-0.0210	
5-3				0.15230	0.15002	-0.0228	
6-1	#57 LS	0.0	14 days	0.11050	0.10960	-0.0090	-0.010
6-2				0.13400	0.13310	-0.0090	
6-3				0.16850	0.16745	-0.0105	
0-1	#57	0.0	28 days	0.17550	0.17360	-0.0190	-0.018
0-2				0.17800	0.17599	-0.0201	
0-3				0.07100	0.06940	-0.0160	
1-1	#57	0.1	34 days	0.16450	0.16080	-0.0370	-0.040
1-2				0.17300	0.16870	-0.0430	
1-3				0.09800	0.09396	-0.0404	
2-1	#57	0.2	34 days	0.08100	0.07633	-0.0467	-0.047
2-2				0.11890	0.11396	-0.0494	
2-3				0.16440	0.15997	-0.0443	
3-1	#57	0.3	34 days	0.05780	0.05420	-0.0360	-0.035
3-2				0.19662	0.19279	-0.0383	
3-3				0.19000	0.18680	-0.0320	
4-1	#57	0.4	34 days	0.09680	0.09270	-0.0410	-0.044
4-2				0.08200	0.07730	-0.0470	
4-3				0.16700	0.16250	-0.0450	
5-1	#357 LS	0.0	28 days	0.10200	0.09988	-0.0212	-0.024
5-2				0.01285	0.01050	-0.0235	
5-3				0.15230	0.14971	-0.0259	
6-1	#57 LS	0.0	28 days	0.11050	0.10920	-0.0130	-0.013
6-2				0.13400	0.13280	-0.0120	
6-3				0.16850	0.16709	-0.0141	

4.3.2 Restrained Shrinkage

Even though several ring specimens were produced for monitoring restrained shrinkage of the plain, fiber reinforced and low shrinkage concrete mixtures, the samples showed no cracking for an extended period of time, probably due to the strength characteristics of the concrete mixtures considered herein. Thus, no data are

reported for this testing. As indicated in Chapter 2, to date, there is no universally accepted method and standard of testing for restrained shrinkage. The experimental results and conclusions are varying in function of the testing setup geometry, testing conditions and mixture characteristics.

4.4 Toughness

The toughness index measures the energy capacity of the specimen and the ductility of the specimen. The toughness results are shown in Table 4.4 and Figure 4.3. Both toughness indices and residual strength factors are shown in this table for the fiber reinforced mixtures. Plain concrete failed immediately upon cracking, and thus toughness indices I_5, I_{10}, and I_{30} are always equal to 1. Fiber reinforced concrete carried loads after the first crack into the plastic zone. So, ductility and energy capacity was increased with adding fibers. As it can be seen from Table 4.4, the 0.3% and 0.4% fiber reinforced concrete mixtures showed the highest toughness results, 5.5 and 5.6 respectively.

Table 4.4 Toughness

Specimen	Agg. Type	Fiber (%)	First Crack Strength (PSI)	First Crack Strength (PSI)	I_5 Toughness Index	I_{10} Toughness Index	I_{20} Toughness Index	$R_{5,10}$ Residual Strength Factor	$R_{10,20}$ Residual Strength Factor
1-2	#57	0.1	584	667	2.6	3.3	3.6	8	3
1-3			750		2.6	2.7	3.0		
				Average	2.6	3.0	3.3		
2-2	#57	0.2	701	774	2.8	3.1	3.6	6	5
2-3			847		3.5	3.8	4.3		
				Average	3.2	3.5	4.0		
3-2	#57	0.3	701	777	3.1	4.0	5.5	16	14
3-3			853		3.4	4.1	5.4		
				Average	3.3	4.1	5.5		
4-2	#57	0.4	786	774	3.3	4.3	5.9	20	14
4-3			761		3.0	4.0	5.3		
				Average	3.2	4.2	5.6		

* 1 Psi = 6.89 kPa

Toughness

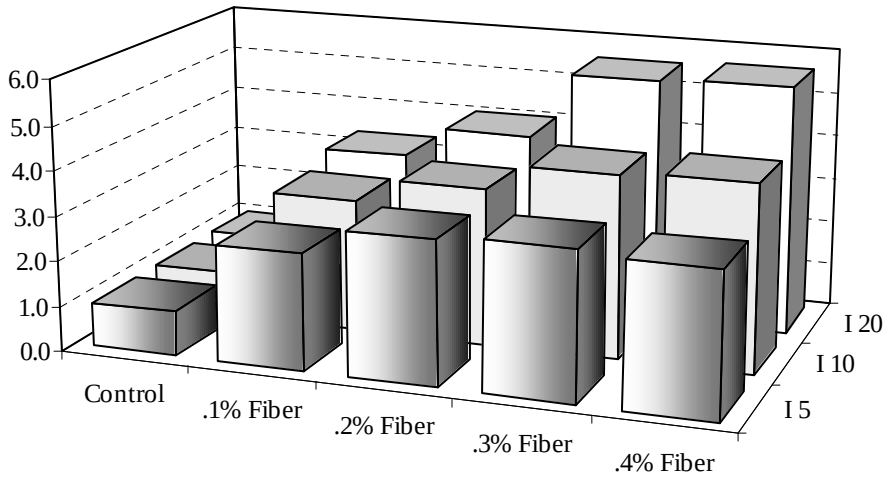

Figure 4.3 Toughness Index

4.5 Fatigue

The fatigue data are shown in Table 4.5. As it can be seen from this Table there is significant variability in fatigue data. However it should be considered that different batch mixtures are included in this table and extensive analysis were undertaken in the fatigue analysis presented in Chapter 6.

Table 4.5 Fatigue Data

TYPE	Slump (in / sec)	AC (%)	UW (pcf)	MOR (psi)	Flexural Stress	STRESS LEVEL	CYCLE ACHIEVED
PL2-1	0.9"	6.2	148.8	868	429	0.49	2,500,000 +
PL1-2	1.38"	5.6	147.8	868	512	0.59	2,255,889
PL2-2	1.38"	5.6	147.8	868	512	0.59	7,000,000 +
PL1-4	0.75"	5.5	151.8	868	510	0.59	1,463,439
PL2-4	0.75"	5.5	151.8	868	511	0.59	2,559,621
PL3-4	0.38"	4.5	148.8	868	516	0.59	2,897,652
PL1-3	1.75"	6.5	144.8	868	598	0.69	502,602
PL2-3	1.75"	6.5	144.8	868	598	0.69	817,372
PL3-3	1.75"	6.5	144.8	868	599	0.69	484,395
1F1-1	0.75" /15sec	5.5	146.8	970	465	0.48	2,500,000 +
1F3-1	0.38" / 18sec	5.4	146.8	970	475	0.49	3,000,000 +
1F1-2	1" / 10sec	5.2	149.8	970	573	0.59	2,385,829
1F2-2	1" / 10sec	5.2	149.8	970	572	0.59	512,852
1F3-2	1" / 10sec	5.2	149.8	970	572	0.59	1,413,298
1F1-3	3/8" / 18sec	5.4	146.8	970	669	0.69	250,348
1F2-3	3/8" / 18sec	5.4	146.8	970	669	0.69	907,577
1F3-3	1" / 10sec	5.2	149.8	970	670	0.69	553,080
1F1-4	1" / 10sec	6	148.8	970	568	0.59	545,691
1F2-4	1" / 10sec	6	148.8	970	572	0.59	375,918
1F3-4	1" / 10sec	5.7	148.8	970	571	0.59	552,290
2F1-1	0" / 19sec	5.0	145.8	981	478	0.49	6,000,000 +
2F2-1	0" / 19sec	5.0	145.8	981	482	0.49	2,500,000 +
2F1-2	0.75" / 11sec	6	147.8	981	579	0.59	790,351
2F2-2	0.75" / 11sec	6	147.8	981	579	0.59	1,279,506
2F3-2	0.75" / 11sec	6	147.8	981	579	0.59	1,328,193
2F4-2	0.75" / 11sec	6	147.8	981	580	0.59	2,096,039

2F1-3	¼ "/ 21sec	5.8	145.8	981	677	0.69	69,175
2F2-3	¼ "/ 21sec	5.8	145.8	981	677	0.69	121,989
2F3-3	¼ "/ 21sec	5.8	145.8	981	674	0.69	118,194
2F1-4	0.75" / 9sec	5.7	148.8	981	582	0.59	524,558
2F2-4	0.75" / 9sec	5.7	148.8	981	582	0.59	612,446
3F1-1	1" / 11sec	5.8	147.8	1,017	500	0.49	1,450,101
3F2-1	1" / 11sec	5.8	147.8	1,017	498	0.49	1,097,318
3F4-2	1.5" / 9sec	7.5	143.8	1,017	499	0.49	3,303,710
3F1-2	1 ½ " / 9sec	7.5	143.8	1,017	600	0.59	268,403
3F2-2	1 ½ " / 9sec	7.5	143.8	1,017	600	0.59	301,809
3F3-2	1 ½ " / 9sec	7.5	143.8	1,017	600	0.59	332,002
3F4-3	0 / 21sec	4.5	145.8	1,017	600	0.59	311,153
3F1-3	0" / 21sec	4.5	145.8	1,017	703	0.69	301,626
3F2-3	0" / 21sec	4.5	145.8	1,017	703	0.69	310,575
3F3-3	0" / 21sec	4.5	145.8	1,017	702	0.69	415,136
4F1-1	0" / 24sec	5.8	143.8	980	479	0.49	1,773,437
4F2-1	0" / 24sec	5.8	143.8	980	484	0.49	2,500,000 +
4F1-2	5/8" / 12sec	6.1	146.8	980	578	0.59	624,844
4F2-2	5/8" / 12sec	6.1	146.8	980	578	0.59	1,190,832
4F3-2	5/8" / 12sec	6.1	146.8	980	578	0.59	603,543
4F4-2	5/8" / 12sec	6.1	146.8	980	585	0.59	1,519,651
4F1-3	¼ " / 21sec	5.4	145.8	980	676	0.69	14,900
4F2-3	¼ " / 21sec	5.4	145.8	980	676	0.69	189,962
4F3-3	¼ " / 21sec	5.4	145.8	980	676	0.69	214,951

* AC = Air Content, UW = Unit Weight, MOR = Modulus of Rupture
* 1 Psi = 6.89 kPa

4.6 Field Data

4.6.1 NDT (Non Destructive Test)

As it can be seen in Table 4.6 and Figure 4.4 the Non Destructive Test Results using a V-meter (ultrasonic pulse velocity method) were obtained both in the laboratory and the field. The static modulus of elasticity for the lab test was obtained by three replicates of 6″x12″ cylinder after 28 days. The dynamic modulus of elasticity for the lab test was obtained by 3 replicates of 6″x6″x21″ beam after 100 days. The beams were tested for longitudinal resonance according to ASTM C 215. The average values for the static and dynamic modulus of elasticity obtained in the lab testing are in the order of 4,004,395 Psi., and 6,611,556 Psi., respectively. The dynamic modulus of elasticity for the field test was obtained by four repeated measurements. Due to the pavement condition NDT was performed for the transverse resonance in each section and the dynamic modulus was corrected with a correction factor. The average field dynamic modulus of elasticity was 5,000,000 Psi.

Table 4.6 Non Destructive Test Results

	Type	Section	CV, %	Modulus (psi)	Sample Size
$E_{Static\ lab}$	Plain	1	1.2	3,966,614	6"x 6 "x21"
	FB	2	1.8	4,145,537	6"x 6 "x21"
	LS	3	1.3	3,901,034	6"x 6 "x21"
$E_{Dynamic\ Lab}$	Plain	1	0.6	6,847,667	6"x 6 "x21"
	FB	2	1.8	6,343,000	6"x 6 "x21"
	LS	3	3.5	6,644,000	6"x 6 "x21"
$E_{Dynamic\ Field}$	Plain	1	-	5,100,000	
	FB	2	-	5,300,000	
	LS	3	-	4,600,000	

* FB = Fiber Reinforced Concrete (0.1% fiber content)
LS = Low Shrinkage Concrete (#357)
CV = Coefficient of variation, Sample Size n = 3
E static Lab = Lab static modulus of elasticity, 28 Days
E Dynamic Lab = Lab dynamic modulus of elasticity, 28 Days + 70 F (72 Days)
E Dynamic Field = Field dynamic modulus of elasticity, After 2 months age

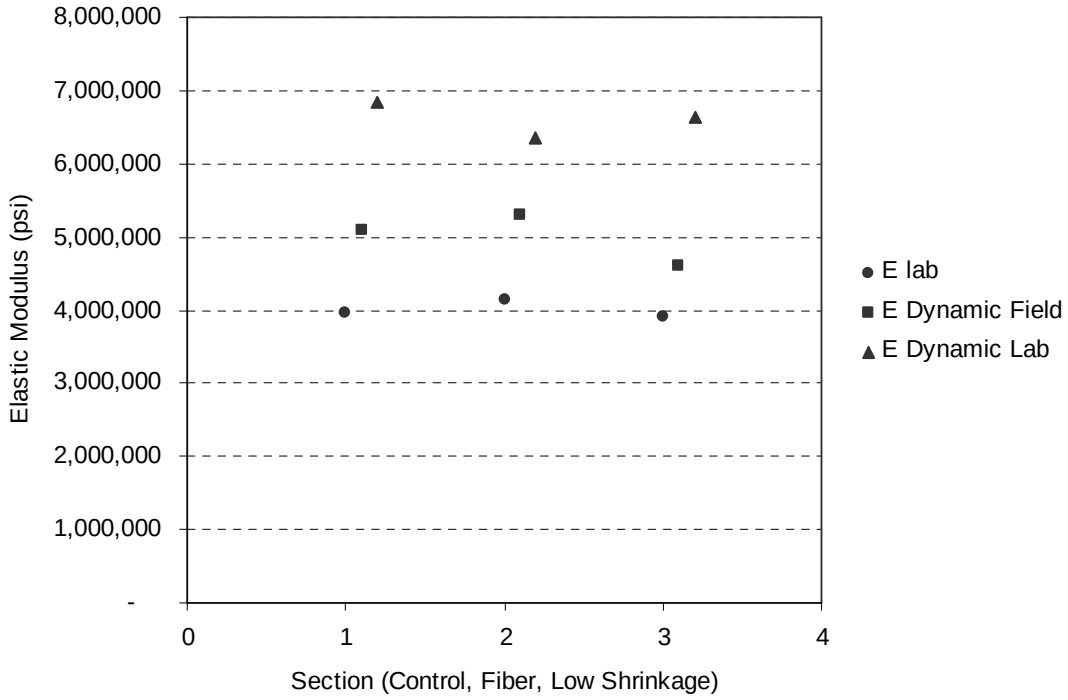

Figure 4.4 Non Destructive Test Results

* E Lab = Lab static modulus of elasticity, 28 Days
E Dynamic Lab = Lab dynamic modulus of elasticity, 28 Days + 70 F (72 Days)
E Dynamic Field = Field dynamic modulus of elasticity, After 2 months age

The equations describing the relationship between the static and dynamic modulus of elasticity for the fiber reinforced concrete and low shrinkage mix are obtained here:

For the fiber reinforced concrete mix the equation is

$$E_{static} = (3E+07) - 3.3868\, E_{dynamic}$$

The R^2 for this model was equal to 0.90. However, it has to be considered that any such relationship is valid only for the specific concrete mix.

For the low shrinkage mix the equation is

$$E_{static} = (4E+06) + 0.0465\, E_{dynamic}$$

The R^2 for this model was equal to 0.99. However, it has to be considered that any such relationship is valid only for the specific concrete mix.

4.6.2 Deflection & Surface Strain

As it is shown in Figure 4.5 (including two data point for the two replicate sections constructed for each mix) the edge pass average deflection in the middle position of the control, fiber, and low shrinkage sections is in the order of 0.00338 inch, 0.00119, and 0.00348 inch respectively for the single axle load. The inner pass average deflection in the middle position of the control, fiber, and low shrinkage sections for the single axle load is in the order of 0.00175 inch, 0.00101 inch, and 0.00152 inch respectively. In Figure 4.6 the edge pass average deflection in the middle position of the control, fiber, and low shrinkage sections for the tandem axle load is in the order of 0.00700 inch, 0.00452 inch, and 0.00742 inch respectively. The inner pass average deflection in middle position of the control, fiber, and low shrinkage sections for the tandem axle load is in the order of 0.00313 inch, 0.00125 inch, and 0.00289 inch respectively

The average strain data are presented in Figure 4.7, 4.8. In Figure 4.7 the average strain data for single axle load at the edge pass in all three sections are presented. The strain at the edge pass location for the control, fiber, low shrinkage sections is in the order of -19 μs, -19 μs, and -27μs respectively. The strain at the 24” location for the control, fiber, low shrinkage sections is in the order of - 16 μs, -17 μs, and -18 μs respectively. The strain at the 48” location for the control, fiber, low shrinkage sections is in the order of - 9 μs, -10 μs, and -9 μs respectively. The edge pass

average strain trend is consistent with the inner pass average strain trend. In Figure 4.8 the average strain at the edge pass location for the control, fiber, low shrinkage sections for the tandem axle load is in the order of -17 μs, -16 μs, and -25 μs respectively. The average strain at the 24" location for the control, fiber, low shrinkage sections is in the order of -11 μs, -13 μs, and -18 μs respectively. The average strain at the 48" location for the control, fiber, low shrinkage sections is in the order of -9 μs, -10 μs, and -8 μs respectively. The edge pass average strain trend is consistent with the inner pass average strain trend.

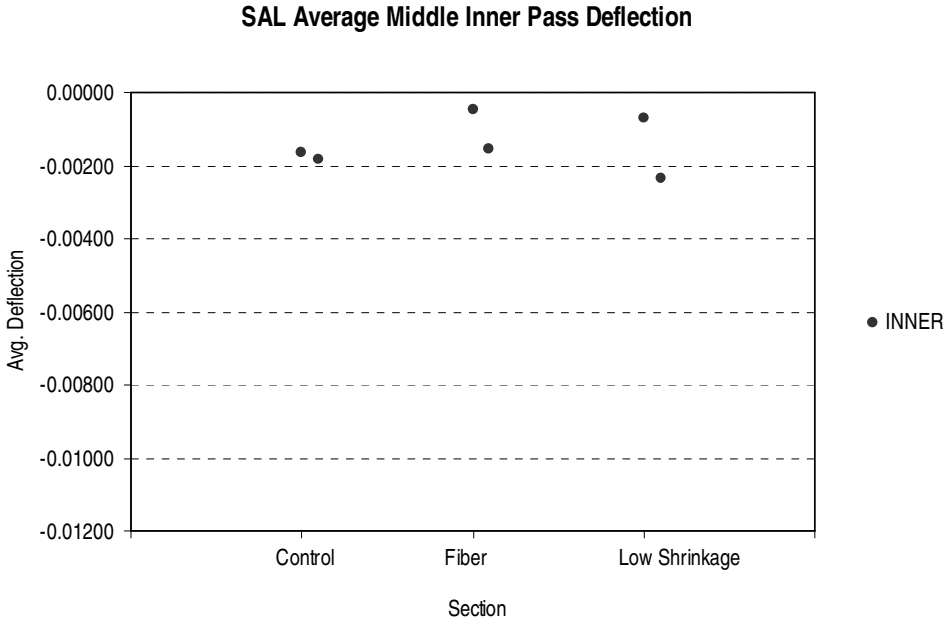

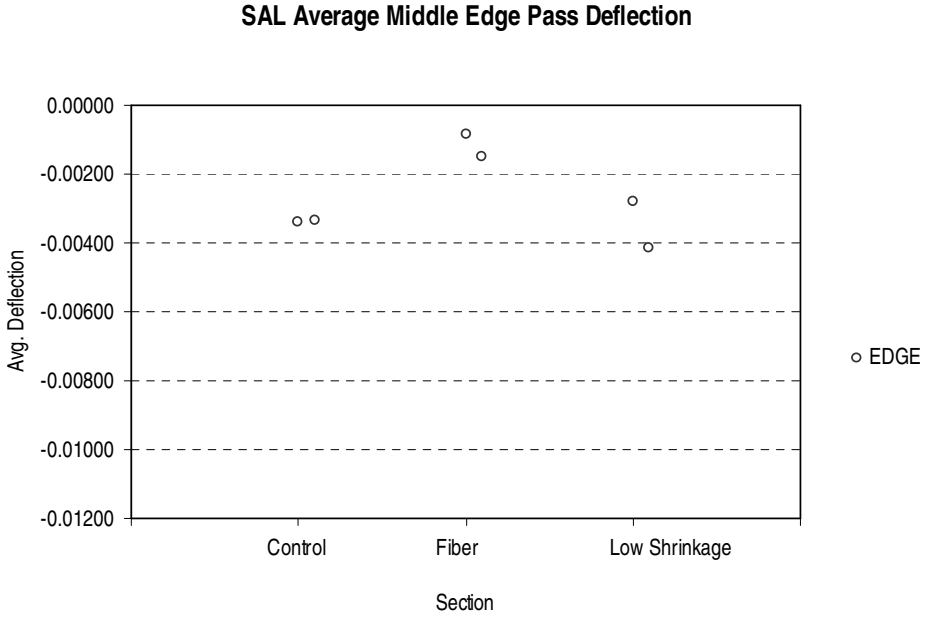

Figure 4.5 Average Middle Deflection for Single Axle Load Testing

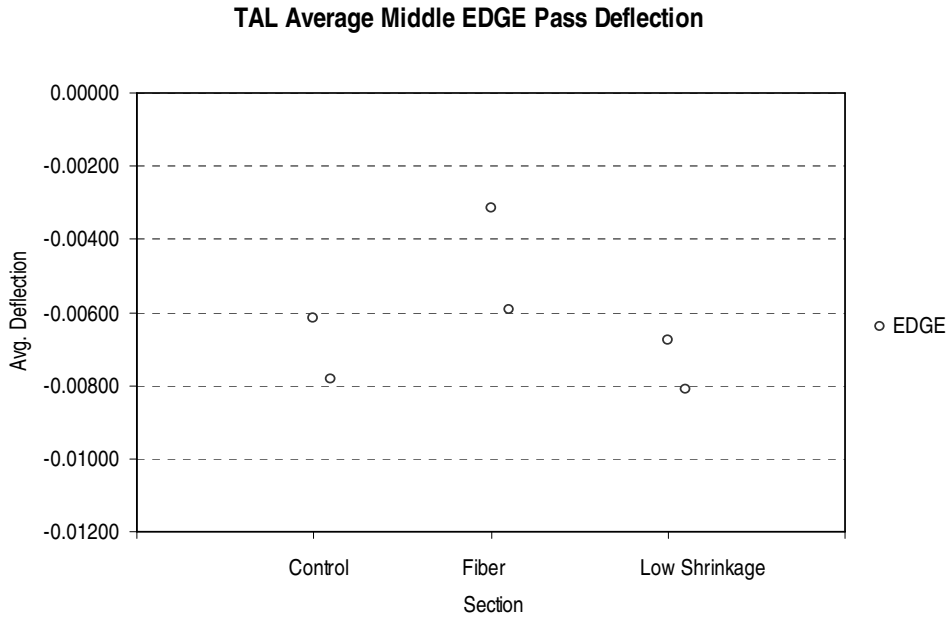

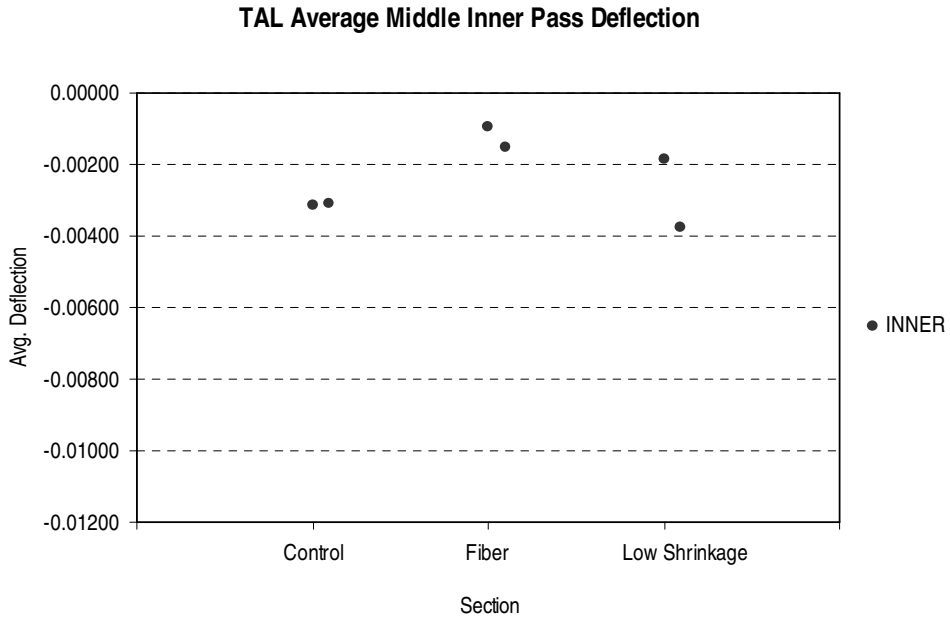

Figure 4.6 Average Middle Deflection for Tandem Axle Load Testing

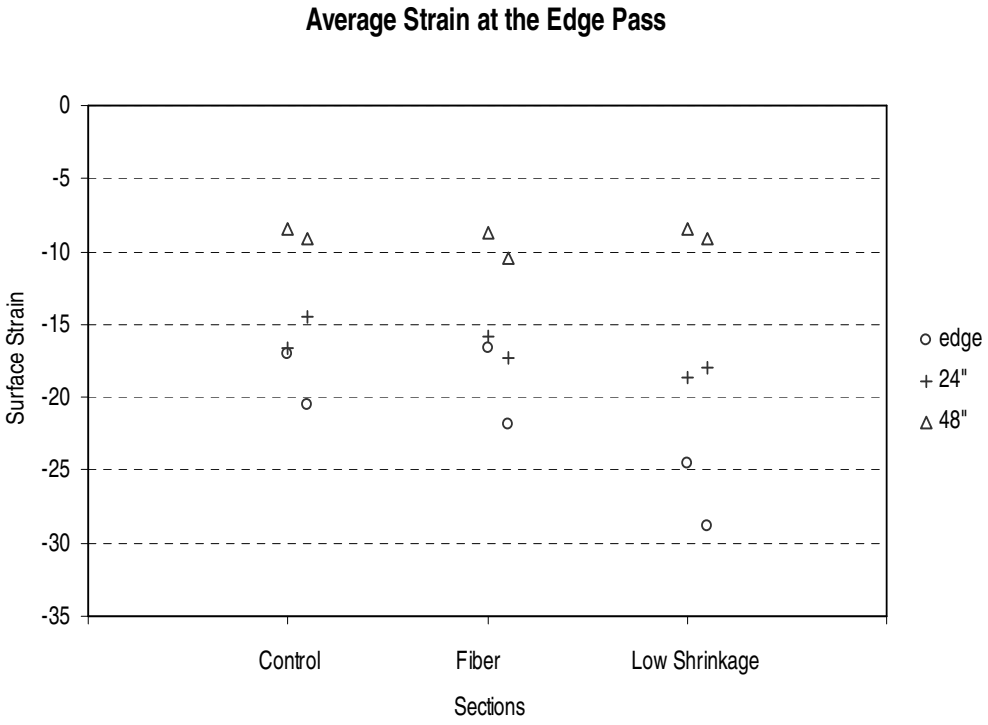

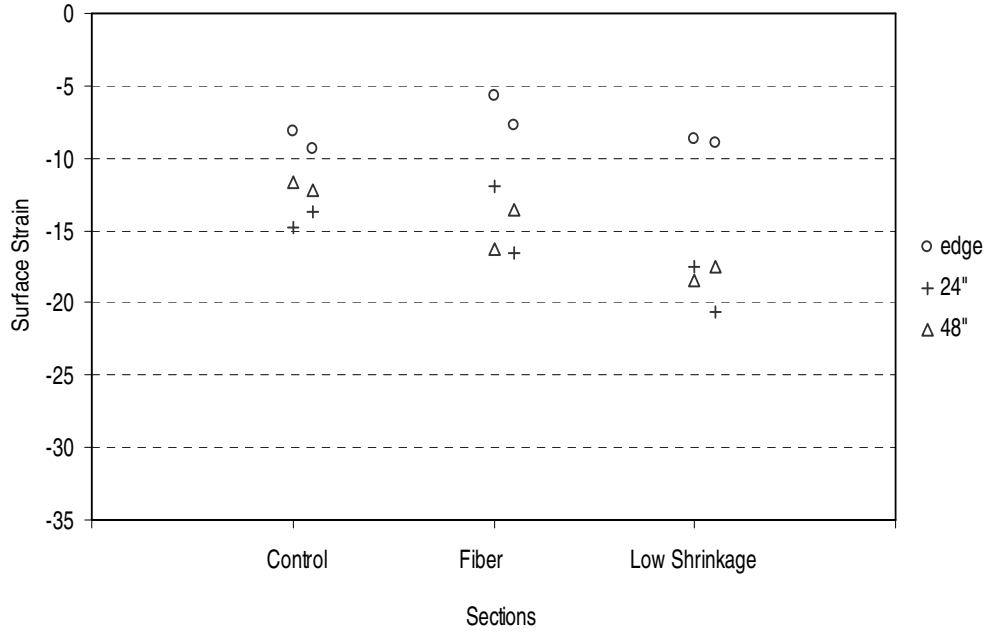

Figure 4.7 Average Strain for the Single Axle Load Test Results

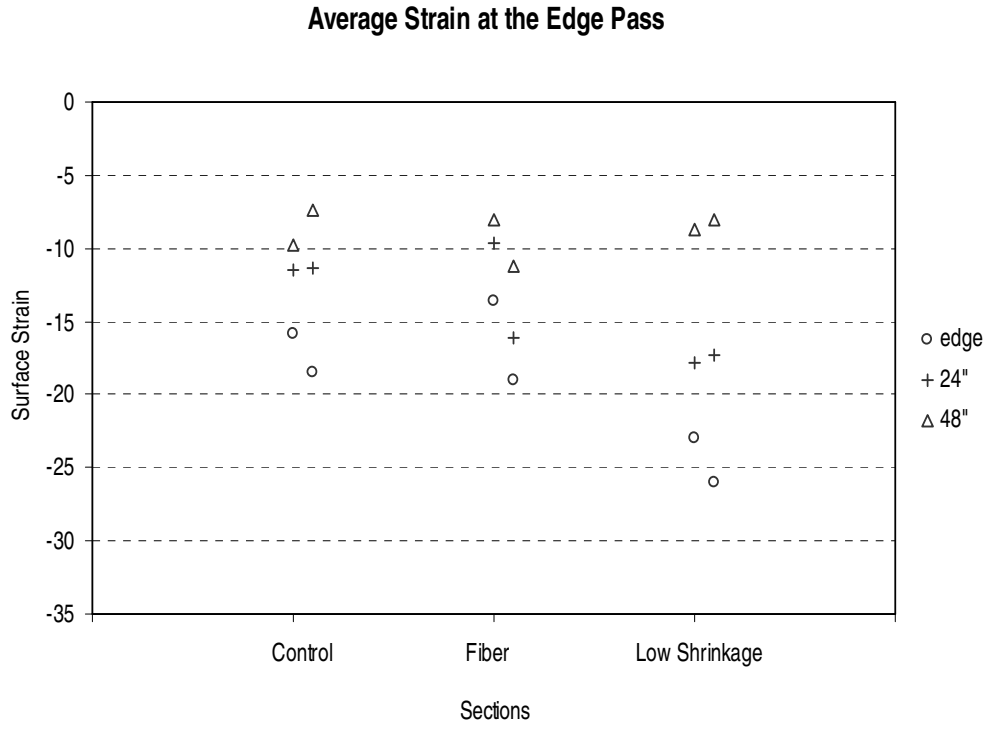

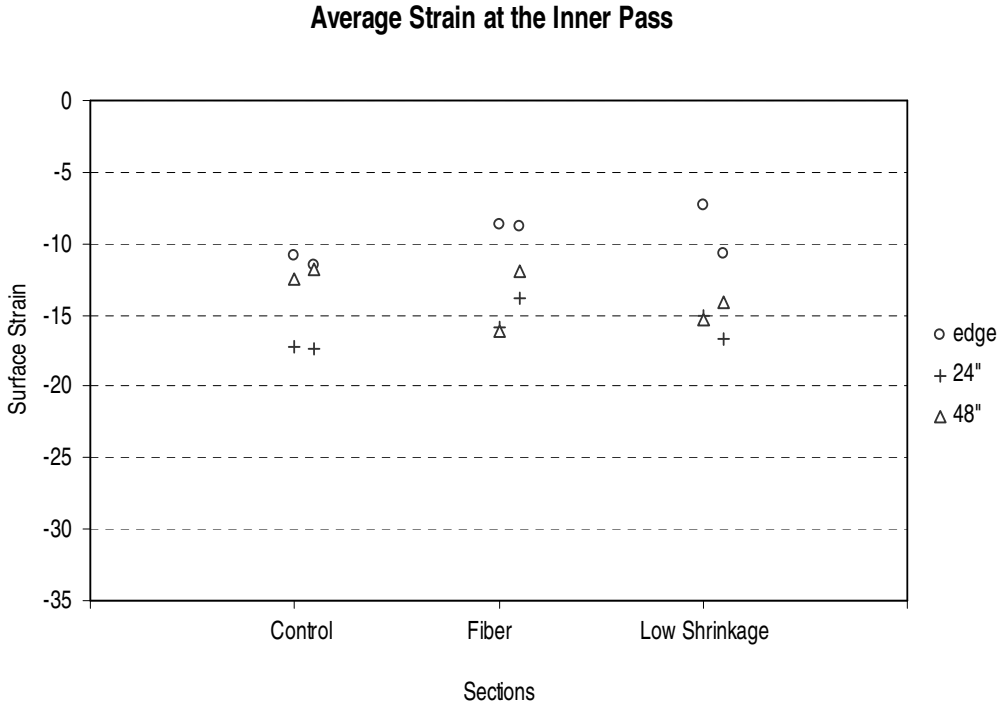

Figure 4.8 Average Strain for the Tandem Axle Load Test Results

CHAPTER 5 FATIGUE

5.1 Introduction

This investigation used ¾-in-long polypropylene fibers. The characteristics for the polypropylene fibers were shown in Chapter 3. The mixtures were prepared using a blend of Type I Portland cement with NewCem as described in Chapter 3, #57 aggregate from Havre De Grace Quarry in Maryland, natural sand, and a middle and high range water reducer admixtures, respectively Daracem 55 and ADVA FLOW for meeting flow/slump requirements, and an air-entraining agent, Daravair 1000.

For the fatigue test, a total of 53 beams of 102 x 102 x 356 mm. (4 x 4 x 14 in.) were cast, 12 for plain concrete , and 41 for 0.1 % fiber, 0.2 % fiber, 0.3 % fiber, and 0.4 % fiber concrete mixtures. The specimens were cast in molds immediately after mixing and then covered with a plastic sheet and cured for 24 hours at room temperature. They were then de-molded and immersed in a water bath for 28days. All the sample properties for fatigue testing are shown in Table 5.1. Since disposable wood molds were used some sample size variability was observed.

Table 5.1 Sample Properties for Fatigue Test Samples.

TYPE	Slump (in / sec)	Air Content (%)	Unit Weight (pcf)	B (in)	D (in)
PL1-1	0.9"	6.2	148.8	4.0	4.0
PL2-1	0.9"	6.2	148.8	3.9	3.9
PL1-2	1.75"	6.5	144.8	4.0	4.1
PL2-2	1.75"	6.5	144.8	4.0	4.1
PL3-2	1.75"	6.5	144.8	3.9	4.1
PL1-3	1.38"	5.6	147.8	4.0	4.1
PL2-3	1.38"	5.6	147.8	4.0	4.0
PL3-3	1.38"	5.6	147.8	4.2	4.2
PL4-3	1.38"	5.6	147.8	4.0	4.0
PL3-4	0.38"	4.5	148.8	4.0	4.0
PL1-5	0.75"	5.5	151.8	4.2	4.1
PL2-5	0.75"	5.5	151.8	4.3	4.1
1F1-1	0.75 / 15	5.5	146.8	4.1	4.0
1F1-2	3/8" / 18	5.4	146.8	4.0	4.1
1F2-2	3/8" / 18	5.4	146.8	3.9	4.0
1F3-2	0.38 / 18	5.4	146.8	4.1	4.1
1F1-3	1" / 10	5.2	149.8	4.0	4.1
1F2-3	1" / 10	5.2	149.8	4.0	4.0
1F3-3	1" / 10	5.2	149.8	3.9	4.1
1F4-3	1" / 10	5.2	149.8	4.0	4.1
1F3-4	1" / 10	5.7	148.8	4.1	4.1
1F1-5	1" / 10	6	148.8	4.2	4.1
1F2-5	1" / 10	6	148.8	4.3	4.1
2F1-1	0" / 19	5.0	145.8	3.8	4.1
2F2-1	0" / 19	5.0	145.8	4.0	4.1
2F1-2	1/4"/ 21	5.8	145.8	3.9	4.1
2F2-2	1/4"/ 21	5.8	145.8	4.0	4.0
2F3-2	1/4"/ 21	5.8	145.8	3.9	4.1
2F1-3	0.75" / 11	6	147.8	3.9	4.2
2F2-3	0.75" / 11	6	147.8	4.0	4.1
2F3-3	0.75" / 11	6	147.8	4.1	4.1
2F4-3	0.75" / 11	6	147.8	3.9	4.1
2F1-5	0.75" / 9	5.7	148.8	4.0	4.1
2F2-5	0.75" / 9	5.7	148.8	4.1	4.0

TYPE	Slump (in / sec)	Air Content (%)	Unit Weight (pcf)	B (in)	D (in)
3F1-1	1" / 11	5.8	147.8	3.9	4.1
3F2-1	1" / 11	5.8	147.8	4.0	4.1
3F1-2	0" / 21	4.5	145.8	3.9	4.1
3F2-2	0" / 21	4.5	145.8	4.0	4.0
3F3-2	0" / 21	4.5	145.8	4.0	4.1
3F4-2	0 / 21	4.5	145.8	3.8	4.1
3F1-3	1 1/2" / 9	7.5	143.8	4.0	4.0
3F2-3	1 1/2" / 9	7.5	143.8	4.1	4.1
3F3-3	1 1/2" / 9	7.5	143.8	3.9	4.1
3F4-3	1.5" / 9	7.5	143.8	4.0	4.1
4F1-1	0" / 24	5.8	143.8	3.8	4.1
4F2-1	0" / 24	5.8	143.8	4.0	4.0
4F1-2	1/4" / 21	5.4	145.8	3.8	4.1
4F2-2	1/4" / 21	5.4	145.8	3.9	4.1
4F3-2	1/4" / 21	5.4	145.8	3.8	4.1
4F1-3	5/8" / 12	6.1	146.8	4.1	4.1
4F2-3	5/8" / 12	6.1	146.8	4.0	4.1
4F3-3	5/8" / 12	6.1	146.8	4.0	4.2
4F4-3	5/8" / 12	6.1	146.8	4.0	4.1

Note:
1F1-1 = 0.1% FRC Sample 1 Batch 1
2F2-3 = 0.2% FRC Sample 2 Batch 3
B = Width of Sample cross section, D = Depth of Sample cross section
1 in. = 25.4 mm.

5.2 Fatigue Testing

Third point loading was used in the flexural fatigue strength test. D uring the testing the sample from support to support was 305 mm (12 in). The machine used for this test was a Material Test System (MTS). The machine was operated in stress control mode.

A sine waveform load (20 Hz, No rest Period) was used simulating the actual field loading conditions in pavements from a moving vehicle. The fatigue behavior

was expressed in terms of the applied flexural stress (as a percentage of the static flexural strength S) versus the number of load cycles to failure N.

In order to evaluate the effects of fibrillated polypropylene FRC on fatigue and evaluate potential benefits as compared to conventional concrete, beams with plain concrete and fiber reinforced concrete with 0.1 %, 0.2 %, 0.3 % and 0.4 % fiber content by volume were prepared and tested in flexural fatigue. Three replicates were tested at each stress level of 0.49, 0.59, and 0.69.

5.2.1 Individual FFS-N Curve

Individual "Flexural Fatigue Stress versus Number of Cycles" (FFS-N) curves were created based on 3 replicates in each stress level for plain concrete and 0.1 %, 0.2 %, 0.3 %, and 0.4 % fiber reinforced concrete. In Figure 5.1, flexural fatigue stress vs. number of cycles is presented for plain PCC. The graph illustrates the results for plain concrete with 2 flexural fatigue stresses with 0.59 and 0.69 vs. number of cycles of failure. Since at low stress level (0.49), most of the samples exceeded 2.5 million cycles without significant damage, and these data were not considered in the analysis. The relationship between N and applied stress for the plain concrete provided a high R^2=0.86. The large variability in testing results has an implication on the coefficient of correlation (R^2) for the linear model. For the large variance, statistical analysis needs to be undertaken for further examining the experimental data.

In Figure 5.2, the graph for the 0.1 % fiber reinforced concrete is presented with 2 flexural fatigue stress levels of 0.59 and 0.69. Again, at low stress level, 0.49, most of the samples exceeded 2.5 million cycles without significant damage. One

significant parameter on this graph is that data from two different batches were used for the 0.59 flexural fatigue stress testing. A large difference in number of load applications to failure, N, was observed between the two batches. For the first batch N was about 1,500,000 cycles and for the second batch N was of the order of 500,000 cycles. So the analysis considered the mixtures that have similar material properties such as, slump, air content, and unit weight, see Table 5.2. The relationship between N and applied stress for 0.1 % fiber reinforced concrete provided a low R^2=0.35. The adequacy of the data was further examined with statistical analysis as indicated in a follow up section.

In Figure 5.3, the graph for the 0.2 % fiber reinforced concrete is presented with two flexural fatigue stress level 0.59 and 0.69. The samples from the 0.49 stress level were not considered since they exceeded 2.5 million cycles to failure without significant damage. Data from two different batches were used for the 0.59 flexural fatigue stress level testing. A large difference in N was observed between the two batches. For the first batch N was about 1,350,000 cycles and for the second batch N was of the order of 600,000 cycles. So analysis was performed with the first batch because its mixture properties such as slump, air content and unit weight were close to the target mixture properties. The relationship between N and applied stress for the 0.2 % fiber reinforced concrete showed a R^2=0.94.

Figure 5.4 illustrates the results for the 0.3 % fiber reinforced concrete. Data from two different batches were used for the 0.49 flexural fatigue stress level testing. A large difference in N was observed between the two batches. For the first batch N was about 1,2500,000 cycles and for the second batch N was of the order of

3,000,000 cycles. So analysis was performed with the first batch because it's mixture properties such as slump, air content and unit weight were close to the target mixture properties. The relationship between N and applied stress for the 0.3% fiber reinforced concrete showed a R^2=0.57. The fatigue results indicate that at high flexural fatigue stresses there is no benefit in fatigue (about the same number of cycles to failure observed). This implies that polypropylene fiber is not effective at high fatigue stresses for the 0.3% fiber reinforced case.

Figure 5.5 illustrates the results for the 0.4% fiber reinforced concrete. The relationship between N and applied stress for the 0.4% fiber reinforced concrete showed a R^2=0.68. The fatigue results for the 0.4 % fiber reinforced concrete is shown, providing a good linear relationship. The sample characteristics and N are presented in Table 5.2

Table 5.2 Fatigue Results and Testing Variability

TYPE	Slump (in/sec)	AC (%)	UW (pcf)	STRESS LEVEL	CYCLE ACHIEVED	CV (%)
PL2-1	0.9"	6.2	148.8	0.49	2,500,000 +	
PL1-1	0.9"	6.2	148.8	0.59	584059*	
PL1-3	1.38"	5.6	147.8	0.59	2,255,889	
PL2-3	1.38"	5.6	147.8	0.59	7,000,000 +	
PL3-3	1.38"	5.6	147.8	0.59	362613*	
PL4-3	1.38"	5.6	147.8	0.59	379312*	
PL1-5	0.75"	5.5	151.8	0.59	1,463,439	
PL2-5	0.75"	5.5	151.8	0.59	2,559,621	
PL3-4	0.38"	4.5	148.8	0.59	2,897,652	27
PL1-2	1.75"	6.5	144.8	0.69	502,602	
PL2-2	1.75"	6.5	144.8	0.69	817,372	
PL3-2	1.75"	6.5	144.8	0.69	484,395	31
1F1-1	0.75 / 15	5.5	146.8	0.48	2,500,000 +	
1F3-2	0.38 / 18	5.4	146.8	0.49	3,000,000 +	
1F1-3	1" / 10	5.2	149.8	0.59	2,385,829	
1F2-3	1" / 10	5.2	149.8	0.59	512,852	
1F3-3	1" / 10	5.2	149.8	0.59	1,413,298	
1F1-5	1" / 10	6	148.8	0.59	545691**	
1F2-5	1" / 10	6	148.8	0.59	375918**	
1F3-4	1" / 10	5.7	148.8	0.59	552290**	36
1F1-2	3/8" / 18	5.4	146.8	0.69	250,348	
1F2-2	3/8" / 18	5.4	146.8	0.69	907,577	
1F4-3	1" / 10	5.2	149.8	0.69	553,080	58
2F1-1	0" / 19	5.0	145.8	0.49	6,000,000 +	
2F2-1	0" / 19	5.0	145.8	0.49	2,500,000 +	
2F1-3	0.75" / 11	6	147.8	0.59	790,351	
2F2-3	0.75" / 11	6	147.8	0.59	1,279,506	
2F3-3	0.75" / 11	6	147.8	0.59	1,328,193	
2F4-3	0.75" / 11	6	147.8	0.59	2,096,039	
2F1-5	0.75" / 9	5.7	148.8	0.59	524558**	
2F2-5	0.75" / 9	5.7	148.8	0.59	612446**	39
2F1-2	1/4"/ 21	5.8	145.8	0.69	69,175	
2F2-2	1/4"/ 21	5.8	145.8	0.69	121,989	
2F3-2	1/4"/ 21	5.8	145.8	0.69	118,194	29
3F1-1	1" / 11	5.8	147.8	0.49	1,450,101	
3F2-1	1" / 11	5.8	147.8	0.49	1,097,318	
3F4-3	1.5" / 9	7.5	143.8	0.49	3,303,710	20

TYPE	Slump (in/sec)	AC (%)	UW (pcf)	STRESS LEVEL	CYCLE ACHIEVED	CV (%)
3F1-3	1 1/2" / 9	7.5	143.8	0.59	268,403	
3F2-3	1 1/2" / 9	7.5	143.8	0.59	301,809	
3F3-3	1 1/2" / 9	7.5	143.8	0.59	332,002	
3F4-2	0 / 21	4.5	145.8	0.59	311,153**	11
3F1-2	0" / 21	4.5	145.8	0.69	301,626	
3F2-2	0" / 21	4.5	145.8	0.69	310,575	
3F3-2	0" / 21	4.5	145.8	0.69	415,136	18
4F1-1	0" / 24	5.8	143.8	0.49	1,773,437	
4F2-1	0" / 24	5.8	143.8	0.49	2,500,000 +	
4F1-3	5/8" / 12	6.1	146.8	0.59	624,844	
4F2-3	5/8" / 12	6.1	146.8	0.59	1,190,832	
4F3-3	5/8" / 12	6.1	146.8	0.59	603,543	
4F4-3	5/8" / 12	6.1	146.8	0.59	1,519,651	46
4F1-2	1/4" / 21	5.4	145.8	0.69	14,900	
4F2-2	1/4" / 21	5.4	145.8	0.69	189,962	
4F3-2	1/4" / 21	5.4	145.8	0.69	214,951	78

Note :
UW = Unit Weight, AC = Air Content
CV = Coefficient of Variation
* Testing failure
** Different Batches
Unit: 1 lbs/ft^3 = 16 kg/m^3

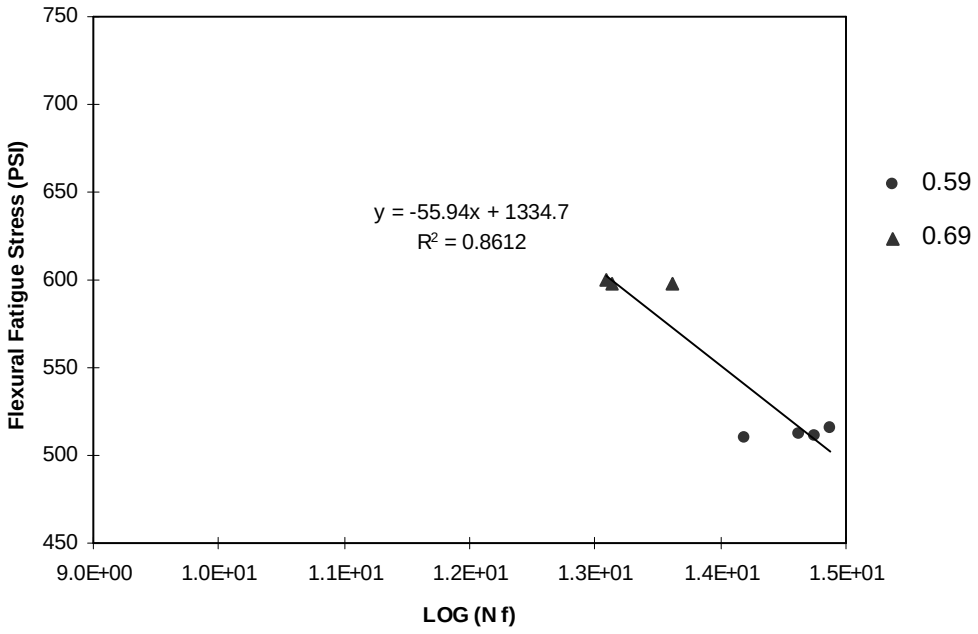

Figure 5.1 FFS-N for Plain Concrete

Units : 100 Psi = 0.69 mPa

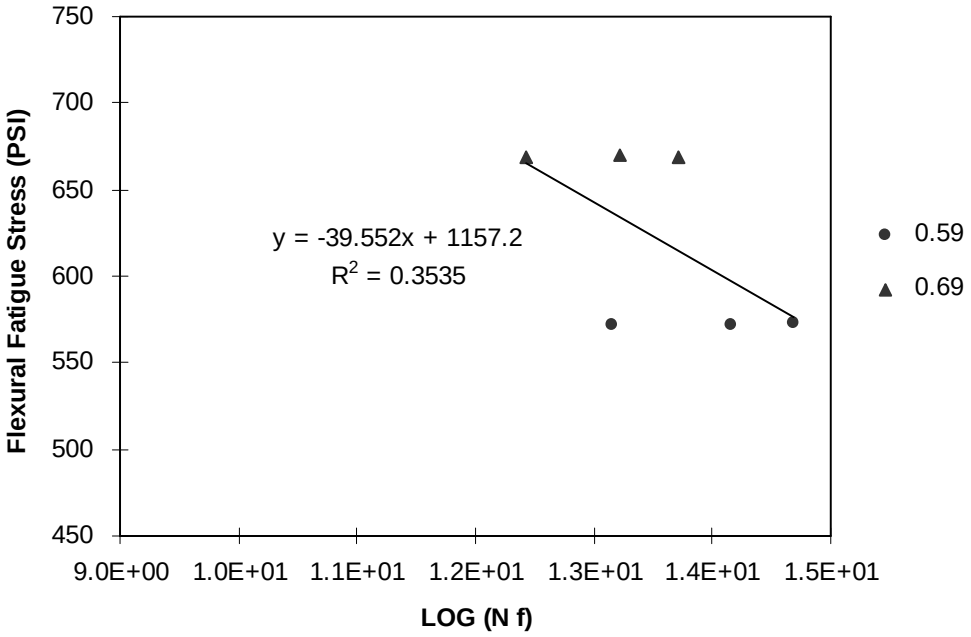

Figure 5.2 FFS-N for 0.1 % Fiber Reinforced Concrete

Units : 100 Psi = 0.69 mPa

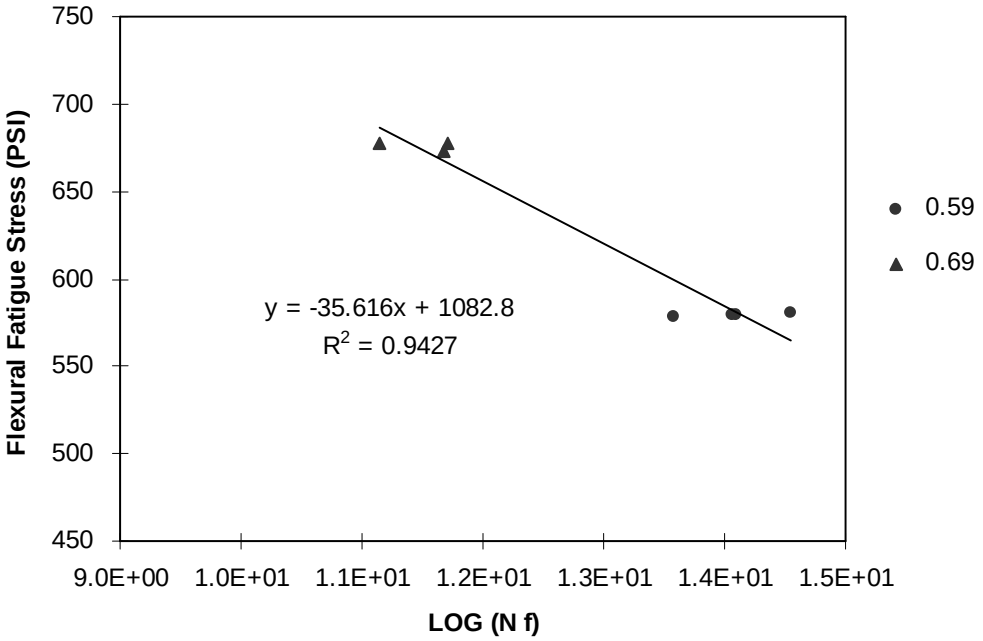

Figure 5.3 FFS-N for 0.2 % Fiber Reinforced Concrete

Units : 100 Psi = 0.69 mPa

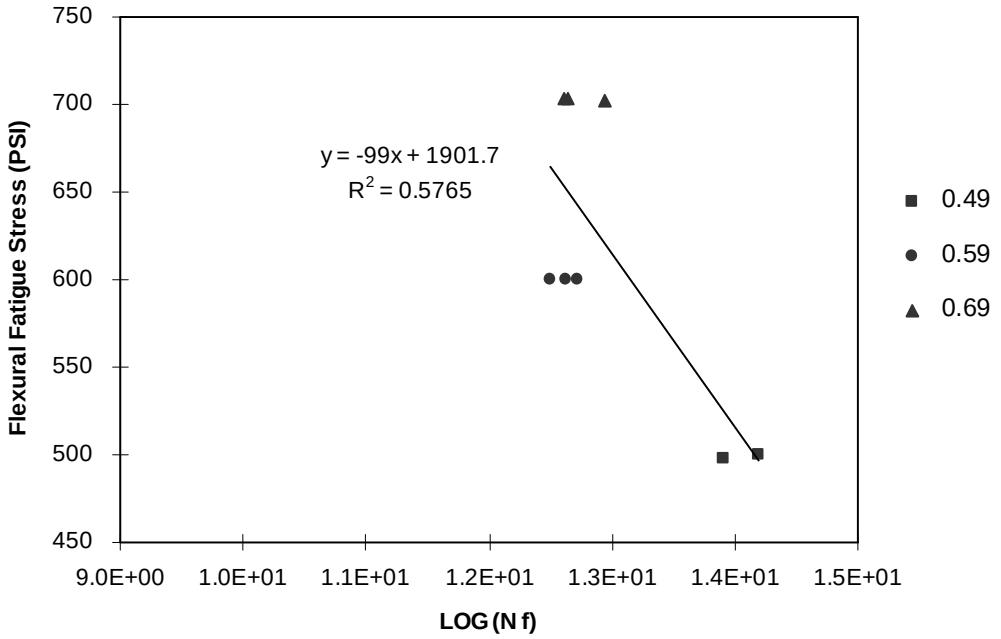

Figure 5.4 FFS-N for 0.3 % Fiber Reinforced Concrete

Units : 100 Psi = 0.69 mPa

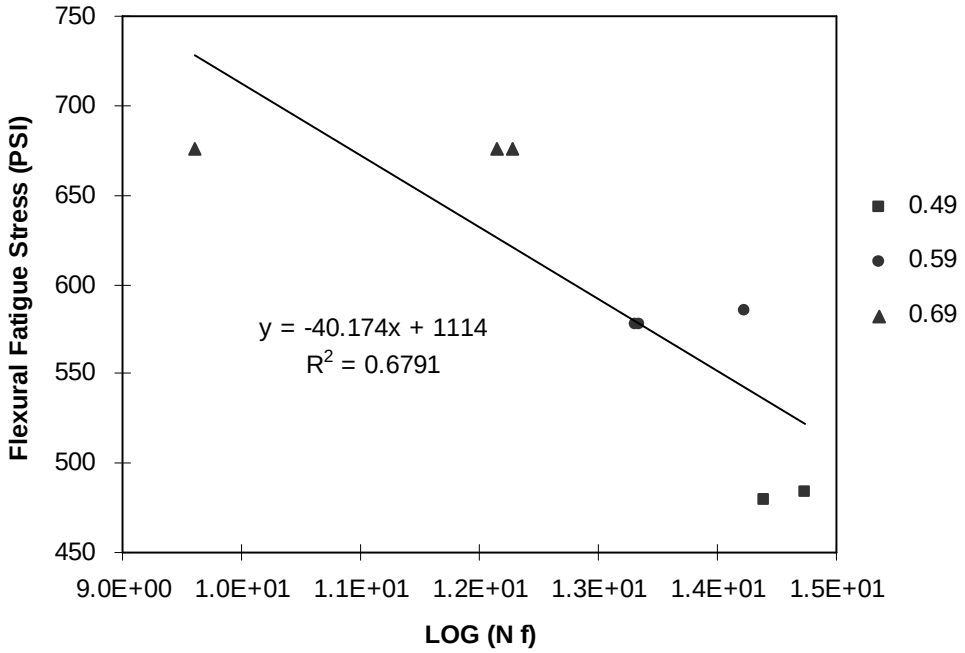

Figure 5.5 FFS-N for 0.4 % Fiber Reinforced Concrete

Units : 100 Psi = 0.69 mPa

5.2.2 Combined FFS-N Curve

The relationship of Flexural Fatigue Stress (FFS) vs. Number of Cycles (N) for plain concrete and the fiber reinforced concrete with 0.1 %, 0.2 %, 0.3 %, and 0.4 % fiber content by volume are shown in Figure 5.6. In this graph, the 0.1 % fiber reinforced concrete provides an advantage, in terms of fatigue, over the remaining mixtures. Because the 2 million cycle limit is chosen to approximate the life span of a structure that may typically be subjected to fatigue loading, such as a bridge deck or a highway pavement (as indicated by M. Nagabhushanam et. al., TRR 1226), from Figure 5.6 it can be observed that at 2 million cycles the corresponding flexural fatigue stress for the 0.1%, 0.2%, 0.3% and 0.4% FRC concrete was in the order of 3999 kPa (580 psi), 3792 kPa (550 psi), 3654 kPa (530 psi), 3516 kPa (510 psi). This indicates that the 0.1% fiber reinforced concrete provides a higher fatigue performance among the remaining mixtures.

The linear model based on all the data does not provide strong correlation (R2). Since fatigue results from mixture with different characteristics were grouped together, it seems appropriate to further examine the data with statistical analysis and reviewing mixture characteristics, such as slump, unit weight, and air content.

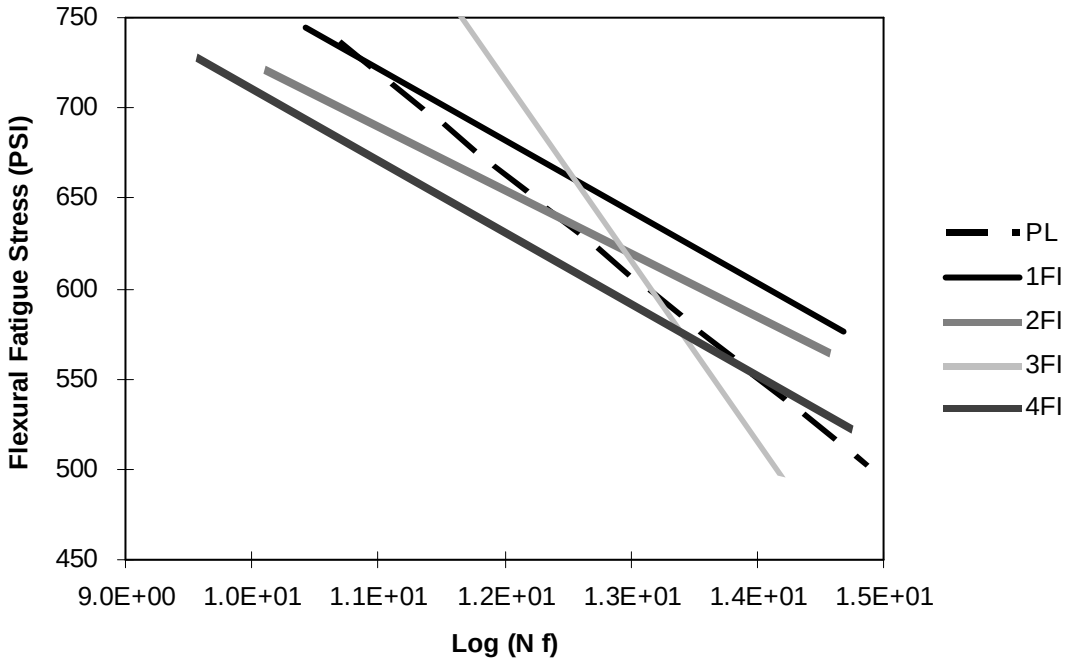

Figure 5.6 FFS-N for Concrete Mixtures

* PL = Plain Concrete, 1F = 0.1% Fiber Reinforced Concrete, 2F = 0.2% Fiber Reinforced Concrete
Units : 100 Psi = 0.69 mPa

5.3 Evaluation of fatigue data for outliers

5.3.1 Introduction

Since the fatigue testing data of concrete show considerable variability due to inherent material variability, testing variability, equipment response and accuracy, the data were examined for identifying potential outliers. Because of the uncertainty associated with estimating the true population mean value of samples, the 95 percent confidence limit was used as a criterion. With this consideration, confident limits were considered in the outlier analysis.

5.3.2 Analysis based on Mix Design Properties

In evaluating the quality of the fatigue data, the mix design properties, such as unit weight, air content, and slump were analyzed for identifying potential outliers. In this analysis, central tendency (μ) and sample variance (σ^2) were used along with the assumption of normal distribution for mixtures properties. As can be seen in Figure 5.7, 5.8, and 5.9, the normal distribution of mix design properties such as unit weight, air content, and slump was obtained by the normality test (Shapiro-Wilk W test) by which we are able to see the distribution of the data set such as unit weight, air content, and slump. According to the normality test, the normal distribution of the mixture properties such as unit weight, air content, and slump was obtained. The confidence interval for 1 standard deviation (1σ), 2 standard deviation (2σ), and 3 standard deviation (3σ) were calculated and used in analyzing the data. Thus, at 1σ from the mean, in either direction, the data should contain 68% of the values of unit weight, air content, and slump. In the same way, at $\mu \pm 2\sigma$ is 95% of the samples and

at $\mu \pm 3\sigma$ is 99% of the samples. Considering a 95% confidence, samples outside the $\mu \pm 2\sigma$ were assured to be outliers. Also Grubbs' test (Z test) for detecting outliers was used to compare the outliers obtained from the samples outside the $\mu \pm 2\sigma$.

In Figure 5.10 the unit weight for concrete mixtures is presented with lines representing 1σ, 2σ, and 3σ. Most of the samples were within $\mu \pm 2\sigma$ 95% of the sample mean except 2 samples PL1-5, PL2-5 of plain concrete. So these 2 samples were considered potential outliers and were removed from the analysis.

In Figure 5.11 the air content concrete mixtures are presented with 1σ, 2σ, and 3σ. Most of the samples were within $\mu \pm 2\sigma$ (95%) of the sample mean except 4 samples 3F1-3, 3F2-3, 3F3-3 and 3F4-3 of 0.3% FRC concrete. So these 4 samples were removed from the analysis.

Similarly, in Figure 5.12 the slump of concrete mixtures are presented with 1σ, 2σ, and 3σ. Most of the samples were within $\mu \pm 2\sigma$ 95% of the samples mean. As it can be seen from Figure 5.12, 3 samples from plain concrete were in the border of the $\mu \pm 2\sigma$ and thus were not excluded from the analysis.

	Sample	SR	UW
1	PL2-1	0.49	148.8
2	PL3-4	0.59	148.8
3	PL1-2	0.59	147.8
4	PL1-4	0.59	151.8
5	PL1-3	0.69	144.8
6	1F1-1	0.48	146.8
7	1F3-1	0.49	146.8
8	1F1-2	0.59	149.8
9	1F3-4	0.59	148.8
10	1F1-4	0.59	148.8
11	1F3-3	0.69	149.8
12	1F1-3	0.69	146.8
13	2F1-1	0.49	145.8
14	2F1-4	0.59	148.8
15	2F1-2	0.59	147.8
16	2F1-3	0.69	145.8
17	3F1-1	0.49	147.8
18	3F4-2	0.49	143.8
19	3F4-3	0.59	145.8
20	3F1-2	0.59	143.8
21	3F1-3	0.69	145.8
22	4F1-1	0.49	143.8
23	4F1-2	0.59	146.8
24	4F1-3	0.69	145.8

Shapiro-Wilk Test for Normality
(Sample Size 50 or Less)

Alpha = 0.05

W= 0.9582

Critical Value = 0.916 (If W < Critical Value, Reject Normality)

Decision: Do Not Reject Normality Hypothesis

Figure 5.7 Normality test for unit weight.

* UW = Unit Weight, SR = Stress Ratio

	Sample	SR	Air Content
1	PL2-1	0.49	6.2
2	PL3-4	0.59	4.5
3	PL1-2	0.59	5.6
4	PL1-4	0.59	5.5
5	PL1-3	0.69	6.5
6	1F1-1	0.48	5.5
7	1F3-1	0.49	5.4
8	1F1-2	0.59	5.2
9	1F3-4	0.59	5.7
10	1F1-4	0.59	6.0
11	1F3-3	0.69	5.2
12	1F1-3	0.69	5.4
13	2F1-1	0.49	5.0
14	2F1-4	0.59	5.7
15	2F1-2	0.59	6.0
16	2F1-3	0.69	5.8
17	3F1-1	0.49	5.8
18	3F4-2	0.49	7.8
19	3F4-3	0.59	4.5
20	3F1-2	0.59	7.2
21	3F1-3	0.69	4.5
22	4F1-1	0.49	5.8
23	4F1-2	0.59	6.1
24	4F1-3	0.69	5.4

Shapiro-Wilk Test for Normality
(Sample Size 50 or Less)

Alpha = 0.05

W= 0.9227

Critical Value = 0.916 (If W < Critical Value, Reject Normality)

Decision: Do Not Reject Normality Hypothesis

Figure 5.8 Normality test for air content

* SR = Stress Ratio

	Sample	SR	Slump
1	PL2-1	0.49	0.9
2	PL3-4	0.59	0.4
3	PL1-2	0.59	1.4
4	PL1-4	0.59	0.8
5	PL1-3	0.69	1.8
6	1F1-1	0.48	0.8
7	1F3-1	0.49	0.4
8	1F1-2	0.59	1.0
9	1F3-4	0.59	1.0
10	1F1-4	0.59	1.0
11	1F3-3	0.69	1.0
12	1F1-3	0.69	0.4
13	2F1-1	0.49	0.0
14	2F1-4	0.59	0.8
15	2F1-2	0.59	0.8
16	2F1-3	0.69	0.3
17	3F1-1	0.49	1.0
18	3F4-2	0.49	1.5
19	3F4-3	0.59	0.0
20	3F1-2	0.59	1.5
21	3F1-3	0.69	0.0
22	4F1-1	0.49	0.0
23	4F1-2	0.59	0.6
24	4F1-3	0.69	0.3

Shapiro-Wilk Test for Normality
(Sample Size 50 or Less)

Alpha = 0.05

W= 0.9427

Critical Value = 0.916 (If W < Critical Value, Reject Normality)

Decision: Do Not Reject Normality Hypothesis

Figure 5.9 Normality test for slump

* SR = Stress Ratio

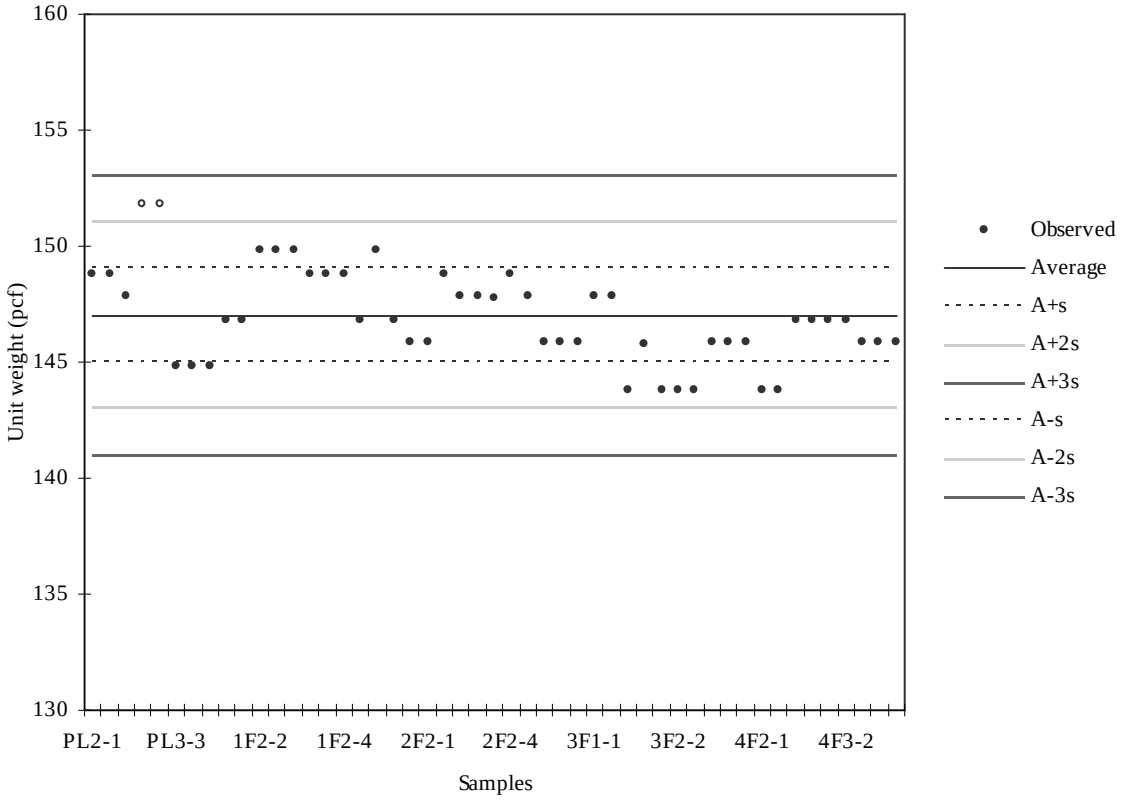

Figure 5.10 Unit Weight for concrete mixtures

* PL2-1 = Plain Concrete Sample 2, Batch 1
  1F2-2 = 0.1% Fiber Reinforced Concrete Sample 2, Batch 2
  3F1-1 = 0.3% Fiber Reinforced Concrete Sample 1, Batch 1

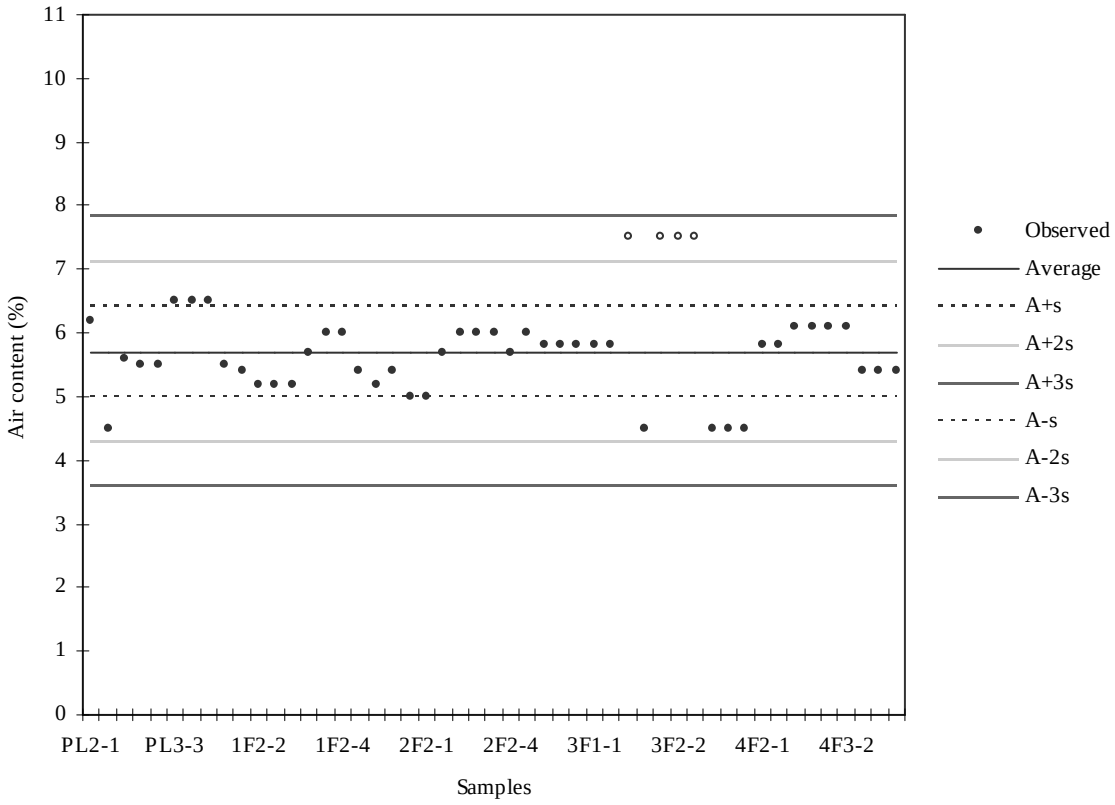

Figure 5.11 Air content for concrete mixtures

* PL2-1 = Plain Concrete Sample 2, Batch 1
  1F2-2 = 0.1% Fiber Reinforced Concrete Sample 2, Batch 2
  3F1-1 = 0.3% Fiber Reinforced Concrete Sample 1, Batch 1

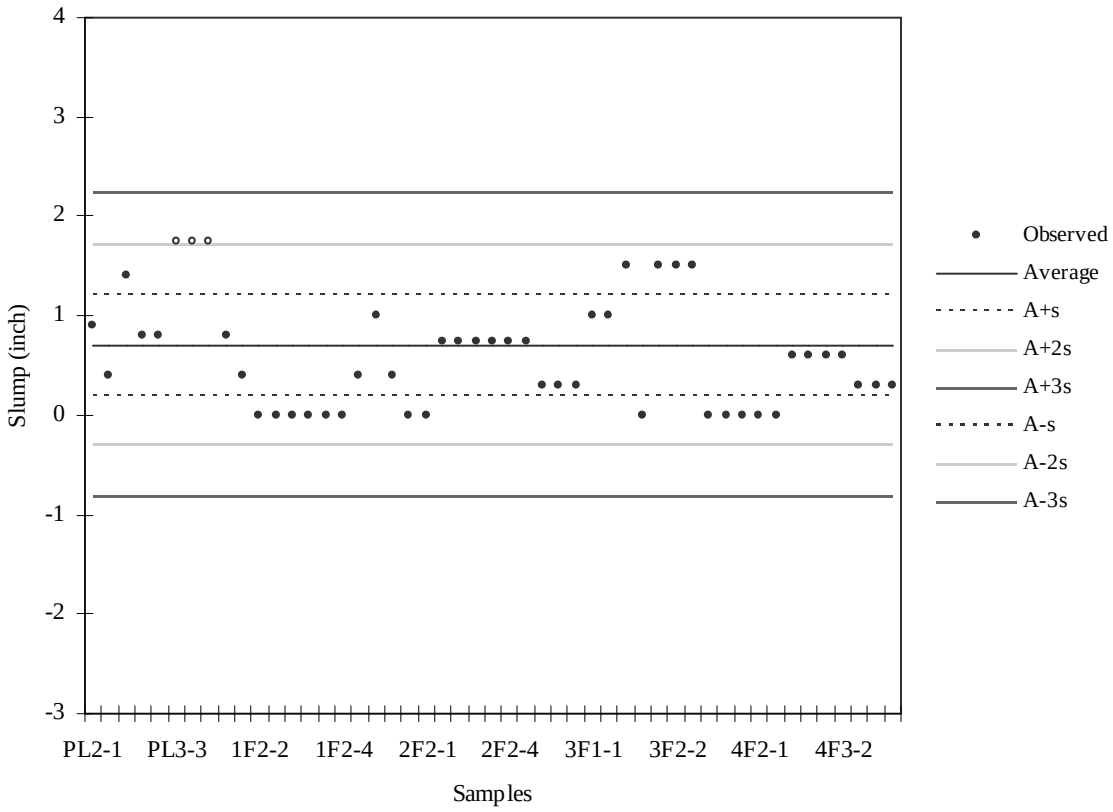

Figure 5.12 Slump for concrete mixtures

* PL2-1 = Plain Concrete Sample 2, Batch 1
  1F2-2 = 0.1% Fiber Reinforced Concrete Sample 2, Batch 2
  3F1-1 = 0.3% Fiber Reinforced Concrete Sample 1, Batch 1

5.3.3 Fatigue Data

Based on the confidence intervals analysis identified in the previous section, the data used for the fatigue analysis along with the respective coefficient of variation is shown in Table 5.3.

Table 5.3 Fatigue Data

TYPE	Slump (in / sec)	AC (%)	UW (pcf)	AGE (DAYS)	f_{max} (PSI)	STRESS LEVEL	CYCLE ACHIEVED	CV (%)
PL2-1	0.9"	6.2	148.8	91	429	0.49	2,500,000 +	
PL1-3	1.38"	5.6	147.8	30	512	0.59	2,255,889	
PL2-3	1.38"	5.6	147.8	31	512	0.59	7,000,000 +	
PL3-4	0.38"	4.5	148.8	41	516	0.59	2,897,652	18
PL1-2	1.75"	6.5	144.8	43	598	0.69	502,602	
PL2-2	1.75"	6.5	144.8	43	598	0.69	817,372	
PL3-2	1.75"	6.5	144.8	44	599	0.69	484,395	31
1F1-1	0.75" / 15 sec	5.5	146.8	96	465	0.48	2,500,000 +	
1F3-2	0.38" / 18 sec	5.4	146.8	42	475	0.49	3,000,000 +	
1F1-3	1" / 10 sec	5.2	149.8	42	573	0.59	2,385,829	
1F3-3	1" / 10 sec	5.2	149.8	45	572	0.59	1,413,298	36
1F1-2	3/8" / 18 sec	5.4	146.8	38	669	0.69	250,348	
1F2-2	3/8" / 18 sec	5.4	146.8	41	669	0.69	907,577	
1F4-3	1" / 10 sec	5.2	149.8	47	670	0.69	553,080	58
2F1-1	0" / 19 sec	5.0	145.8	79	478	0.49	6,000,000 +	
2F2-1	0" / 19 sec	5.0	145.8	82	482	0.49	2,500,000 +	
2F1-3	0.75" / 11 sec	6	147.8	39	579	0.59	790,351	
2F2-3	0.75" / 11 sec	6	147.8	39	579	0.59	1,279,506	
2F3-3	0.75" / 11 sec	6	147.8	40	579	0.59	1,328,193	
2F4-3	0.75" / 11 sec	6	147.8	58	580	0.59	2,096,039	39
2F1-2	1/4"/ 21 sec	5.8	145.8	39	677	0.69	69,175	
2F2-2	1/4"/ 21 sec	5.8	145.8	39	677	0.69	121,989	
2F3-2	1/4"/ 21 sec	5.8	145.8	40	674	0.69	118,194	29
3F1-1	1" / 11 sec	5.8	147.8	77	500	0.49	1,450,101	
3F2-1	1" / 11 sec	5.8	147.8	79	498	0.49	1,097,318	20

3F4-2	0 / 21 sec	4.5	145.8	62	600	0.59	311,153	
3F1-2	0" / 21 sec	4.5	145.8	28	703	0.69	301,626	
3F2-2	0" / 21 sec	4.5	145.8	28	703	0.69	310,575	
3F3-2	0" / 21 sec	4.5	145.8	34	702	0.69	415,136	18
4F1-1	0" / 24 sec	5.8	143.8	78	479	0.49	1,773,437	
4F2-1	0" / 24 sec	5.8	143.8	80	484	0.49	2,500,000 +	
4F1-3	5/8" / 12 sec	6.1	146.8	28	578	0.59	624,844	
4F2-3	5/8" / 12 sec	6.1	146.8	28	578	0.59	1,190,832	
4F3-3	5/8" / 12 sec	6.1	146.8	45	578	0.59	603,543	
4F4-3	5/8" / 12 sec	6.1	146.8	86	585	0.59	1,519,651	46
4F2-2	1/4" / 21 sec	5.4	145.8	29	676	0.69	189,962	
4F3-2	1/4" / 21 sec	5.4	145.8	30	676	0.69	214,951	9

Note:
AC = Air Content, UW = Unit Weight
PL2-1 = Plain Concrete Sample 2, Batch 1
3F1-2 = 0.3% Fiber Reinforced Concrete Sample 1, Batch 2

5.4 Fatigue Models

Fatigue models were developed based on regression analysis from the above data. The linear relationship was used for stress levels between 0.49 and 0.69. The fatigue testing of 0.49 stress level with plain concrete and 0.1%, 0.2%, 0.4% fiber reinforced concrete exceeded 2.5 million cycles without significant damage. According to PCA (Portland Concrete Association) when the stress level is not more than about 0.55, concrete will withstand virtually infinite number of load repetitions. And the fatigue result of 0.49 stress level with plain concrete and 0.1%, 0.2%, 0.4% fiber reinforced concrete agrees with PCA with the exception of the 0.3% fiber reinforced.

5.4.1 Plain Concrete

The relationship of flexural fatigue stress versus number of cycles (LOG N_f) for plain concrete is shown in Figure 5.13. Such a relationship had a 0.93 coefficient of correlation. Since at low 0.49 stress level, fatigue exceeded 2.5 million cycles without significant damage. The linear relationship model is used for higher stress levels. The stress for 0.59 was 3544 kPa (514 psi) with 2,500,000 cycles and for 0.69 was 4123 kPa (598 psi) with 600,000 cycles to failure. The linear model is thus as follows:

$$\text{Log } (N_f) = 1298 - 53\, f_c$$

where,

f_c = flexural fatigue stress (PSI) = Stress Level * MOR
ex. 69% f_c = 0.69 * MOR
0.69 < Stress Level < 0.59
N_f = number of failure cycles.

5.4.2 0.1 % Fiber Reinforced Concrete

The relationship of flexural fatigue stress versus number of cycles (N) for 0.1 % fiber reinforced concrete is shown in Figure 5.14. Such a relationship had a 0.67 coefficient of correlation. Since at 0.49 stress level fatigue exceeded 2.5 million cycles without significant damage, the linear relationship model is used for higher stress levels. The stress for 0.59 was 3944 kPa (572 psi) with 1,400,000 cycles and for 0.69 was 4613 kPa (669 psi) with 570,000 cycles to failure. The linear model is thus as follows:

$$\text{Log}\,(N_f) = 1314 - 50\,f_c$$

where,

f_c = flexural fatigue stress (PSI) = Stress Level * MOR
ex. 69% f_c = 0.69 * MOR
0.69 < Stress Level < 0.59
N_f = number of failure cycles.

5.4.3 0.2 Percent Fiber Reinforced Concrete

The relationship of flexural fatigue stress versus number of cycles (N) for 0.2 % fiber reinforced concrete is shown in Figure 5.15. Such a relationship had a 0.94 coefficient of correlation. Since at low 0.49 stress level, fatigue exceeded 2.5 million cycles without significant damage. The linear relationship model is used for higher stress levels. The stress for 0.59 was 3992 kPa (579 psi) with 1,500,000 cycles and for 0.69 was 4661 kPa (676 psi) with 100,000 cycles to failure. The linear model is thus as follows:

$$\text{Log}\,(N_f) = 1083 - 36\,f_c$$

where,

f_c = flexural fatigue stress (PSI) = Stress Level * MOR

ex. 69% f_c = 0.69 * MOR

0.69 < Stress Level < 0.59

N_f = number of failure cycles.

5.4.4 0.3 Percent Fiber Reinforced Concrete

The relationship of flexural fatigue stress versus number of cycles for 0.3 % fiber reinforced concrete is shown in Figure 5.16. Such a relationship had a 0.77 coefficient of correlation. The stress for 0.49 was 3440 kPa (499 psi) with 1,200,000 cycles and for 0.59 was 4137 kPa (600 psi) with 300,000 cycles and for 0.69 was 4847 kPa (703 psi) with 340,000 cycles to failure. The linear model is thus as follows:

$$\text{Log}\,(N_f) = 2261 - 125\,f_c$$

where,

f_c = flexural fatigue stress (PSI) = Stress Level * MOR

ex. 69% f_c = 0.69 * MOR

0.69 < Stress Level < 0.49

N_f = number of failure cycles.

5.4.5 0.4% Fiber reinforced concrete

The relationship of flexural fatigue stress versus number of cycles for 0.4 % fiber reinforced concrete is shown in Figure 5.17. Such a relationship had a 0.64 coefficient of correlation. The stress for 0.49 was 3323 kPa (482 psi) with 2,000,000 cycles and for 0.59 was 3999 kPa (580 psi) with 980,000 cycles and for 0.69 was 4661 kPa (676 psi) with 140,000 cycles to failure. The linear model is thus as follows:

$$\text{Log}\,(N_f) = 953 - 26\,f_c$$

where,

f_c = flexural fatigue stress (PSI) = Stress Level * MOR

ex. 69% f_c = 0.69 * MOR

0.69 < Stress Level < 0.49

N_f = number of failure cycles.

5.4.6 Models for Plain Concrete and 0.1%, 0.2%, 0.3%, and 0.4% Fiber Reinforced Concrete

All the linear models for the plain concrete and fiber concrete of 0.1%, 0.2%, 0.3% and 0.4% fiber content are shown in Figure 5.18. The 0.1% fiber reinforced concrete performed higher fatigue cycles than any other concretes. For a given 600 psi flexural fatigue stress, 0.1% fiber reinforced concrete failed at around 2,000,000 cycles and plain concrete failed at around 500,000 cycles. Apparently 0.1% fiber reinforced concrete showed 25% increment of the fatigue performance.

5.4.7 Effect of Mix Properties on Fatigue

Multiple regression was used to examine potential effects of mix properties on fatigue. In this analysis, two types of models were examined. In the first case, models relating the number of failure cycles to mix properties were examined. In the second case, models relating number of failures to fiber content were examined. The linear form of the model for multiple regression was :

$$y = \beta_0 + \beta_1 x_1 + \beta_2 x_2 + ... + \beta_k x_k + \varepsilon$$

where y is dependent variable, $x_1 \ldots x_i$ are independent variables and $\beta_0 \ldots \beta_i$ are experimental coefficients of regression model. F test and T test were used to test the

validity of the models and testing the coefficients of the multiple regression models with 95% significance.

In the first case, multiple regression analysis was performed and provided a model with 0.697 R^2 (Table 5.4). Next, the F test was used to test the validity of the model, and the T test was used for testing the coefficients of the multiple regression model. According to the results shown in Table 5.4, an acceptable F test (Significance F < 0.05; f theoretical equal to 7.559, $f > F_{0.05,5,23} = 2.44$) was obtained but no variable was significantly related to the fatigue failure cycles except the Stress Level, T test (P-value < 0.05); t theoretical equal to $t > t_{0.25,29} = 2.045$ or $t < -2.045$. The third step for this analysis is to remove any one of the non-significant independent variables one by one. For example, in Table 5.4 the variables with the least significance were percent Fiber (%), and B/D ratio (B is the width of specimen's cross section, D is the depth of specimen's cross section) that had a P-value of 0.60 and 0.53 respectively (t theoretical equal to $t > t_{0.25,29} = 2.045$ or $t < -2.045$, P value indicates 95% of significance which also indicates P-value < 0.05). So these two variables were removed and multiple regression analysis was performed again. The result is shown in Table 5.5.

Table 5.4 Multiple Regression for Plain Concrete and Fiber Concrete.

SUMMARY OUTPUT	
Regression Statistics	
R Square	0.697
Adjusted R Square	0.605
Observations	31

ANOVA

	df	*SS*	*MS*	*F*	*Significance F*
Regression	7	3.695	0.528	7.559	0.000092
Residual	23	1.606	0.070		
Total	30	5.301			

	Coefficients	*Standard Error*	*t Stat*	*P-value*	*Lower 95%*	*Upper 95%*
Intercept	24.627	11.434	2.154	0.042	0.973	48.280
LOG(MOR)	-8.468	4.191	-2.021	0.055	-17.138	0.201
Fiber (%)	0.354	0.679	0.522	0.607	-1.051	1.760
B/D ratio	1.458	2.314	0.630	0.535	-3.330	6.245
Slump	0.106	0.196	0.540	0.594	-0.300	0.512
Air Cont.	-0.106	0.127	-0.830	0.415	-0.369	0.158
Unit Wet.	0.056	0.047	1.194	0.245	-0.041	0.152
Stress L	-4.322	0.932	-4.636	0.000	-6.251	-2.394

* Stress L = Stress Level

Table 5.5 Step Wise Regression for Plain Concrete and Fiber Concrete.

SUMMARY OUTPUT	
Regression Statistics	
R Square	0.688
Adjusted R Square	0.626
Observations	31

ANOVA

	df	*SS*	*MS*	*F*	*Significance F*
Regression	5	3.648	0.730	11.032	0.000011
Residual	25	1.653	0.066		
Total	30	5.301			

	Coefficients	*Standard Error*	*t Stat*	*P-value*	*Lower 95%*	*Upper 95%*
Intercept	23.117	10.091	2.291	0.031	2.334	43.900
LOG(MOR)	-7.559	3.296	-2.293	0.031	-14.348	-0.771
Slump	0.065	0.180	0.363	0.719	-0.305	0.435
Air Cont.	-0.082	0.118	-0.694	0.494	-0.324	0.161
Unit Wet.	0.057	0.040	1.443	0.161	-0.024	0.139
Stress L.	-4.398	0.816	-5.392	0.000	-6.077	-2.718

Even though the two variables Fiber(%), and B/D ratio were removed from the model (Table 5.5), none of the remaining variables were significant except Stress Level. So according to the first case multiple regression analysis there is no potential effects of mix properties between plain and fiber concrete. In the second case, only the fiber reinforced concrete was considered and the analysis is shown in Table 5.6. For this model a value of 0.784 for R^2 value was obtained, indicating that 78.4 percent of the variation was explained by the linear regression model. According to the F and T tests in the multiple regression analysis, the model is able to represent the data (Significant F < 0.05; f theoretical equal to 9.345, $f > F_{0.05,5,23} = 2.44$), and all the variables are significant except Fiber(%), B/D ratio. So these two variables were removed and performed multiple regression analysis again. That is shown in Table 5.7. For this model a value of 0.765 for R^2 value was obtained, indicating that 76.5 percent of the variation in the measure of profitability is explained by the linear regression model. The model is able to explain the data variability, valid F test (Significance F < 0.05), and all of variables are significantly related to the fatigue failure cycles, T test (P-value < 0.05). So the final proposed model is :

$$y = 130.29 - 25.85x_1 - 0.0115x_2 - 0.57x_3 - 0.27x_4 - 3.847x_5$$

where y = LOG(NFC) *NFC = Number of failure cycles,
x_1 = LOG(MOR), *MOR = Modulus of Rupture
x_2 = Invert Slump
x_3 = Air Content
x_4 = Unit Weight
x_5 = Stress Level

Table 5.6 Multiple Regression for Fiber Concrete.

SUMMARY OUTPUT	
Regression Statistics	
R Square	0.784
Adjusted R Square	0.700
Observations	26

ANOVA

	df	*SS*	*MS*	*F*	*Significance F*
Regression	7	3.513	0.502	9.345	0.00007
Residual	18	0.967	0.054		
Total	25	4.480			

	Coefficients	*Standard Error*	*t Stat*	*P-value*	*Lower 95%*	*Upper 95%*
Intercept	153.379	47.222	3.248	0.004	54.169	252.588
LOG(MOR)	-26.487	10.088	-2.625	0.017	-47.681	-5.292
Fiber (%)	-0.955	0.755	-1.265	0.222	-2.541	0.631
B/D ratio	0.031	2.205	0.014	0.989	-4.600	4.663
Invert Slump	-0.147	0.045	-3.254	0.004	-0.242	-0.052
Air Cont.	-0.650	0.201	-3.231	0.005	-1.072	-0.227
Unit Wet.	-0.407	0.156	-2.612	0.018	-0.734	-0.080
Stress L	-3.960	1.035	-3.825	0.001	-6.136	-1.785

*Stress L. = Stress Level

Table 5.7 Step Wise Regression for Fiber Concrete.

SUMMARY OUTPUT	
Regression Statistics	
R Square	0.765
Adjusted R Square	0.706
Observations	26

ANOVA

	Df	*SS*	*MS*	*F*	*Significance F*
Regression	5	3.425	0.685	12.990	0.00001
Residual	20	1.055	0.053		
Total	25	4.480			

	Coefficients	*Standard Error*	*t Stat*	*P-value*	*Lower 95%*	*Upper 95%*
Intercept	130.285	43.143	3.020	0.007	40.290	220.281
LOG(MOR)	-25.853	9.961	-2.595	0.017	-46.631	-5.075
Invert Slump	-0.115	0.036	-3.219	0.004	-0.190	-0.041
Air Cont.	-0.570	0.189	-3.012	0.007	-0.965	-0.175
Unit Wet.	-0.271	0.111	-2.438	0.024	-0.502	-0.039
Stress L.	-3.847	0.955	-4.027	0.001	-5.839	-1.854

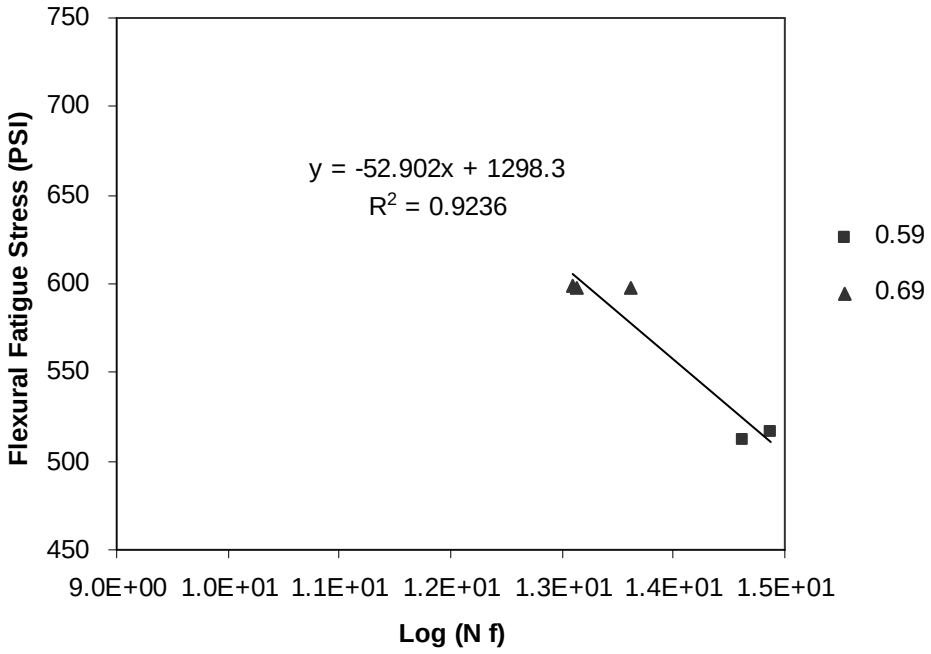

Figure 5.13 Plain Concrete

Units : 100 Psi = 0.6.9 mPa

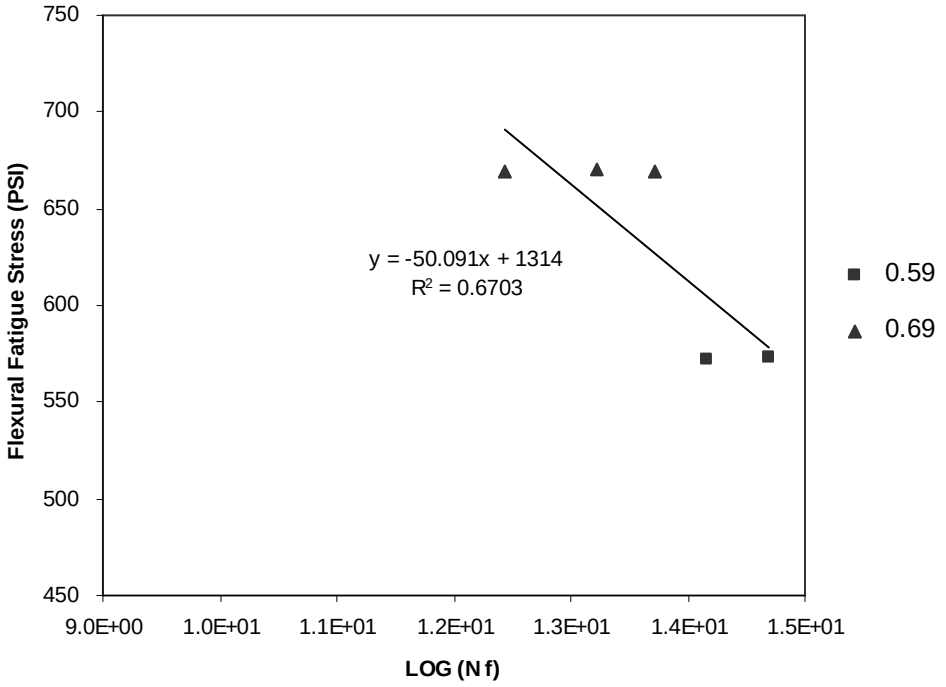

Figure 5.14 0.1% Fiber Reinforced Concrete

Units : 100 Psi = 0.6.9 mPa

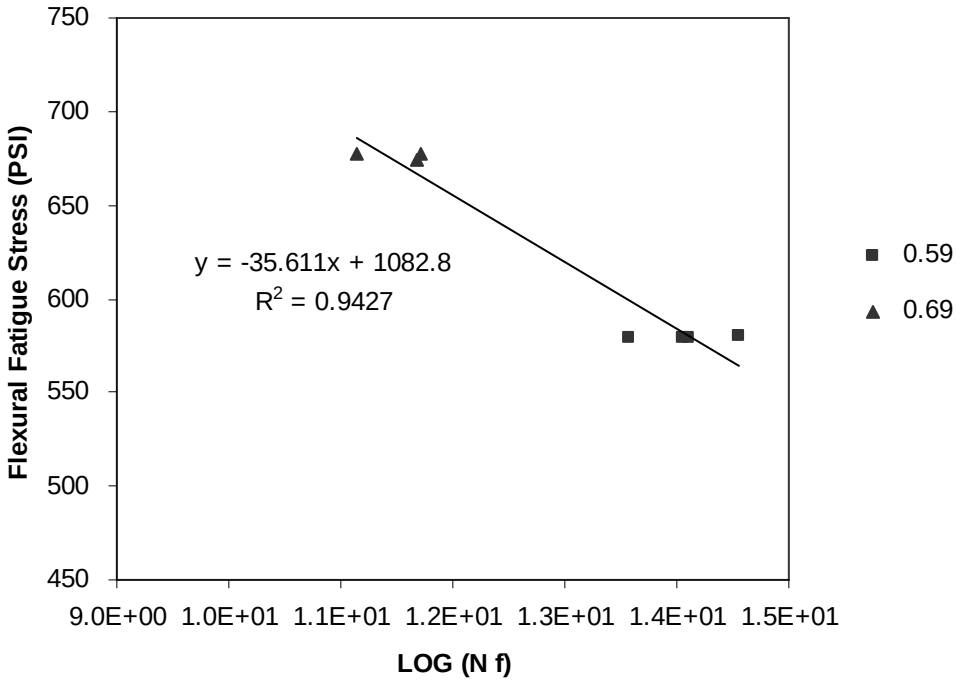

Figure 5.15 0.2% Fiber Reinforced Concrete

Units : 100 Psi = 0.6.9 mPa

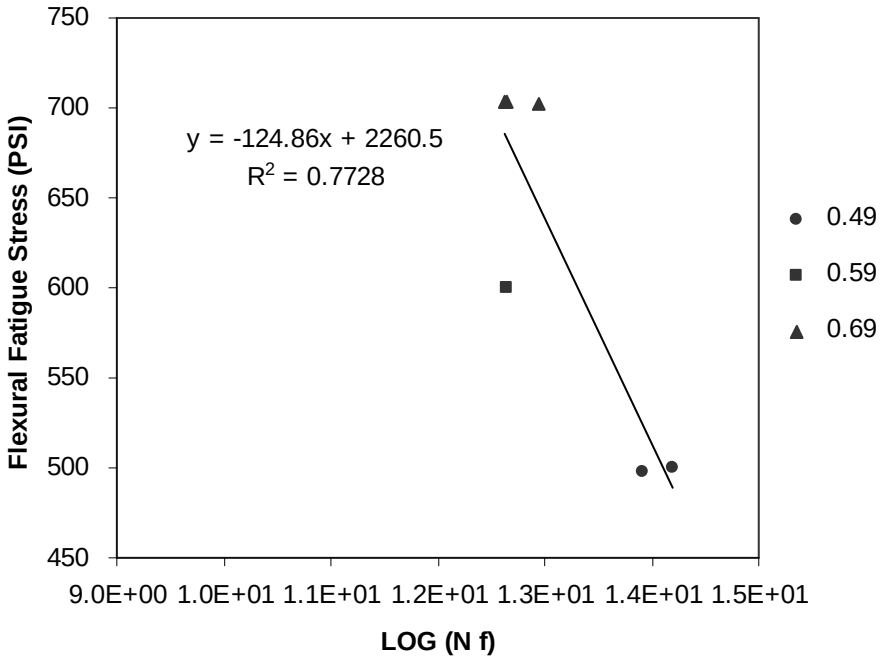

Figure 5.16 0.3% Fiber Reinforced Concrete.

Units : 100 Psi = 0.6.9 mPa

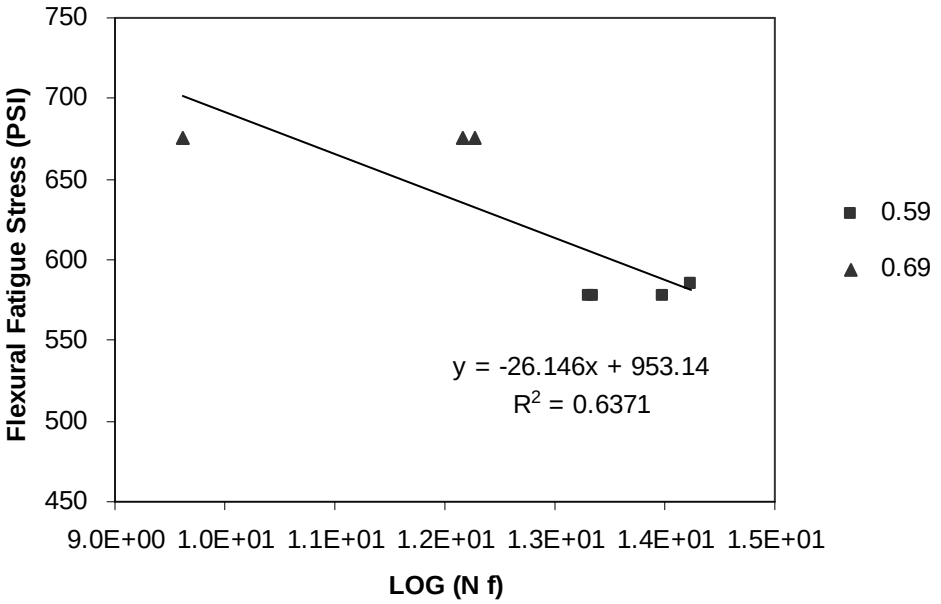

Figure 5.17 0.4% Fiber Reinforced Concrete

Units : 100 Psi = 0.6.9 mPa

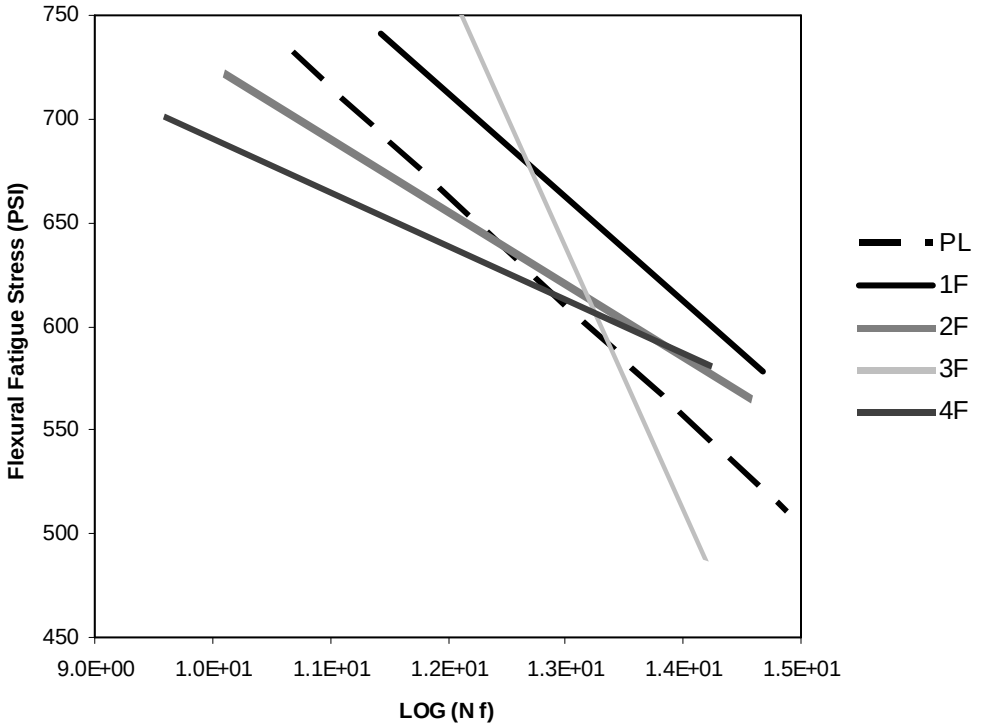

Figure 5.18 Plain Concrete and Fiber Reinforced Concrete

Units : 100 Psi = 0.6.9 mPa

5.5 Endurance Limits

5.5.1 Fatigue Strength

Fatigue strength (V. Ramakrishnan et. al., TRR 1226) is defined as the maximum flexural fatigue stress at which the beam can withstand 2 million cycles of fatigue loading. The 2 million cycle limit was chosen to approximate the life span of a structure that may typically be subjected to fatigue loading, such as a bridge deck or a highway pavement. The fatigue strength was increased with the addition of fibers to the concrete until the 0.2 % fiber content, as shown in Table 5.8 and Figure 5.19.

The fatigue strength was 3730 kPa (541 psi) for plain concrete and 4075 kPa (591 psi), 3834 kPa (556 psi), 3351 kPa (486 psi), and 3489 kPa (506 psi) respectively for concrete mixes reinforced with 0.1 %, 0.2 %, 0.3 %, and 0.4 % polypropylene fiber. Graphs of flexural fatigue stress versus the number of cycles are shown in Figure 5.20. For a given 600 psi flexural fatigue stress, 0.1% Fiber reinforced concrete gave 25% better fatigue performance than plain concrete.

5.5.2 Endurance Limit Expressed as a Percentage of Modulus of Rupture of Plain Concrete

The endurance limit (EL_1) is defined as the maximum flexural fatigue stress at which the beam could withstand 2 million cycles of non-reversed fatigue loading, expressed as a percentage of modulus of rupture of plain concrete. It is evident in Figure 5.21 that for the beams with 0.1 % and 0.2 % fiber content, there in an increase in endurance limit expressed as a percentage of modulus of plain concrete. The 0.1 % fiber content concrete showed the best fatigue performance. However, in

0.3 % fiber content, the endurance limit was the lowest. Figure 5.21 compares the endurance limit values for all fiber concretes and plain concrete.

5.5.3 Endurance Limit Expressed as a Percentage of the Modulus of Rupture of the Mix

The Endurance limit of concrete (EL_2) can also be defined as the flexural fatigue stress at which the beam could withstand 2 million cycles of fatigue loading, expressed as a percentage of the mixture modulus of rupture. This indicates that the increased benefit due to the increased fiber content is not proportional at higher quantities of fibers. The limit (EL_2) for fiber mix is lower than that of plain concrete because its modulus of rupture was high compared with that of plain concrete. Hence, the improvement in endurance limit is evident only when the endurance limit is expressed as a percentage of plain concrete modulus of rupture for relative comparisons. Figure 5.22 compares the endurance limit values for all fiber concrete and plain concrete.

Table 5.8 Fatigue Properties of Concrete Mixtures

	Fiber Content				
	0.1	0.2	0.3	0.4	Plain
f_{max}	591	556	486	506	541
EL_1	68	64	56	58	62
EL_2	61	57	48	52	62

* f_{max} (psi) – Maximum Flexural Stress.
EL_1(%)– Endurance limit expressed as a percentage of modulus of rupture of plain concrete.
EL_2(%)– Endurance limit expressed as a percentage of its modulus of rupture.

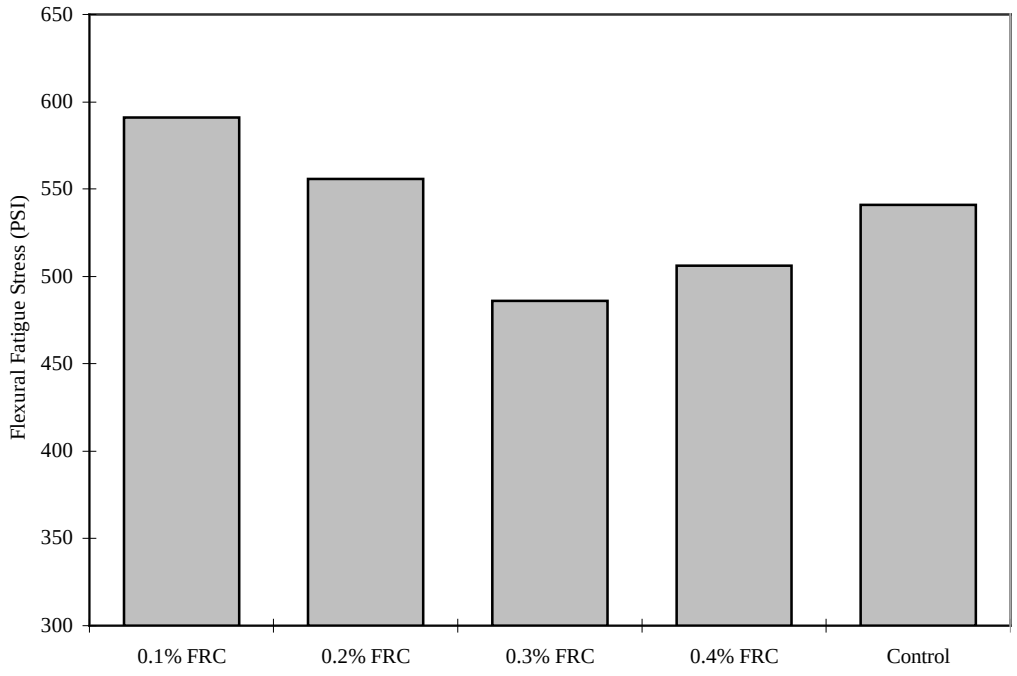

Figure 5.19 Fatigue Strength

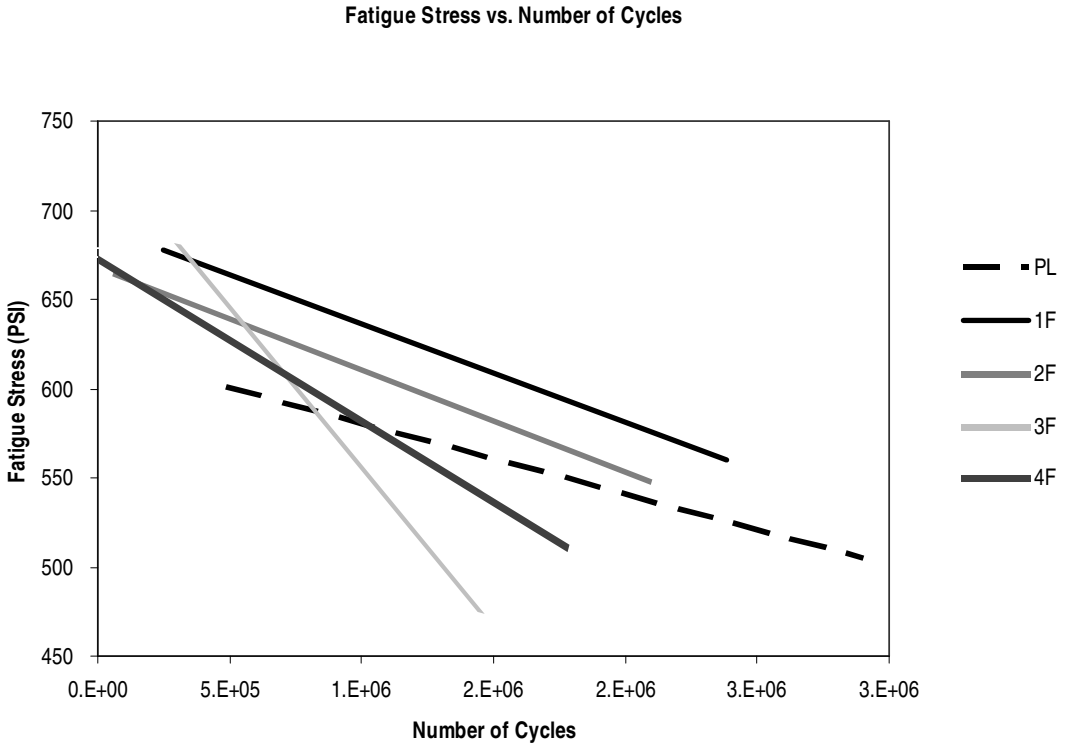

Figure 5.20 Number of cycles versus fatigue stress

Unit : 100 Psi = 0.6.9 mPa

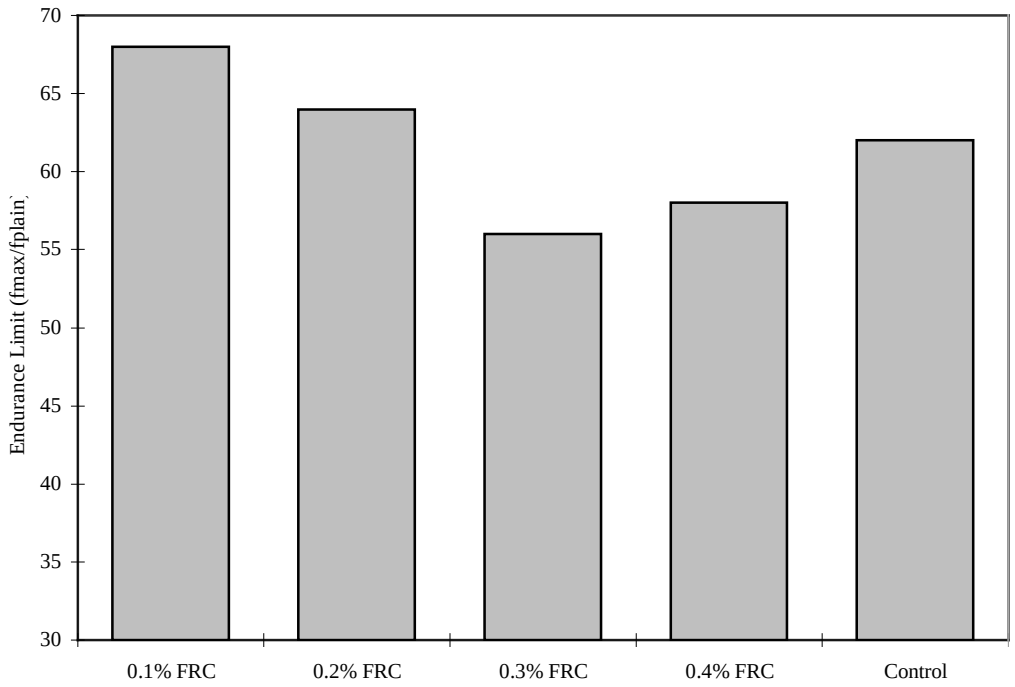

Figure 5.21 Comparison of FRC and plain concrete for endurance limit EL_1.

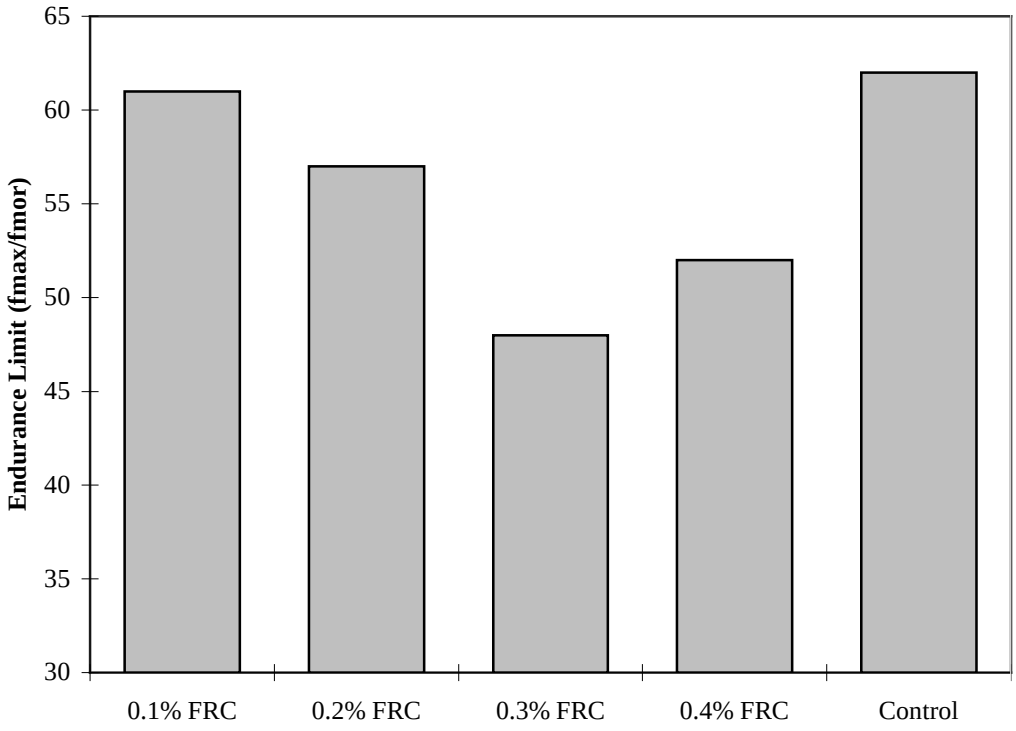

Figure 5.22 Comparison of FRC and plain concrete for endurance limit EL_2.

5.6 Conclusions

The following conclusions were reached based on the fatigue analysis:

1. The addition of polypropylene fibers resulted in higher fatigue strengths.
2. The fatigue strength of FRC increases with decreasing fiber content until 0.3 percent.
3. The endurance limit expressed as a percentage of modulus of rupture increases with decreasing fiber content until 0.3 percent.
4. The optimum fiber content was 0.1 percent based on the fatigue analysis.

CHAPTER 6 BACK CALCULATION ANALYSIS

6.1 Objectives of analyses

The objective of the analyses described in this chapter is the backcalculation of pavement material properties using the measured load test data. The modulus of subgrade reaction k is usually the most uncertain material parameter in the rigid pavement system. In addition, the back calculation analysis can provide estimates of the in situ elastic modulus of the concrete after field aging. A key concern for the back calculation analyses is the variability of foundation stiffness (i.e., k) between slabs and between sections. This variability can be estimated by examining the deflection measurements from the load tests.

6.2 Variability analysis

The deflection measured during the load tests can be used to evaluate the variability between slabs and sections. Each test section was subjected to two passes of both the tandem axle load and single axle load truck loads at a slow-moving speed (about 5 mph), with the first pass along the shoulder-lane joint (edge pass) and the second pass along a line about two feet in from the joint (inner pass).

Figure 6.1, 6.2, and 6.3 summarize the maximum deflections measured at the midpoint LVDT for the control, fiber reinforced, and low shrinkage sections, respectively. Figure 6.4, 6.5, and 6.6 show the corresponding results for the maximum corner LVDT measurements. Generally deflections in all three sections decreased with increasing of temperature. It indicates lower deflection later in the day when the average temperature is higher.

The first item examined was the between slab variability within an individual test section. In Figure 6.1, the average differences in the measured middle position deflection between slab1 and slab2 in the control section were 3% and 24% for the single axle load and tandem axle load, respectively, for the edge pass. The corresponding average differences between slab1 and slab2 were 56% and 61% for the fiber reinforced section (Figure 6.2) and 39% and 18% for the low shrinkage mix (Figure 6.3). The inner pass deflection trends were consistent with those for the edge pass.

In Figure 6.4, the average differences in the measured corner position deflection between slab1 and slab2 in the control section were 77% and 47% for the single axle load and tandem axle load, respectively, for the edge pass. The corresponding deflection trends between slab1 and slab2 were 18% and 5% for the fiber reinforced section (Figure 6.5) and 41% and 3% for the low shrinkage section (Figure 6.6). The inner pass deflection trends were consistent with those for the edge pass in all cases. Slab variations of the measured deflections for all sections at the mid slab and corner positions for the single axle load and tandem axle load were summarized in Figure 6.7.

As can be seen from Figure 6.7 the control and low shrinkage sections were observed some modest variability in the mid slab deflection between slab1 and slab2, but the variability in the fiber section was much higher at more than 50%. For the corner slab deflection variations between slab1 and slab2, the fiber reinforced and low shrinkage sections exhibited relatively a small variability of less than 40% but the control section exhibited a higher variability of 77% for the single axle load.

The conclusions drawn from these data are that the slab variations for the control and low shrinkage sections at the mid slab deflections and for the fiber and low shrinkage sections at the corner deflection were acceptably small. For the fiber section at the mid slab deflection and the control section at the corner deflection, slightly higher variations were observed.

The next item examined was the variation of deflection among sections. Each section had mid slab and corner slab deflection measurements for 3 passes each of inner and edge loading on 2 slabs. Thus, each section has 6 mid slab and 6 corner data points that can be averaged into one representative value for the mid slab and corner deflection for the section. These averaged results are shown in Figure 6.8, 6.9, 6.10, and 6.11.

As shown in Figure 6.8, the average deflections for the mid slab LVDT in the control, fiber, and low shrinkage sections were 0.00338 inch, 0.00129 inch, and 0.00348 inch respectively for the edge pass of the single axle load. The corresponding values for the inner pass of the single axle load were 0.00175 inch, 0.00101 inch, and 0.00152 inch. In Figure 6.9, the average deflections for the mid slab LVDT during the edge pass of the tandem axle load in the control, fiber, and low shrinkage sections were 0.00700 inch, 0.00392 inch, and 0.00742 inch respectively. The corresponding values for the inner pass of the tandem axle load were 0.00313 inch, 0.00125 inch, and 0.00289. In Figure 6.10, the average deflections for the corner slab LVDT in the control, fiber, and shrinkage sections were 0.00432 inch, 0.00368 inch, and 0.00614 inch respectively for the edge pass of the single axle load. The corresponding values for the inner pass of the single axle load were 0.00217 inch, 0.00192 inch, and

0.00277. In Figure 6.11 the average deflections for the corner slab LVDT in the control, fiber, and shrinkage sections were 0.00786 inch, 0.00583 inch, and 0.01061 inch respectively for the edge pass of the tandem axle load. The corresponding values for the inner pass for the tandem axle load were 0.00303 inch, 0.00270 inch, and 0.00355 inch. Table 6.1 summarized the average deflection data for all sections.

Table 6.1 Averaged deflections for all sections

Section	Mid Slab Deflection				Corner Deflection			
	Edge/SAL	Inner/SAL	Edge/TAL	Inner/TAL	Edge/SAL	Inner/SAL	Edge/TAL	Inner/TAL
Control	0.00338	0.00175	0.00700	0.00313	0.00432	0.00217	0.00786	0.00308
Fiber	0.00129	0.00101	0.00392	0.00125	0.00368	0.00128	0.00583	0.00270
LS*	0.00348	0.00152	0.00742	0.00280	0.00614	0.00277	0.01061	0.00355

* LS = Low Shrinkage

As can be seen in Figure 6.8 – 6.11 and Table 6.1, the differences on the deflection magnitudes are negligible between the control section and low shrinkage section but the fiber section always gives significantly smaller deflections. Two possible explanations can be offered for the anomalously low deflections in the fiber section. One is that the foundation of the fiber section is much stiffer than for the other two sections. However, this doesn't seem reasonable because all 3 sections were on embankments having the same fill material and compaction procedures. The other explanation is a malfunction of the LVDT due to unstable anchor rod in the fiber section. As will be shown later, the measured strain data support this conclusion of a malfunctioning LVDT.

The principal conclusions from the variability study are:

- The slab to slab variations of deflection between control and low shrinkage sections at the mid slab location are acceptably small.
- The slab to slab variation of deflection for the fiber and low shrinkage sections at the corner slab location are acceptably small.
- The slab to slab variations of deflection observed for the fiber section at the mid slab and for the control section at the corner slab were higher than the other variations.
- The fiber section exhibits a significantly smaller average deflection at the mid slab location as compared to the rest of the sections.
- Section to Section Variations for the control and low shrinkage sections are acceptably small.

6.3 Backcalculation Analysis

6.3.1 Analysis model

The conclusions from the variability analysis enable the construction of a suitable finite element model for back-calculating k and E_c. The principle assumptions underlying the analysis model are as follows:

- A Winkler-Spring (also termed a “dense liquid”) formulation was assumed as a foundation model with the force-deflection relationship characterized by an elastic spring.
- Full joint load transfer was assumed since this brand new rigid pavement. Although the slabs were built with the transverse and longitudinal joints, these joints are assumed to be tightly interlocked. As a matter of fact, the joint load transfer efficiency of the control, fiber reinforced, and low shrinkage sections

was 79%, 43%, and 56% for the single axle load, 95%, 62%, and 74% for the tandem axle load. Those values are from the difference between mid slab LVDT when the load is in the mid slab and corner LVDT when the load is in the corner with the assumption that a big monolithic slab would be expected to have the same deflection in both places. The amount of difference from 100% is a measure of loss of load transfer efficiency. However the back calculation of k value is to be based on the wheel load at the middle of the slab; this is far enough away from the joint that the imperfect load transfer at the joint becomes less important. Thus, the assumption of full load transfer can be justified.

- Thermal stresses and curling were not considered, and the slab was therefore assumed to remain in full contact with the foundation.
- The elastic modulus, Poisson's ratio, and unit weight material properties were based on laboratory measured values as summarized in the Table 6.2.

Table 6.2 Material properties in the laboratory

	Plain concrete (Control Section)	0.1% fiber reinforced concrete (Fiber Section)	Low shrinkage concrete (Low Shrinkage Section)
E_c	3,966,614 psi	4,145,537 psi	3,901,034 psi
UW	142.8 pcf	147.8 pcf	146.8 pcf
υ	0.15	0.15	0.15

Ec = Concrete Elastic Modulus, UW = Unit Weight, υ = Poisson's ratio

- Finite element mesh(es): As the analysis was done using the KENSLAB program which has a limitation on mesh sizes, the mesh was based on results from a careful meshing study. In order to produce a suitable mesh for the analysis, deflection and strain analyses were used with progressively finer meshes and compared with the measured strain data. The final mesh(es) are presented in Figure 6.12.
- Vehicle Load: Two trucks were used in this test. The first had a single rear axle with a measured single axle load (SAL) of 18,050 lb. The second had a tandem rear axle with a measured tandem axle load (TAL) of 37,000 lb. The measured tire pressure at the beginning of the load test was 100 psi for both trucks.

6.3.2 Analysis results

FE analyses were performed using the KENSLAB program for a range of k values to determine the best fit to measured deflections. The key results are shown in Figures 6.13 and 6.14.

In Figure 6.13 the measured deflections of the mid slab for the control and low shrinkage sections, for the single axle load and tandem axle load were presented. The deflections of the fiber reinforced section were not included in the analysis because of the malfunction of the mid slab LVDT as already discussed in the variability analysis. In Figure 6.14 the averaged deflections ± one standard deviation in the control and low shrinkage sections for the single axle load and tandem axle load are superimposed on the predicted deflections vs. k values at the concrete elastic modulus of about 4,000,000 psi obtained in the laboratory. The range of estimated k

value was between 260 pci to 970 pci for the edge pass of the single axle load at the midslab. For the edge pass of the tandem axle load at the midslab the range of the estimated k value was between 280 pci and 500 pci. The mid-range values for the backcalculated estimates of k are 615 pci and 390 pci for the single and tandem axle passes, respectively. The deflections of the tandem axle load for the control and low shrinkage sections are more consistent than those of the single axle load.

Therefore the best estimated k value from the deflection analysis is selected by the mid-range value for the tandem axle load. It is about 400 pci at concrete elastic modulus of about 4,000,000 psi.

6.4 Strain analysis

The objective of strain analysis is the independent check on the k values back calculated from the deflection data. Six strain gages were installed on each test slab, two each at the slab-shoulder joint (edge) and at 24", and 48" offsets from the longitudinal joints.

The first step in the analysis was to examine the variability of the measured strains among sections. Figures 6.15 and 6.16 summarized the averaged strains in all three sections for the single axle load and tandem axle load.

Figure 6.15 shows the averaged strains in all three sections for the single axle load at the edge pass. The averaged strains for the control, fiber reinforced, and low shrinkage sections at the edge location were -19 μs, -19 μs, and -27μs, respectively. The averaged strains for the control, fiber reinforced, low shrinkage sections at the 24" location were -16 μs, -17 μs, and -18 μs, respectively. The averaged strains for the control, fiber reinforced, and low shrinkage sections at the 48" location were -9μs,

-10μs, and -9μs, respectively. As can be seen, the averaged strains in all three sections for the single axle load at the edge pass indicate similar magnitudes of strain except for low shrinkage section which shows a slightly higher value. This could be because of low elastic modulus of the low shrinkage concrete. The inner pass averaged strain trends are consistent with those for the edge pass in all case.

In Figure 6.16 the averaged strains for the control, fiber reinforced, and low shrinkage sections for the tandem axle edge pass were -17μs, -16μs, and -25μs, respectively at the edge strain gauge location. The averaged strains for the control, fiber reinforced, and low shrinkage sections at the 24" location were -11μs, -13μs, and -18μs, respectively. The averaged strains for the control, fiber reinforced, and low shrinkage sections at the 48" location were -9μs, -10μs, and -8μs, respectively. As can be seen, the averaged strains in all three sections for the tandem axle load at the edge pass indicate the same magnitude of strain except low shrinkage section which shows a little bit higher surface strain. The inner pass averaged strain trend is consistent with that for the edge pass.

Therefore the conclusion from the strain analysis is that the section variations in all three sections are negligible. This conclusion is consistent with that drawn from the deflection analysis and also supports the conclusion of a malfunctioning LVDT.

The measured strains enable an independent check on the k values back calculated from the deflection data. The KENSLAB program was used to predict the strain values corresponded to the back calculated k values. The predicted strains were calculated by the generalized Hooke's law with stresses in three directions such as x direction for the transverse way, y direction for the longitudinal way, and z direction

for the vertical way. Since the truck tires weren't directly over the surface strain gages when the load testing was performed, the stress in z direction for the tire pressure was assumed to zero. The equation used to calculate the predicted strains is here:

$$\varepsilon_y = \frac{\sigma_y}{E} - \upsilon \frac{\sigma_x}{E}$$

where σ_x and σ_y are the stress in x direction for the transverse way and y direction for the longitudinal way. E and υ are the concrete elastic modulus and Poisson's ratio. The results are shown in Figure 6.17, 6.18.

In Figure 6.17 the strains were calculated with the k values ranging from 200 pci to 900 pci at the concrete elastic modulus of 4,000,000 psi which was obtained in the laboratory. A k value of 900 pci gave the best agreement between predicted and measured strains. However a k value of 900 pci is very high and probably unrealistic for the foundation conditions of the site. In addition, the back calculated k value estimated from the deflection analysis was only 400 pci, a much lower and more realistic value.

One possible explanation for this discrepancy is that the concrete elastic modulus in the field experienced ageing for 2 months after construction and therefore is larger than the laboratory value used in the backcalculation analysis. Therefore the concrete elastic modulus in the KENSLAB analysis was increased to 5 million psi to simulate aged condition.

In Figure 6.18 the strains were calculated with the k values ranging from 200 pci to 900 pci at the concrete elastic modulus of 5 million psi to simulate aged concrete condition. It indicates that a k value of 400 pci gave the best agreement

between predicted and measured strains except the edge location strains. The discrepancy at the edge is because the FE analysis assumes the transverse stress (x direction) at the edge case is zero. In fact that transverse stress at the edge case is not zero since there is very tight joint between the main slab and the shoulder slab at that point. Consequently the FE analysis overestimates the strain at the edge location. A k value of 400 pci is matches with the backcalculated k value estimated from the deflection analysis.

The next step in the analysis is to evaluate of k values from δanalysis with the concrete elastic modulus of 5 million psi. Figure 6.19 shows deflection versus 3 different k values such as 300 pci, 350 pci, and 400 pci, at the concrete modulus of 5 million psi. It indicates that k value is between 300 pci and 400 pci at the concrete modulus of 5 million psi. So the average k value of 350 pci was selected and compared with the strain data at the concrete modulus of 5 million psi. These results are shown in Figure 6.20, 6.21.

The measured average strains at the edge, 24", and 48" locations for the single axle load and tandem axle load were superimposed on the predicted strains at the concrete modulus of 5 million psi for the control, fiber reinforced, and low shrinkage sections in Figure 6.20, 6.21.

In Figure 6.20 the measured strains for the single axle load give good agreement with the predicted strains at the k of 350 pci and E_c of 5,000,000 psi except the edge location strains.

In Figure 6.21 the measured strains for the tandem axle load show good agreement with the predicted strains at the k of 350 pci and E_c of 5,000,000 psi except again for the edge case strains.

In conclusion, the best estimates of k and E_c both from the measured deflections and measured strains are k of 350 pci and E_c of 5,000,000 psi. These are both reasonable values for the embankment soils and concrete conditions at the site at the time of the load tests.

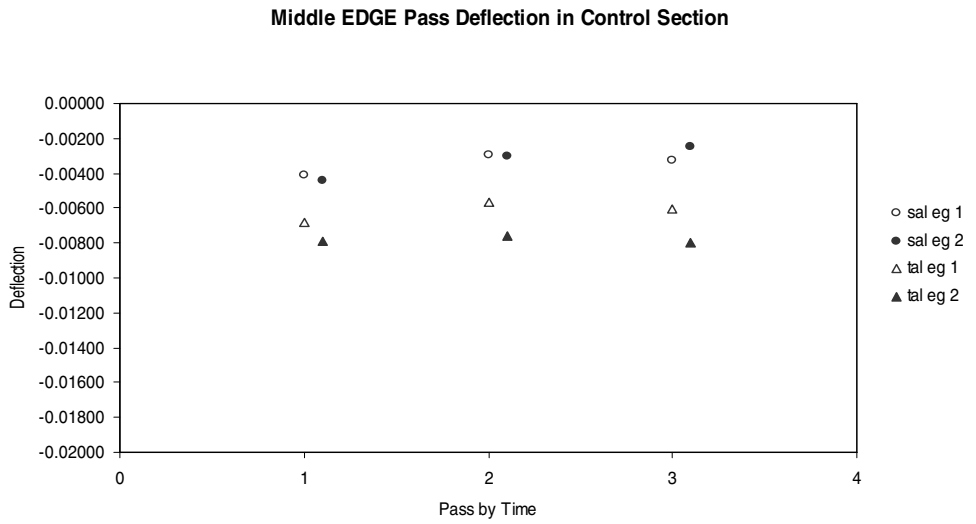

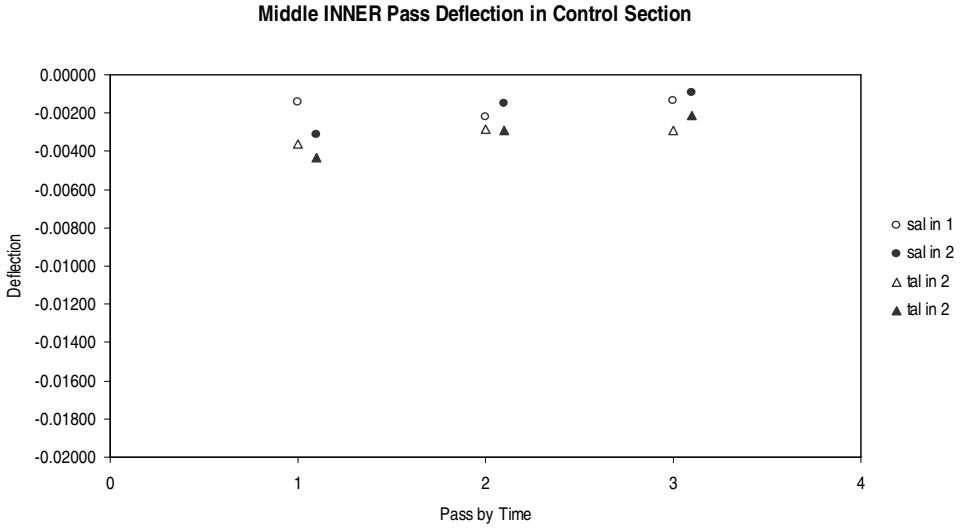

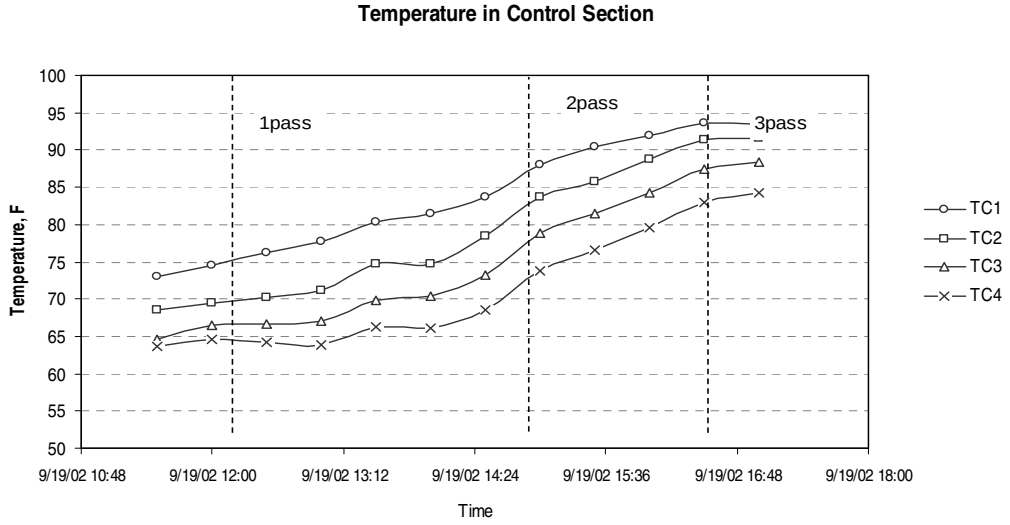

Figure 6.1 Middle Position Deflection & Temperature in Control section

sal eg1 = Single Axle Load Edge pass Slab 1, tal in1 = Tandem Axle Load Inner pass slab 1

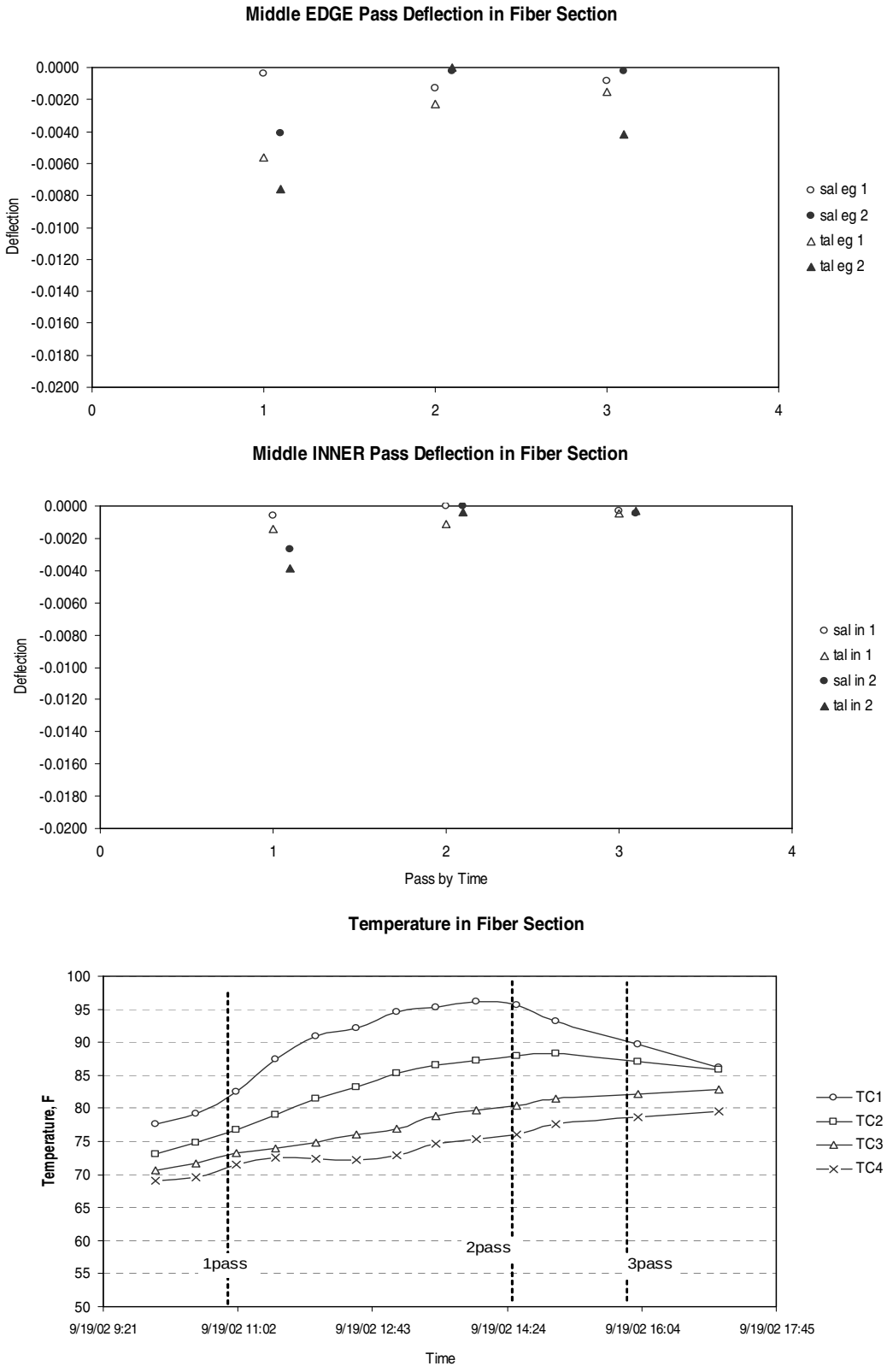

Figure 6.2 Middle Position Deflection & Temperature in Fiber Section sal eg1 = Single Axle Load Edge pass Slab 1, tal in1 = Tandem Axle Load Inner pass slab 1

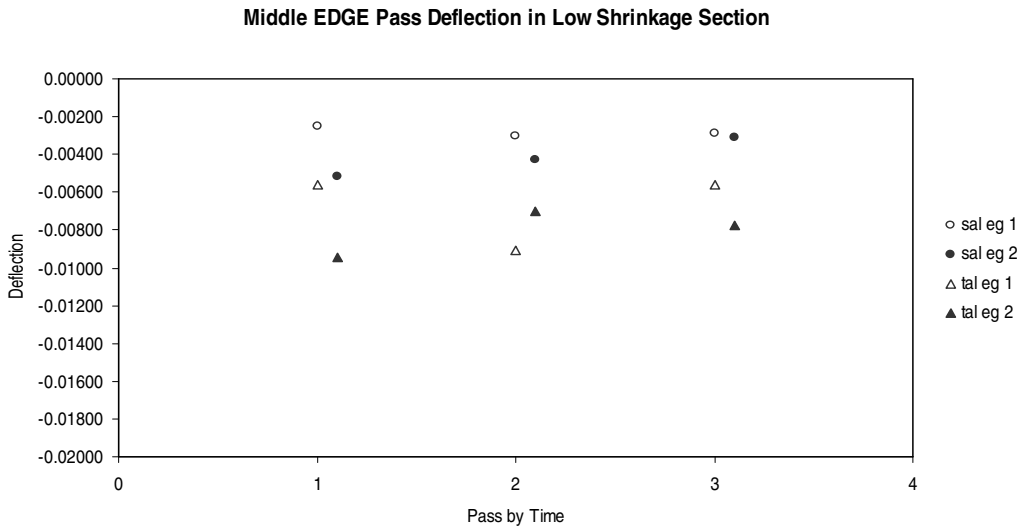

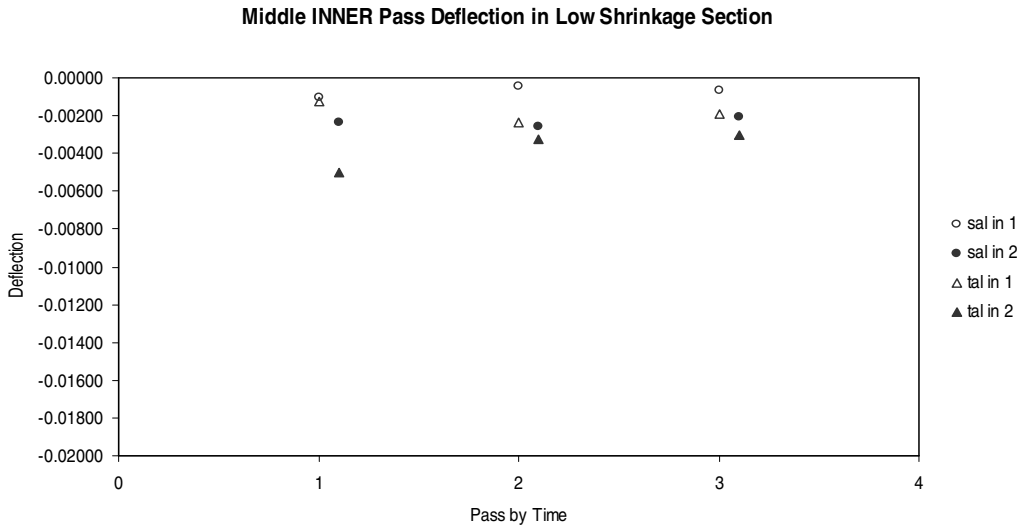

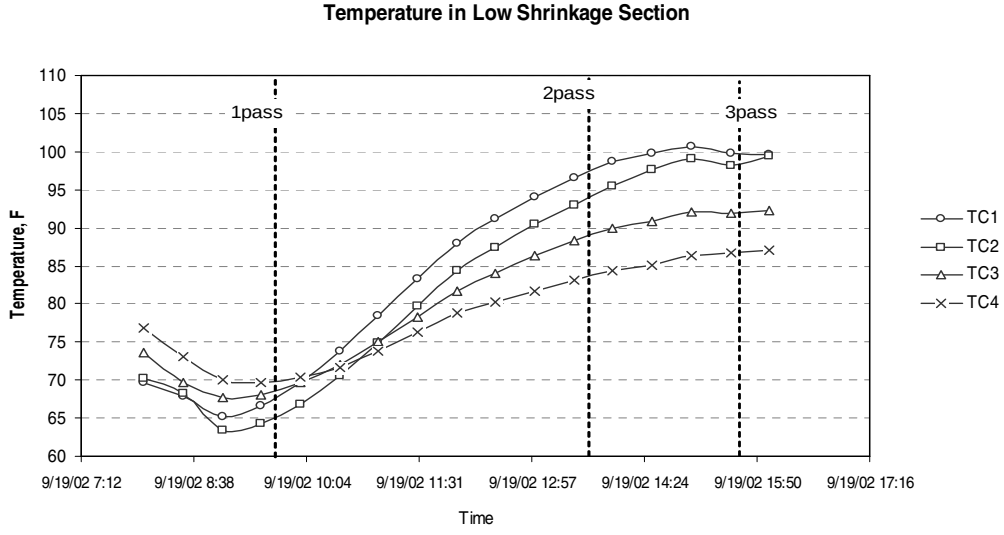

Figure 6.3 Middle Position Deflection & Temperature in Low Shrinkage Section
sal eg1 = Single Axle Load Edge pass Slab 1, tal in1 = Tandem Axle Load Inner pass slab 1

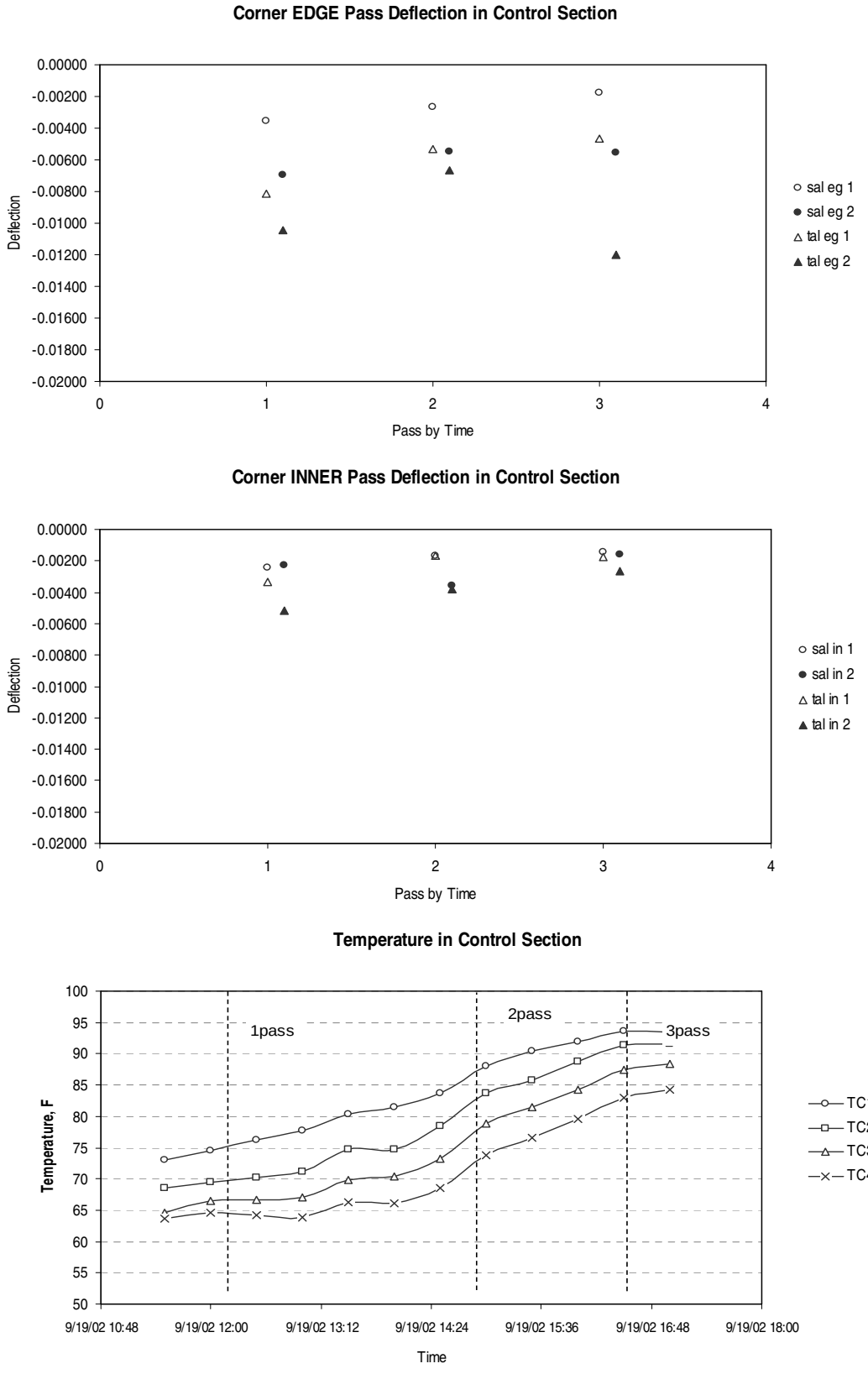

Figure 6.4 Corner Position Deflection & Temperature in Control Section

sal eg1 = Single Axle Load Edge pass Slab 1, tal in1 = Tandem Axle Load Inner pass slab 1

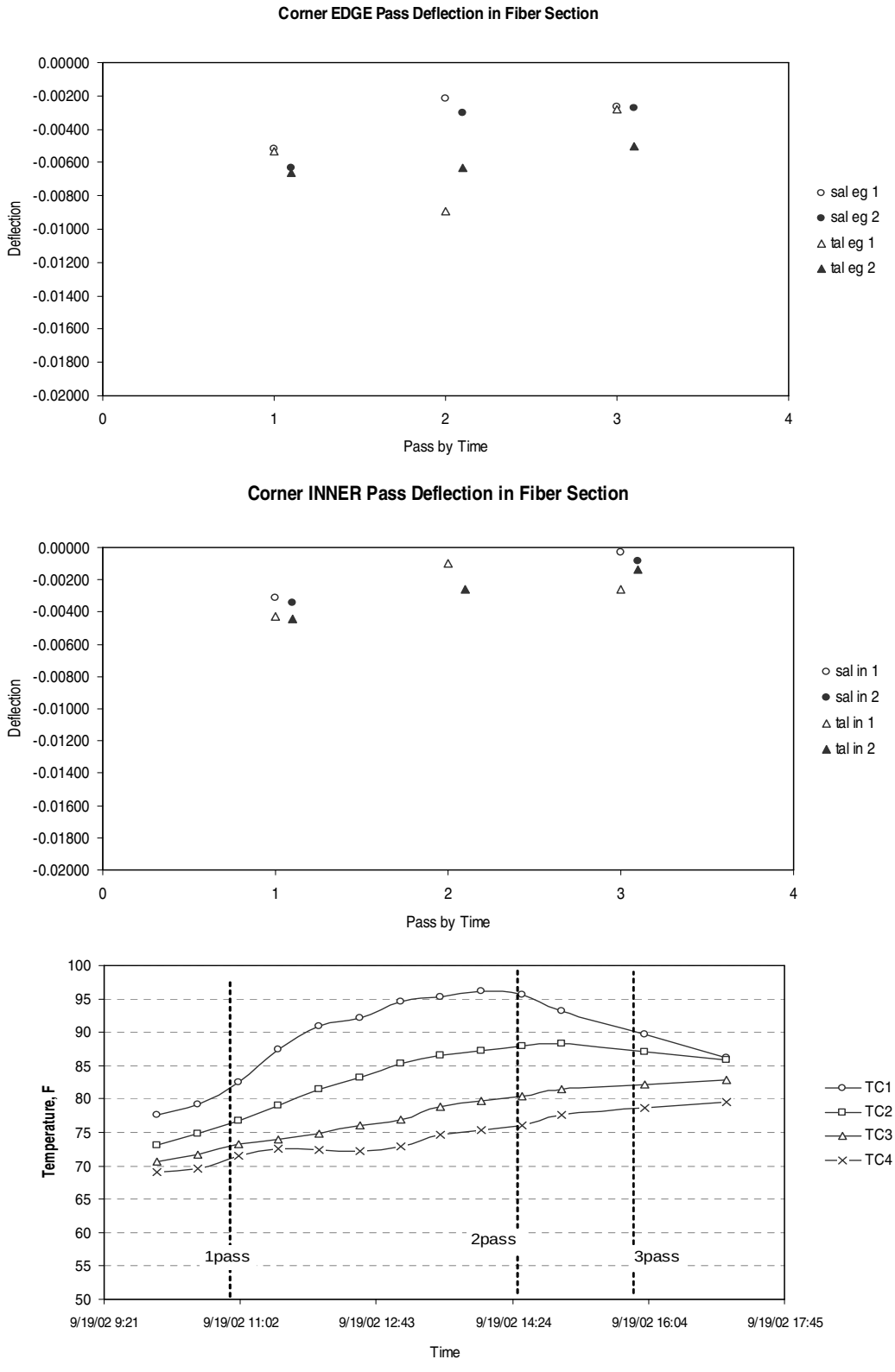

Figure 6.5 Corner Position Deflection & Temperature in Fiber Section

sal eg1 = Single Axle Load Edge pass Slab 1, tal in1 = Tandem Axle Load Inner pass slab 1

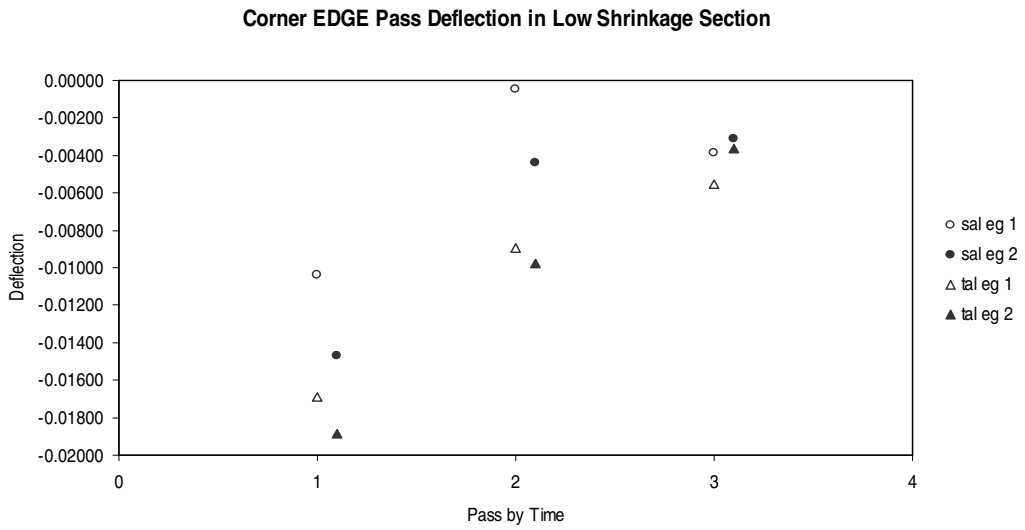

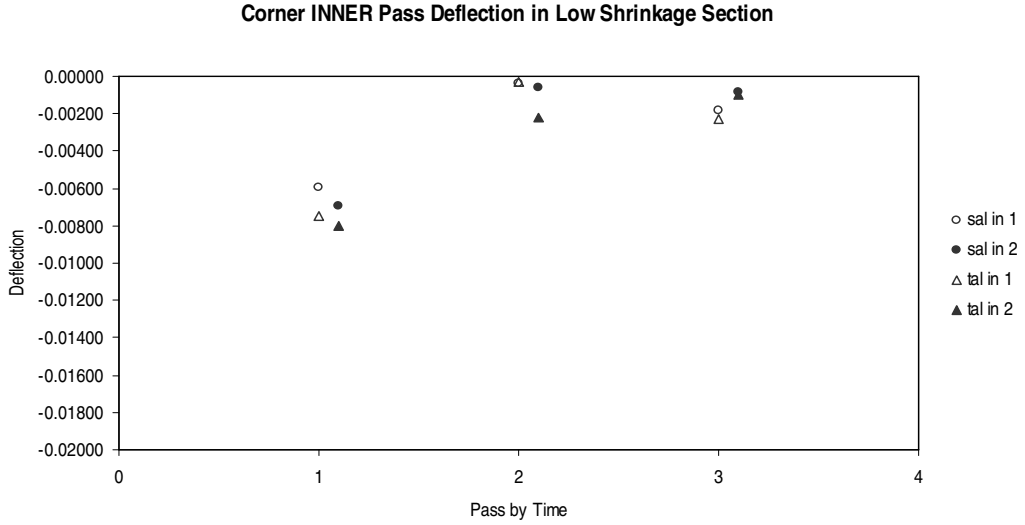

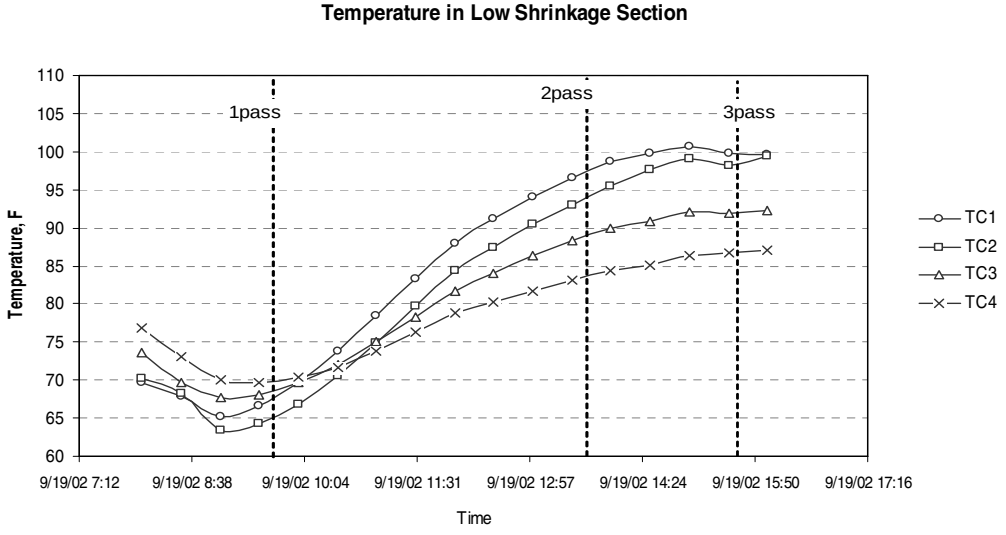

Figure 6.6 Corner Position Deflection & Temperature in Low Shrinkage Section

sal eg1 = Single Axle Load Edge pass Slab 1, tal in1 = Tandem Axle Load Inner pass slab 1

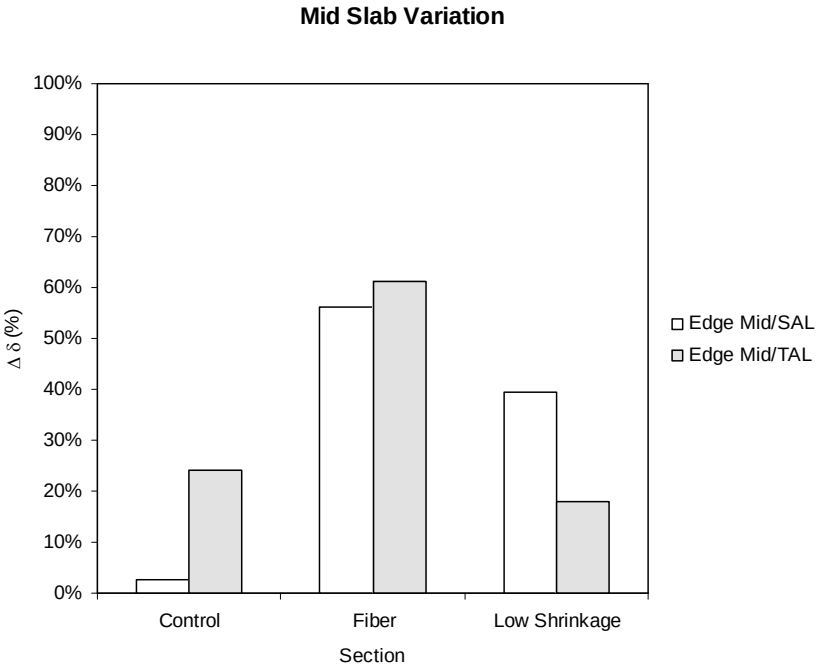

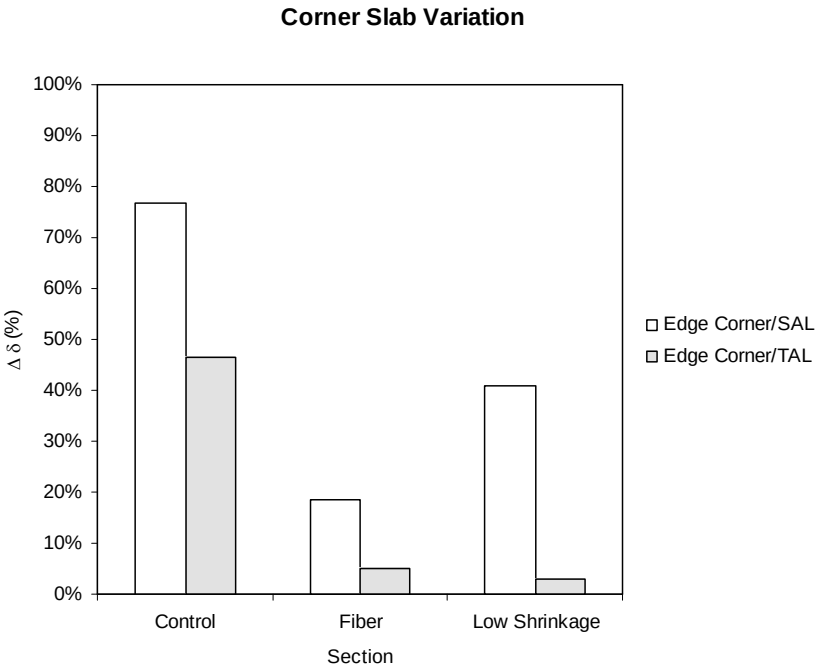

Figure 6.7 Slab variations for all sections

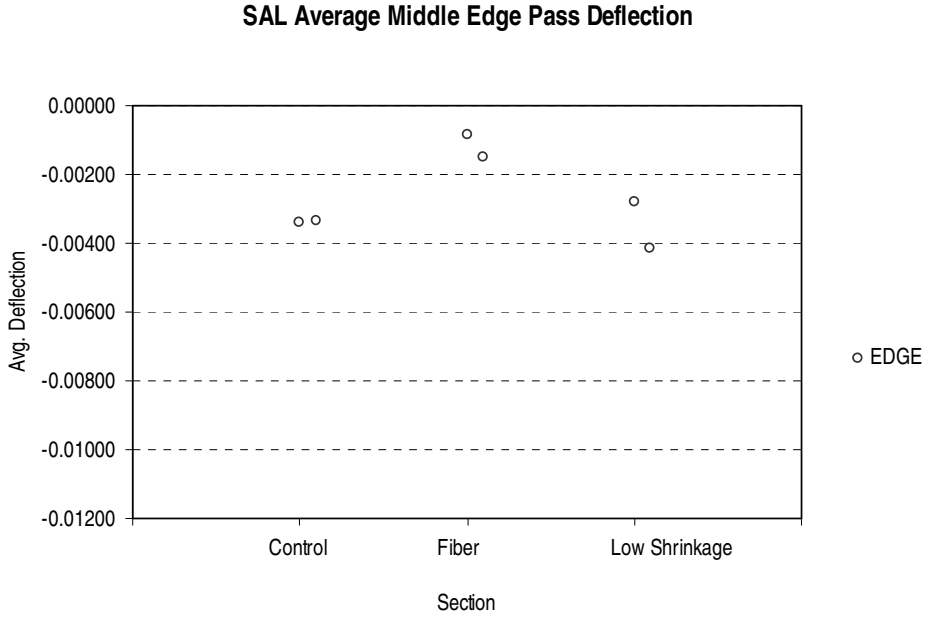

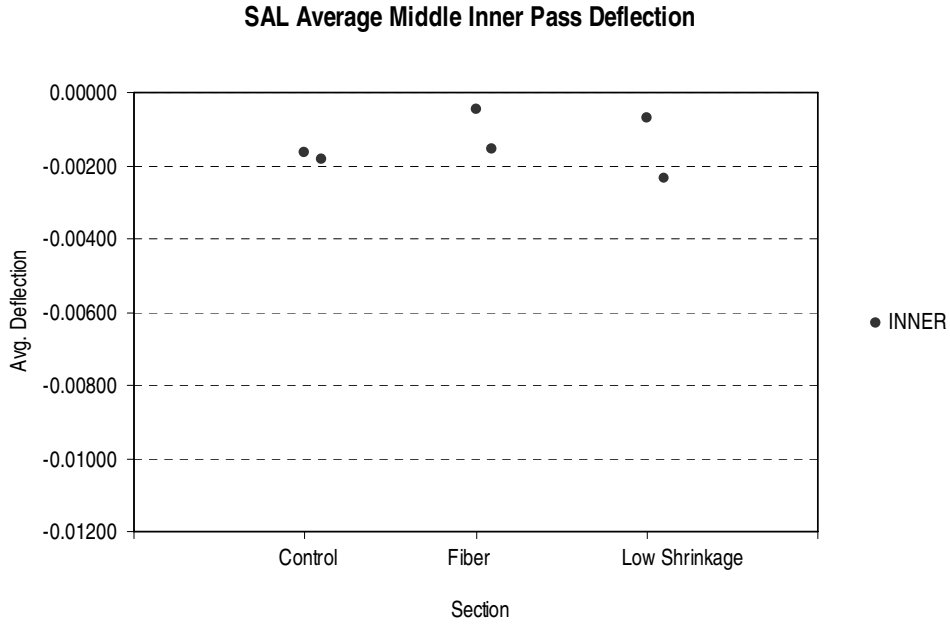

Figure 6.8 Average Middle Deflection for Single Axle Load Testing

*Section 1 = Control section, Section 2 = Fiber reinforced section, Section 3 = Low shrinkage section

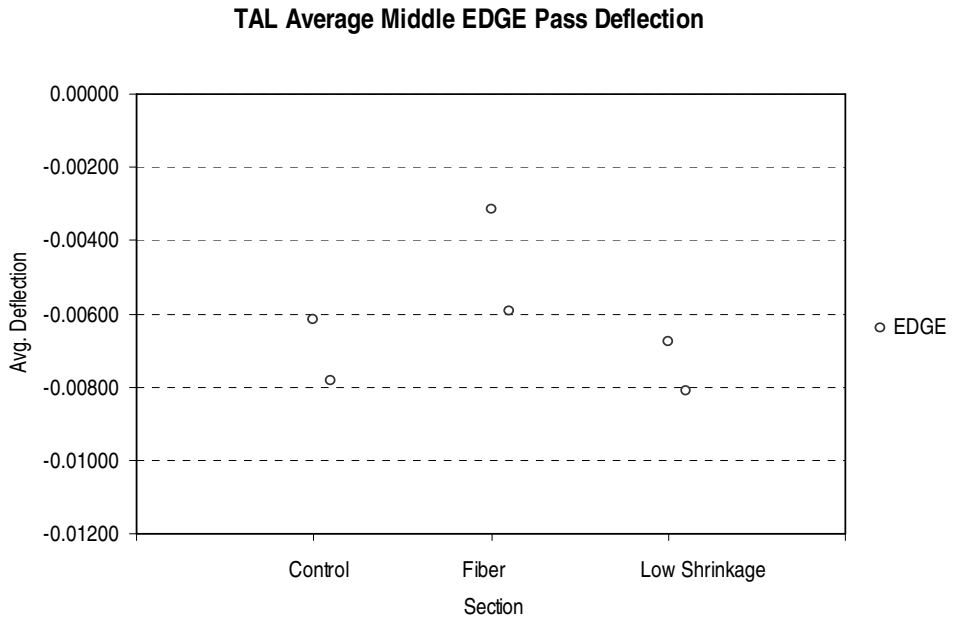

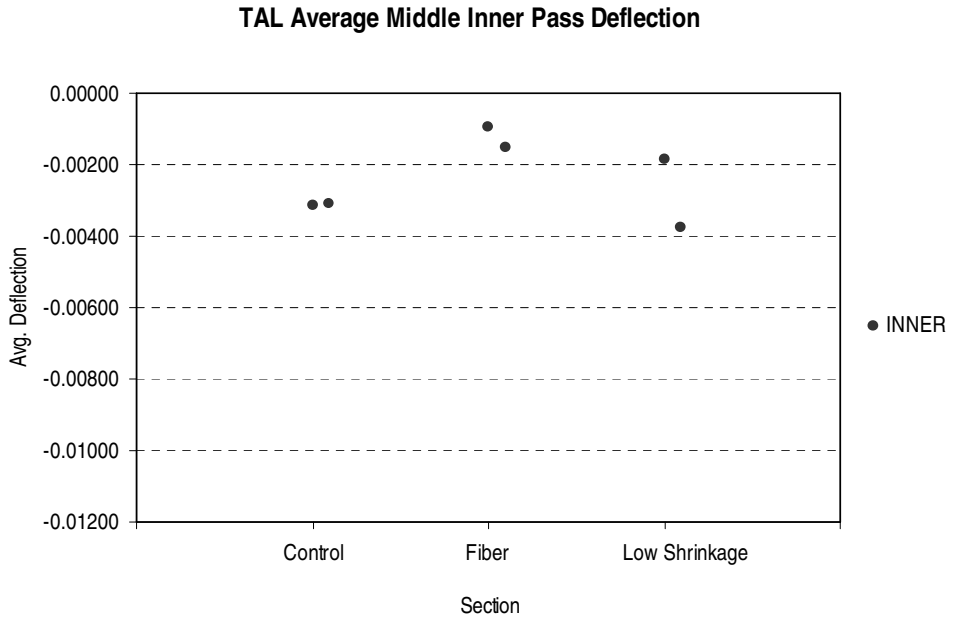

Figure 6.9 Average Middle Deflection for Tandem Axle Load Testing

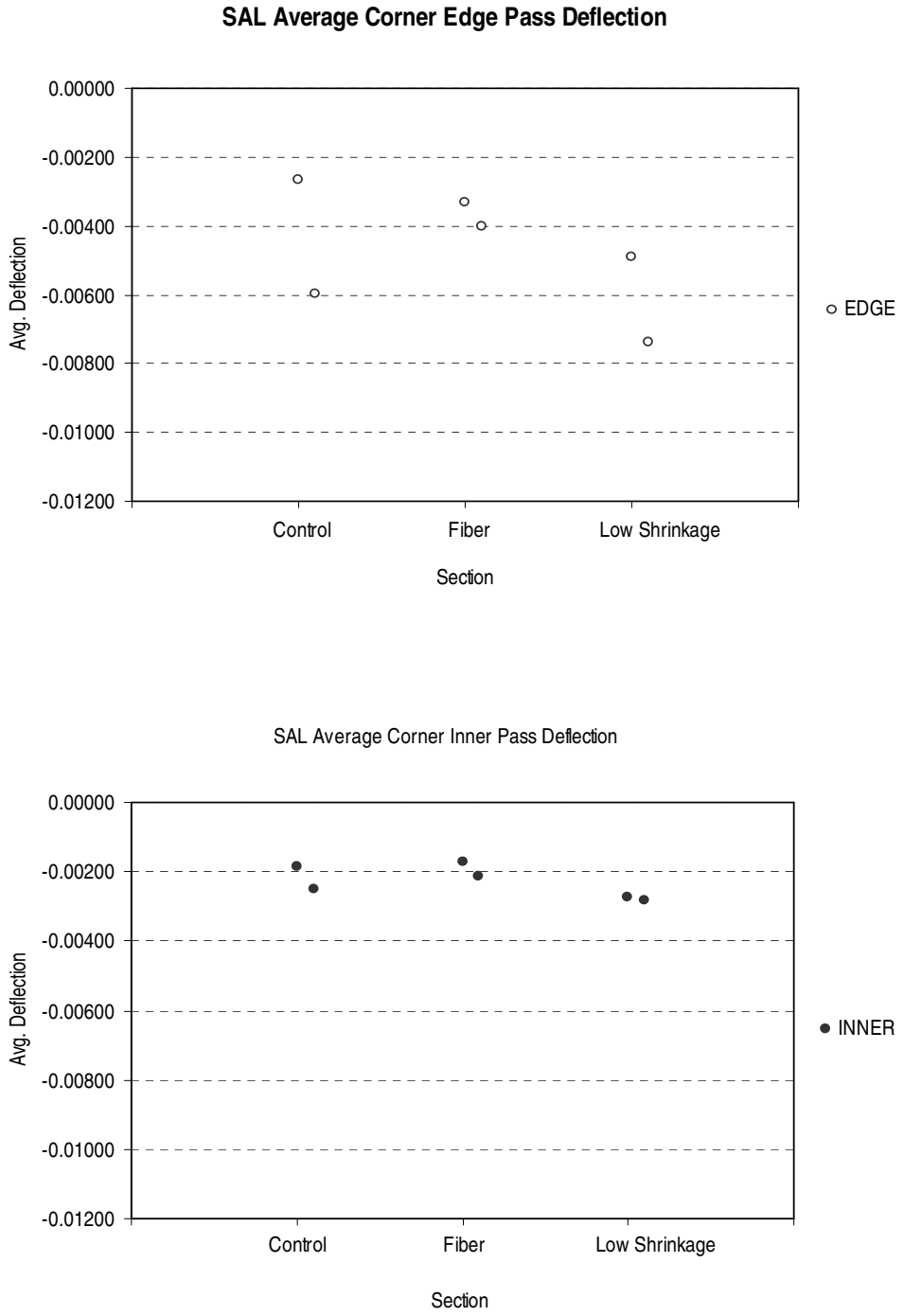

Figure 6.10 Average Corner Deflection for Single Axle Load Testing

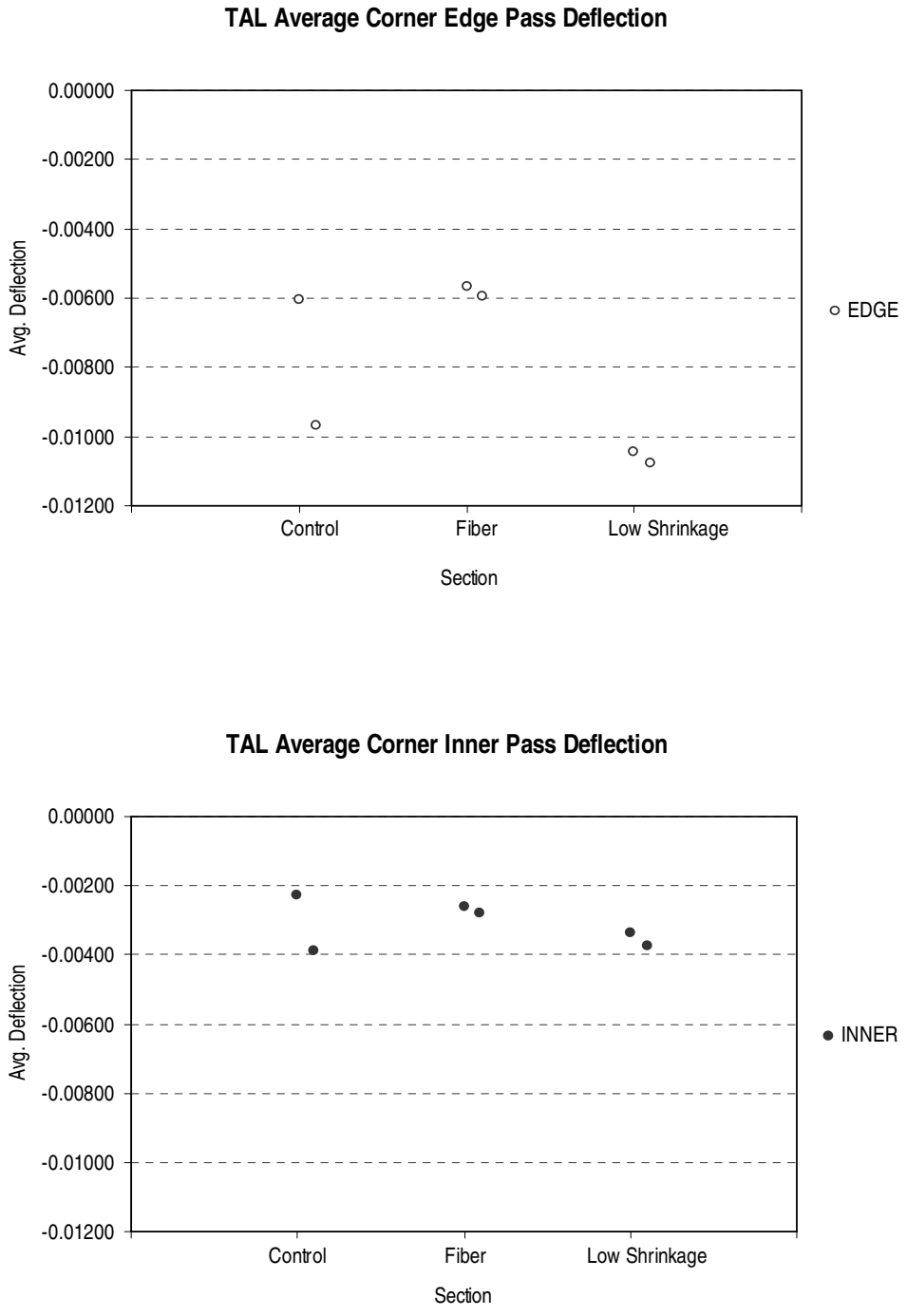

Figure 6.11 Average Corner Deflection for Tandem Axle Load Testing

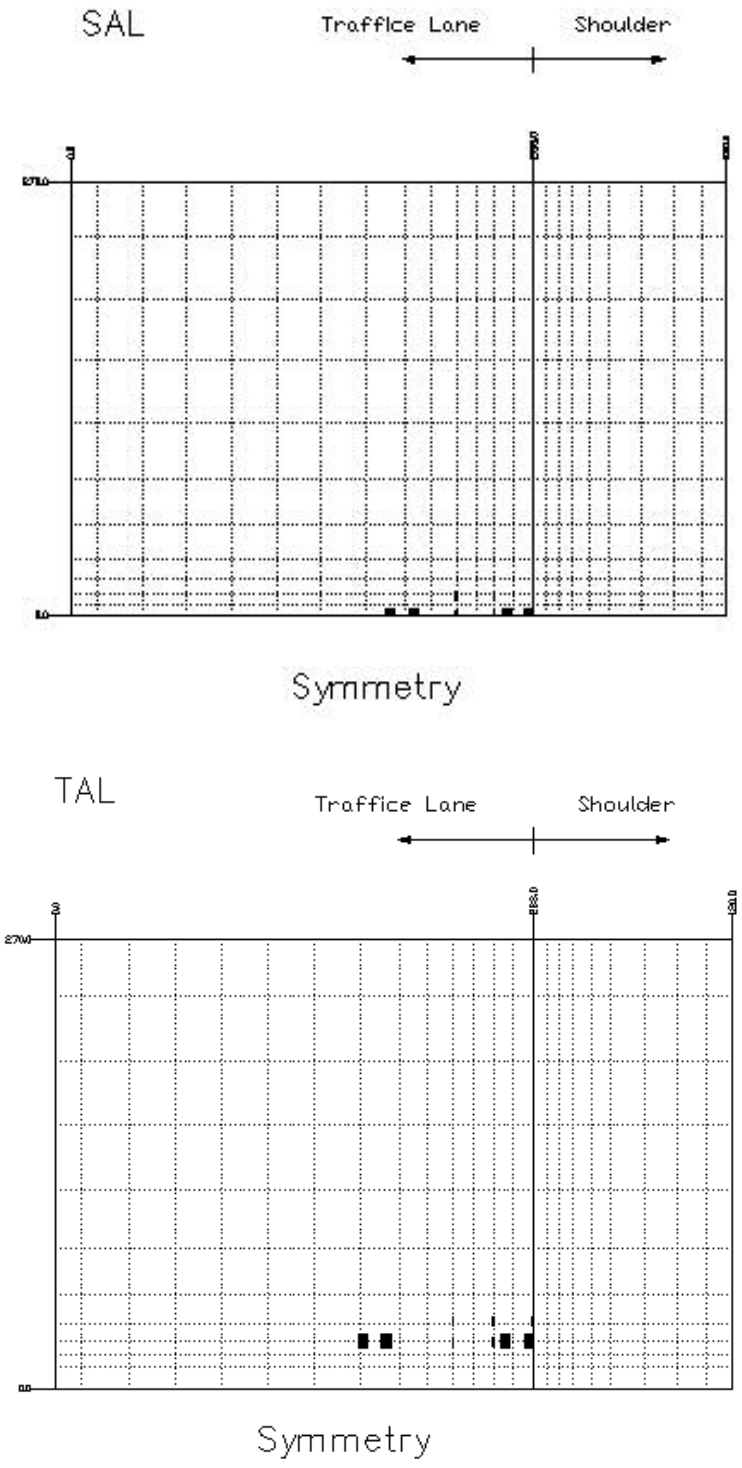

Figure 6.12 Mesh layout for KENSLAB Analysis

*SAL = Single Axle Load, TAL = Tandem Axle Load

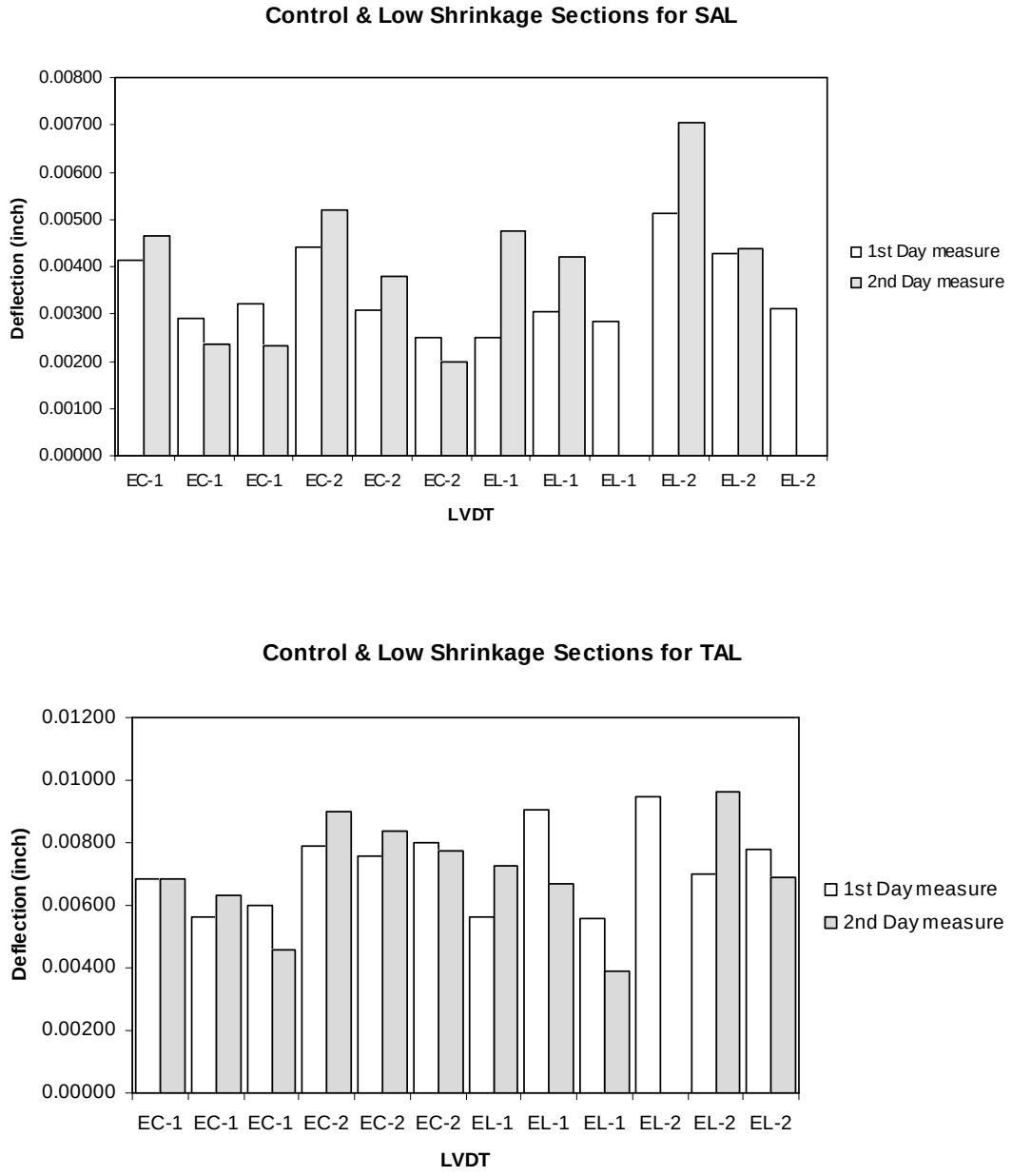

Figure 6.13.The measured deflections of the mid slab for the control & low shrinkage sections

EC-1: Edge Control Section LVDT 1, EC-2: Edge Control Section LVDT 2
EL-1: Edge Low Shrinkage Section LVDT 1, EL-2: Edge Low Shrinkage Section LVDT 2

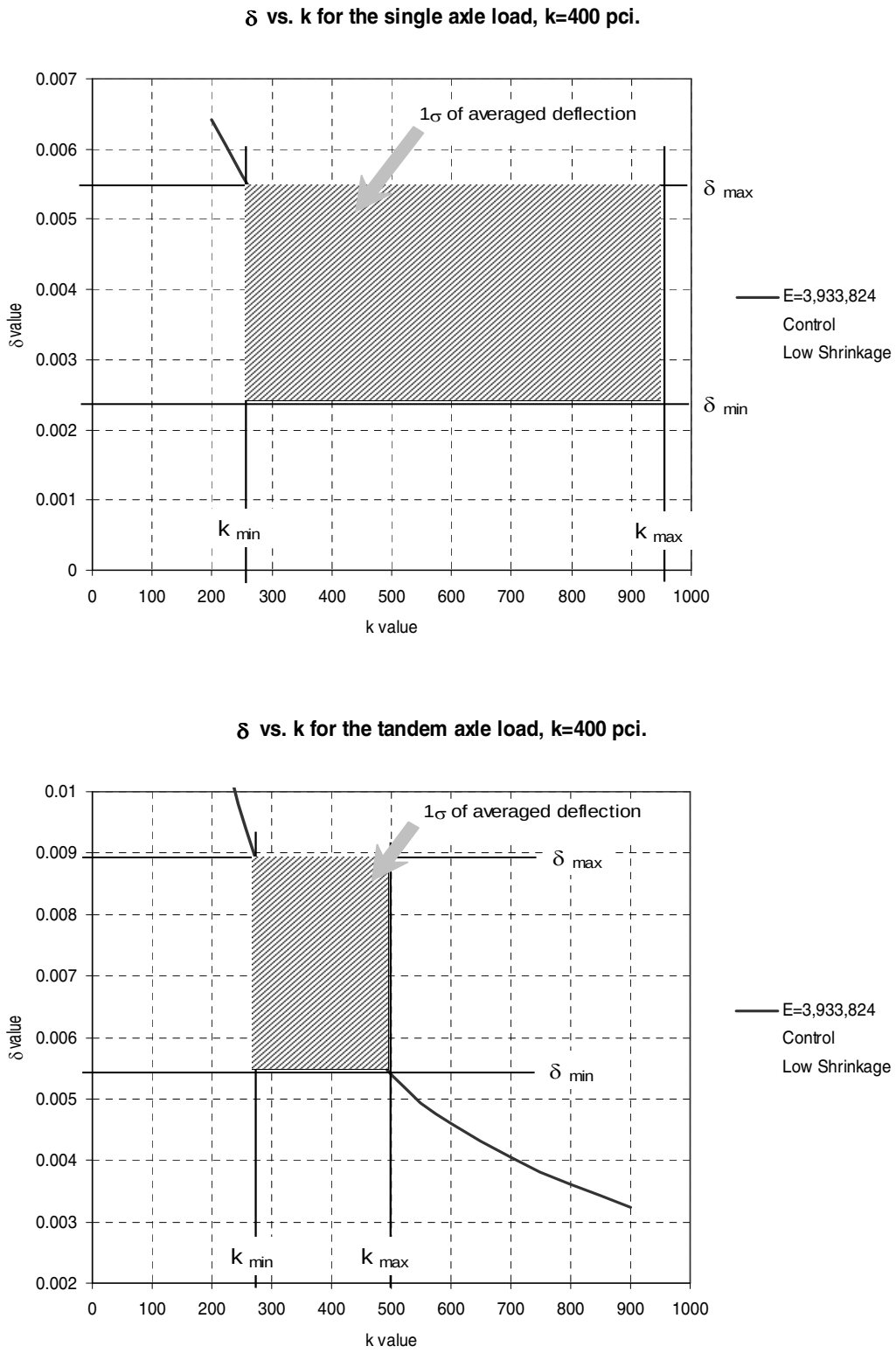

Figure 6.14 Deflection (δ) versus k value for control & low shrinkage sections by KENSLAB with variation.

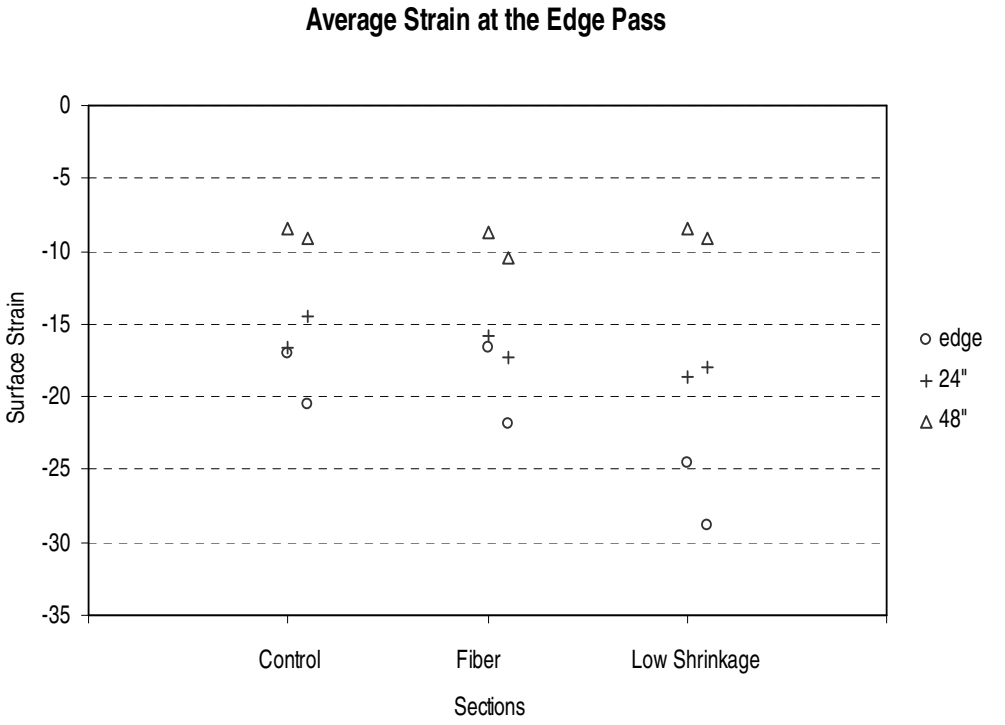

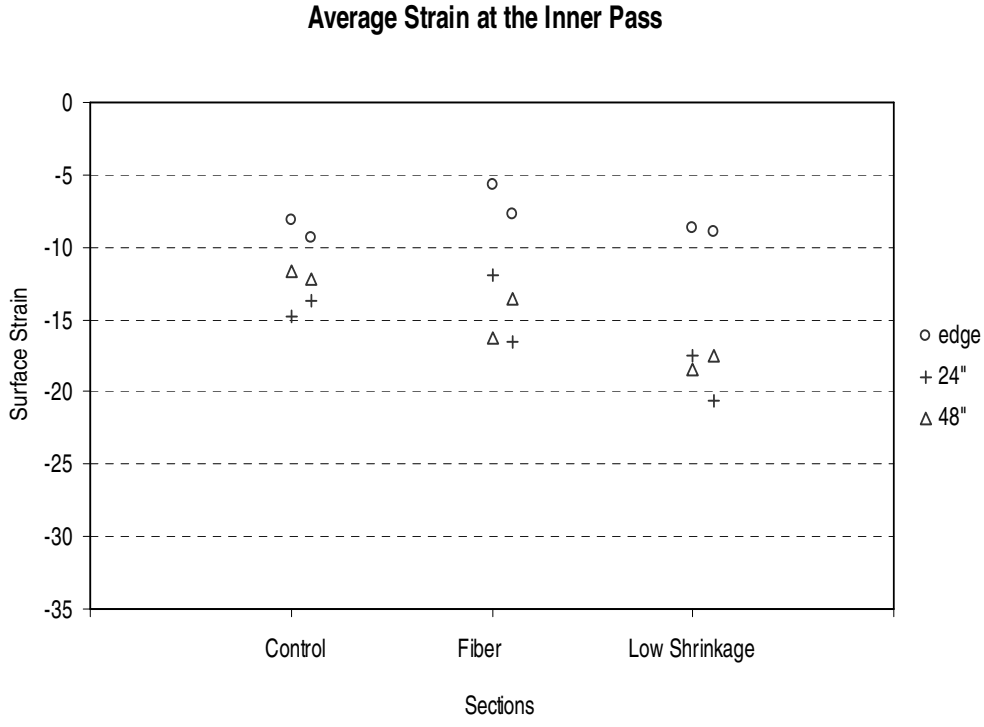

Figure 6.15 Average Strain for the Single Axle Load Test Results

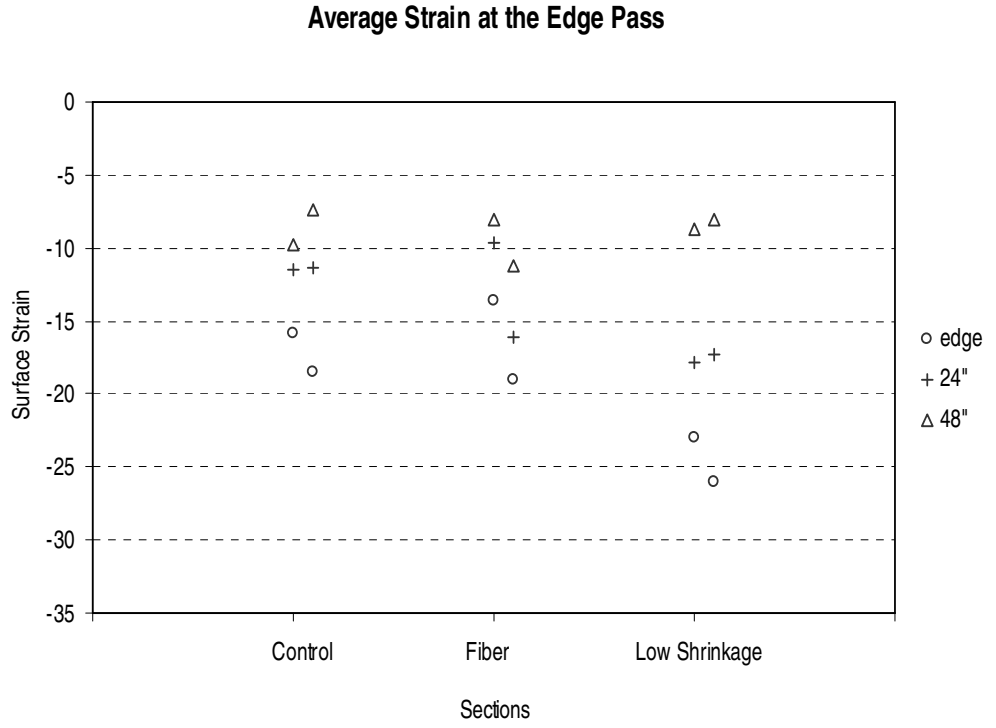

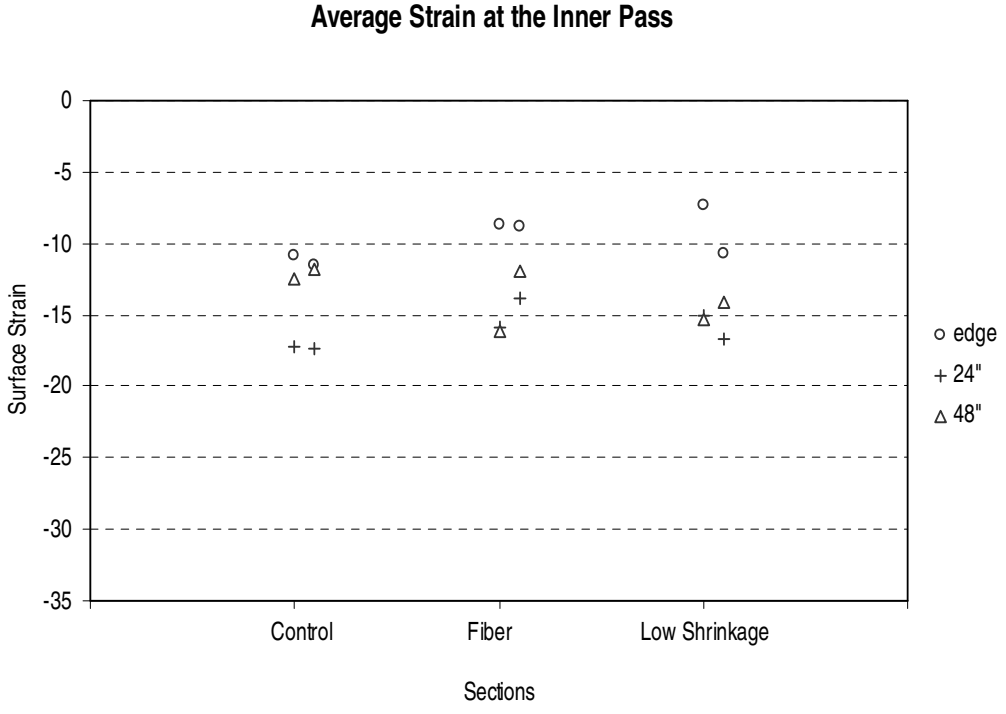

Figure 6.16 Average Strain for the Tandem Axle Load Test Results

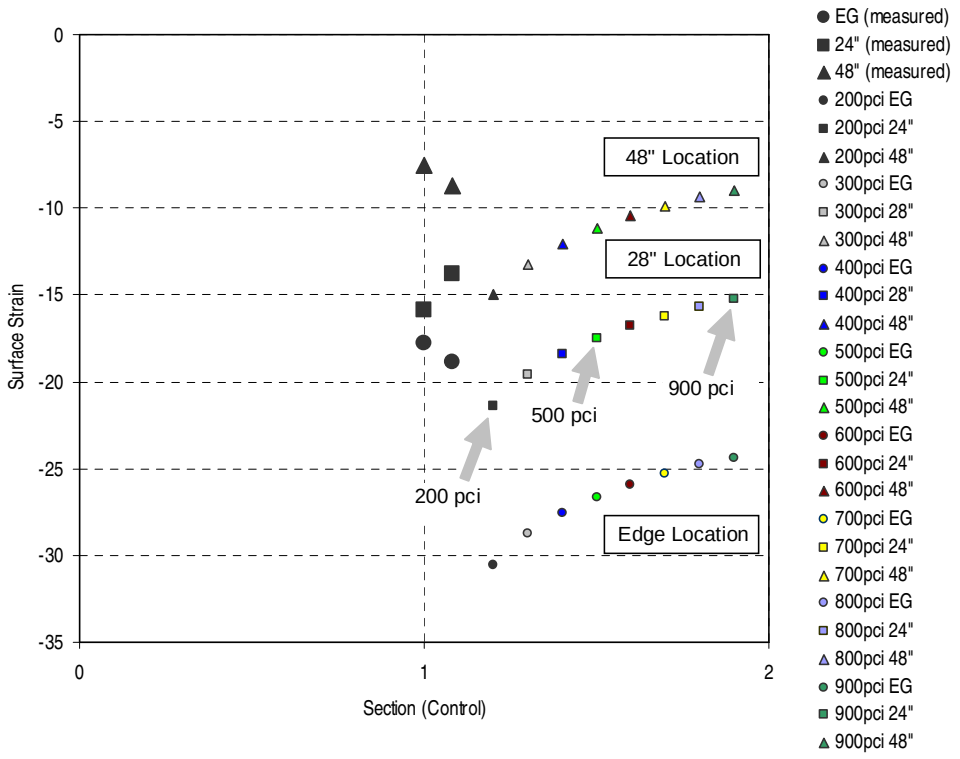

Figure 6.17 Predicted Strain with Various k values at Ec = 4,000,000 psi.

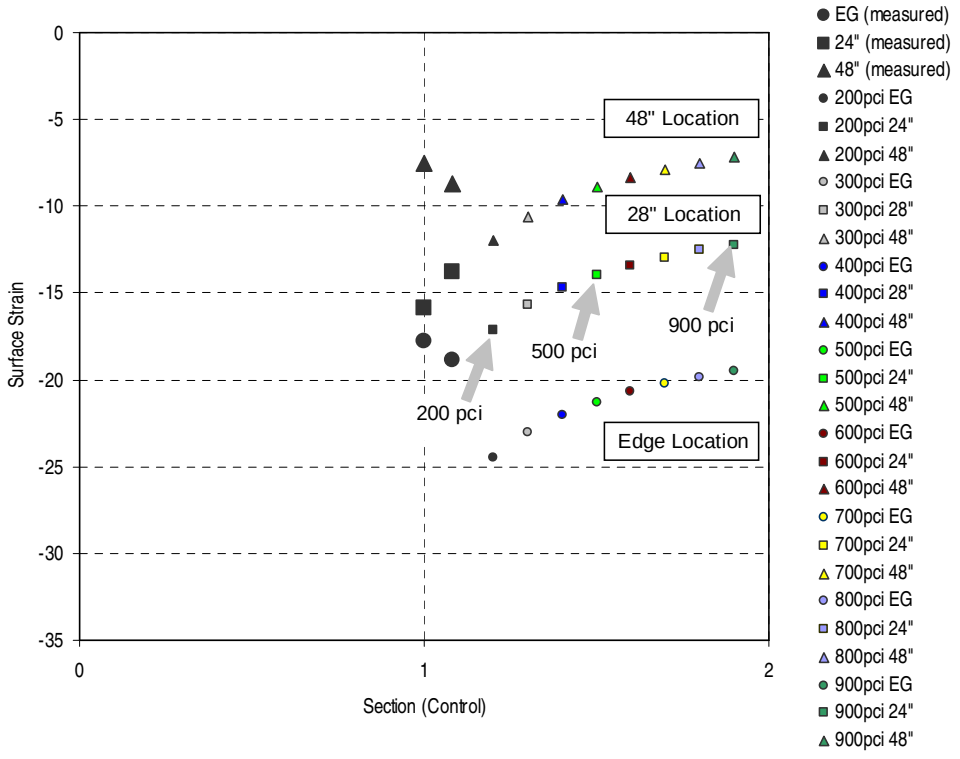

Figure 6.18 Predicted Strain with Various k values at Ec = 5,000,000 psi.

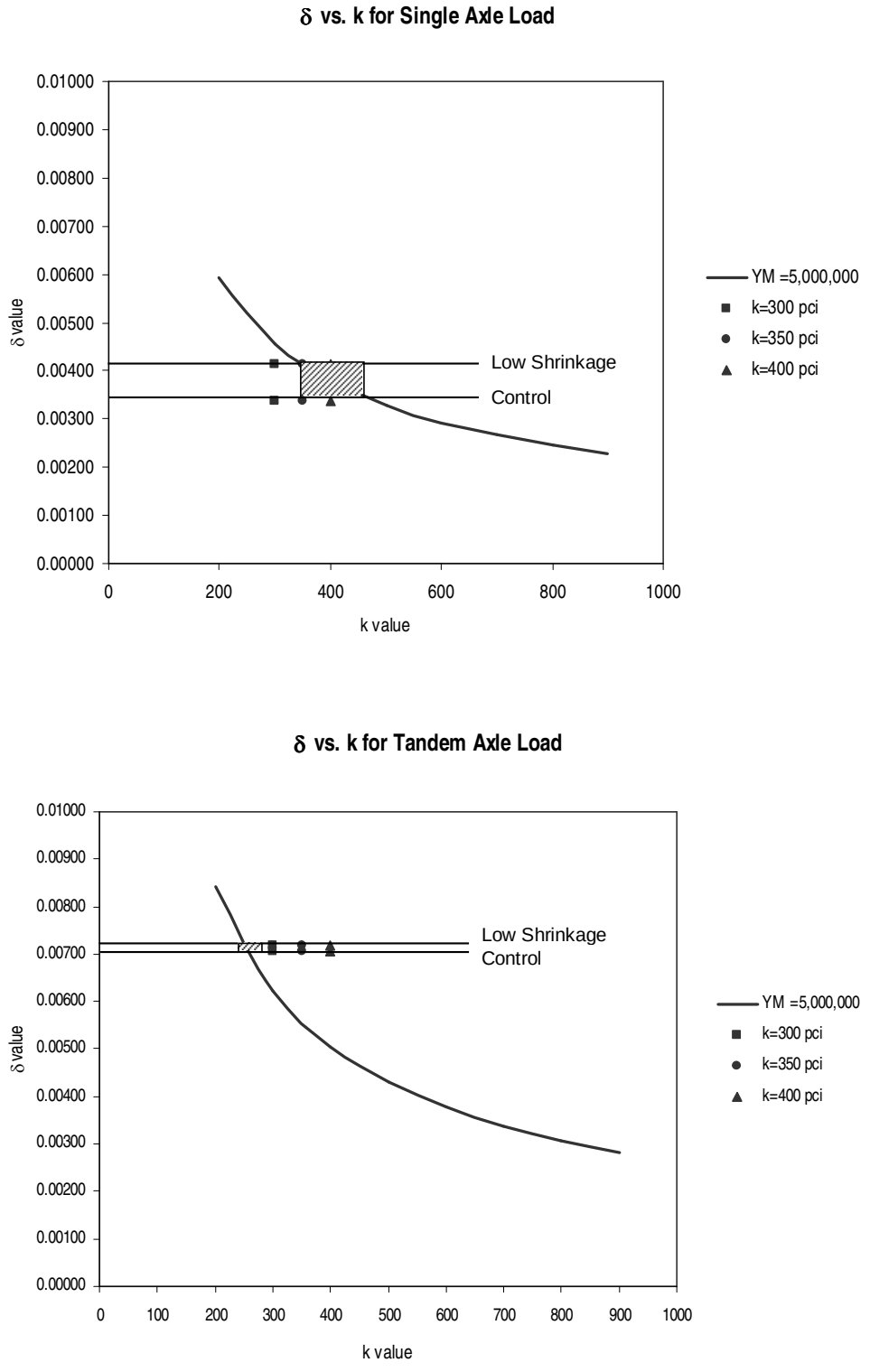

Figure 6.19 Deflection versus k values for the single axle load and tandem axle load

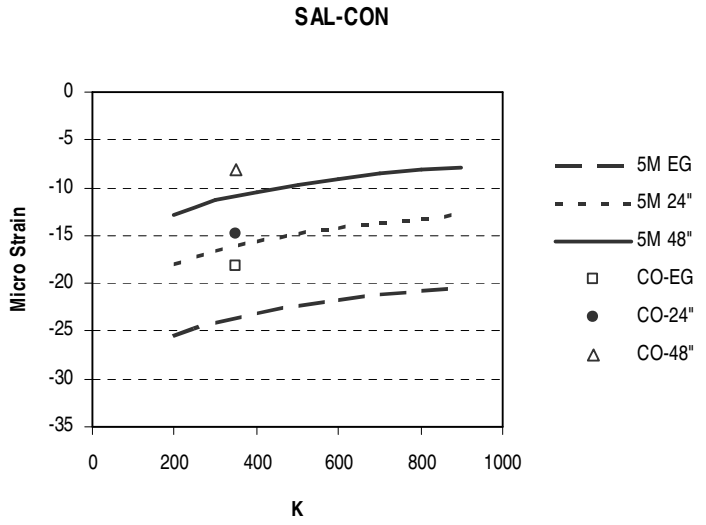

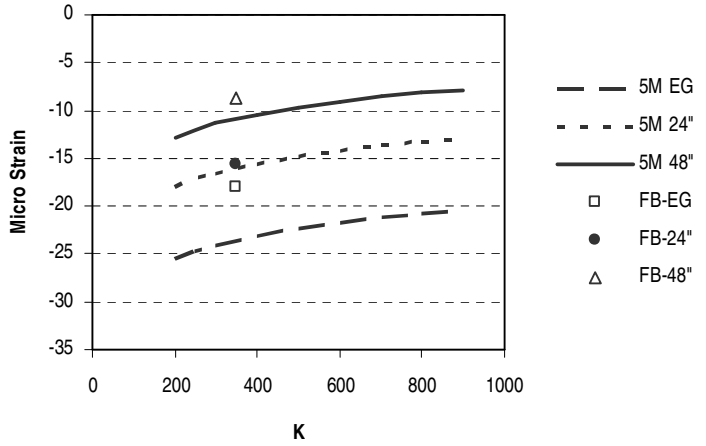

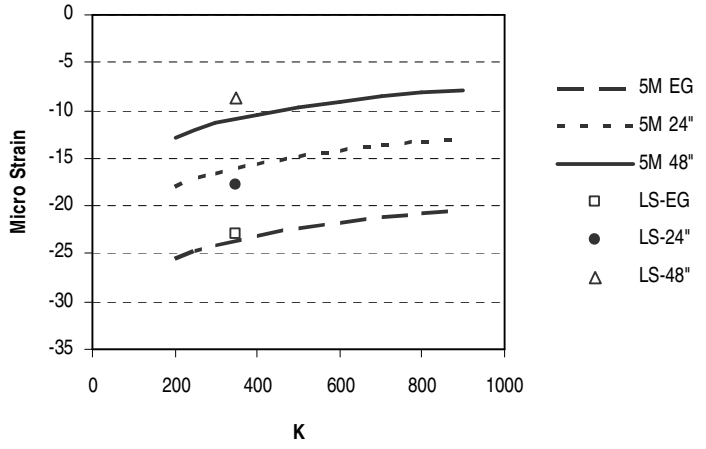

Figure 6.20 FE results & Measured strains for Single Axle Load Test
***SAL-Con = Single Axle Load Control Section,**
SAL-FB = Single Axle Load Fiber Section,
SAL-LS = Single Axle Load Low Shrinkage Section

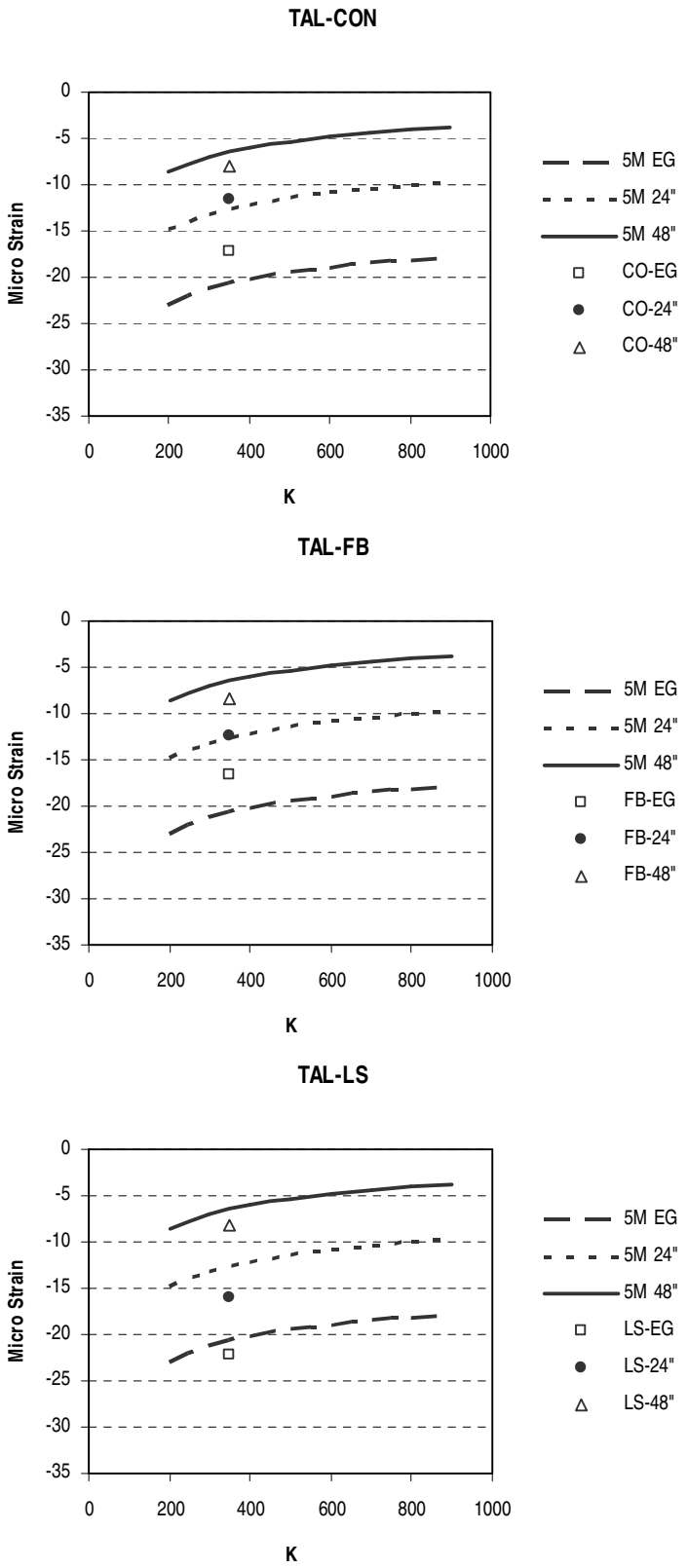

Figure 6.21 FE results & Measured strains for Tandem Axle Load Test
***TAL-Con = Single Axle Load Control Section,**
TAL-FB = Single Axle Load Fiber Section,
TAL-LS = Single Axle Load Low Shrinkage Section

CHAPTER 7 CONCLUSIONS

7.1 Conclusions

This study investigated the potential benefits of using fiber reinforced and low shrinkage concrete in pavements. The study included both laboratory evaluation of these mixtures and field performance through on site instrumentation and analytical evaluation.

The lab results were used for developing fatigue models for the individual mixtures, and all the mixtures together. Such models provide good correlations between fatigue repetitions to failure and applied stress level. The relationship can be used for pavement design since they provide a quantifiable measure of the SN curves for such mixtures. Furthermore, fatigue was related to mixture properties. Such models are particularly valuable when mixture characteristics are changed. Eventually, these relationships can be used to estimate fatigue life of modified mixtures without having to run fatigue testing.

The field data were used in conjunction with FEM analysis for, first estimating field materials and layer properties, such as the modulus of subgrade reaction and the concrete modulus. Then, the analysis were used for comparison between the control and the fiber and low shrinkage concrete pavement test sections. Finally, the analytical evaluation provided the base line for the behavior analysis of these pavement sections. Such analysis can be used for comparison with future condition and behavior of the built experimental test sections.

Some of the specific conclusions from the lab and field study are:

1. Fibers reduce the workability of concrete. However the use of admixtures permits acceptable levels of workability. While no conclusive remarks can be obtained in relation to the effect of fiber content on compressive strength, the flexural strength of concrete for fiber contents > 0.1% was higher than the one of the control concrete mixture. The toughness of concrete increased with increasing fiber content.
2. Shrinkage testing indicated that there were small differences in unrestrained shrinkage for the control and the two low shrinkage mixtures. However, fiber reinforced concrete mixtures exhibited higher levels of shrinkage.
3. The fatigue analysis indicated that the addition of polypropylene fibers resulted in higher fatigue strengths. The fatigue strength of FRC increased with decreasing fiber content until 0.3 percent. The endurance limit expressed as a percentage of the modulus of rupture of the mixture showed an increase with decreasing fiber content until 0.3 percent. Overall the best fatigue performance was obtained with the 0.1 % fiber content.
4. The field data collected from the in-situ instrumentation indicated that overall the sections with the 0.1% fiber reinforced concrete mixture had lower deflections than the control mix and the low shrinkage mixture. The same effect was observed for both single and tandem axle load configurations and for both edge and interior passes. The deflection and strain data were used in the analytical evaluation. This analysis indicated that the best estimates of k and Ec both from the measured deflections and measured strains are k of 350 pci and

Ec of 5,000,000 psi. These are both reasonable values for the embankment soils and concrete conditions at the site at the time of the load tests.

5. The non-destructive testing results provided correlations between the dynamic and static concrete properties. Such relationships could be used in estimating concrete properties from non-destructive testing rather than having to collect cores and running destructive mechanical testing in the lab. Also these relationships become particularly useful in QC operations.

7.2 Recommendations

The fatigue models developed in this research could be further expanded by including additional mixtures into the analysis. Such work will expand the validity and improve the response of the models in a wide variety of cases. Also, due to the high variability in fatigue testing there is a need to better control mixture properties during preparation. This will assure mixture homogeneity and reduce fatigue testing variability.

Furthermore, NDT testing and modeling is needed to expand the relations obtained in this study and to consider the relationships between lab and field mixture parameters. Eventually field NDT parameters should be related with field concrete properties, using in this case the QC data.

The FEM analysis could be used in conjunction with FWD testing and data so as to verify the instrumentation response and further refine the base line analytical model for future analysis.

Finally, periodic monitoring of the test sections will provide the necessary data for monitoring the behavior and performance of these mixtures and pavements, and will provide the necessary data for enhancing the fatigue and NDT models, and improve the FEM modeling.

NORTH

CONCRETE PAVEMENT
CONTROL SECTION

EAS
T

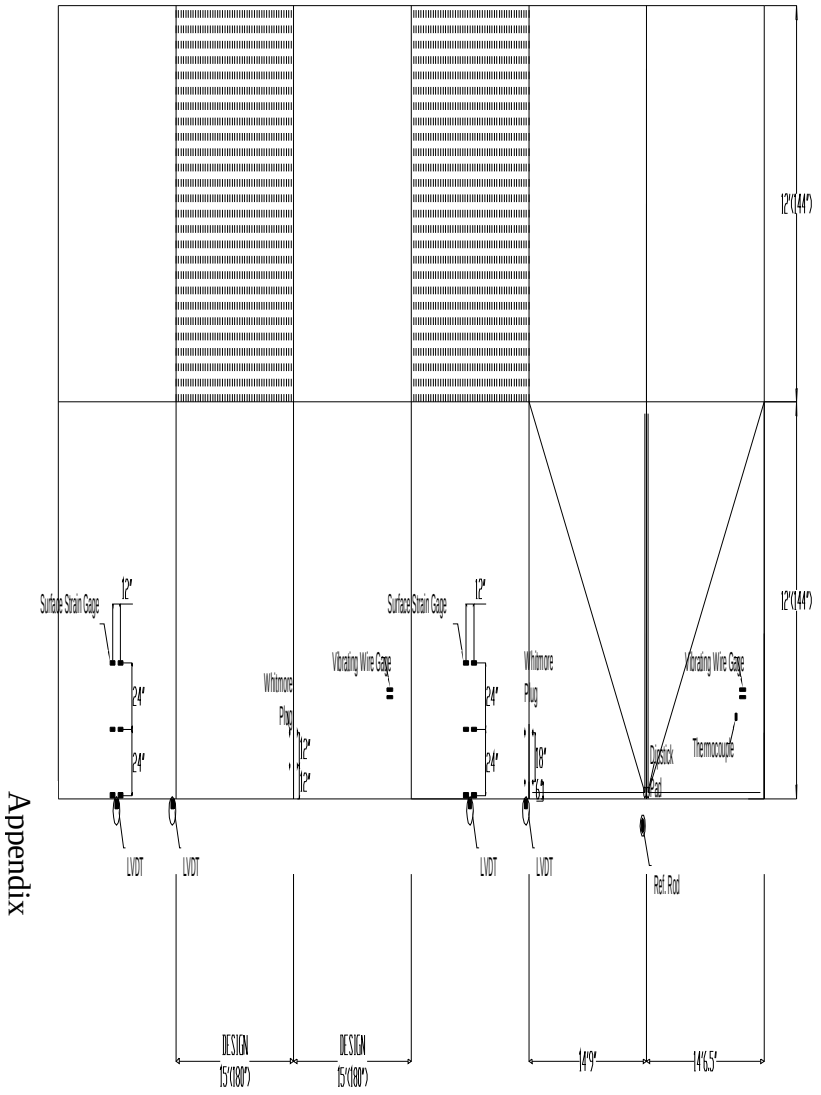

NORTH

EAS

T

CONCRETE PAVEMENT

FIBER SECTION

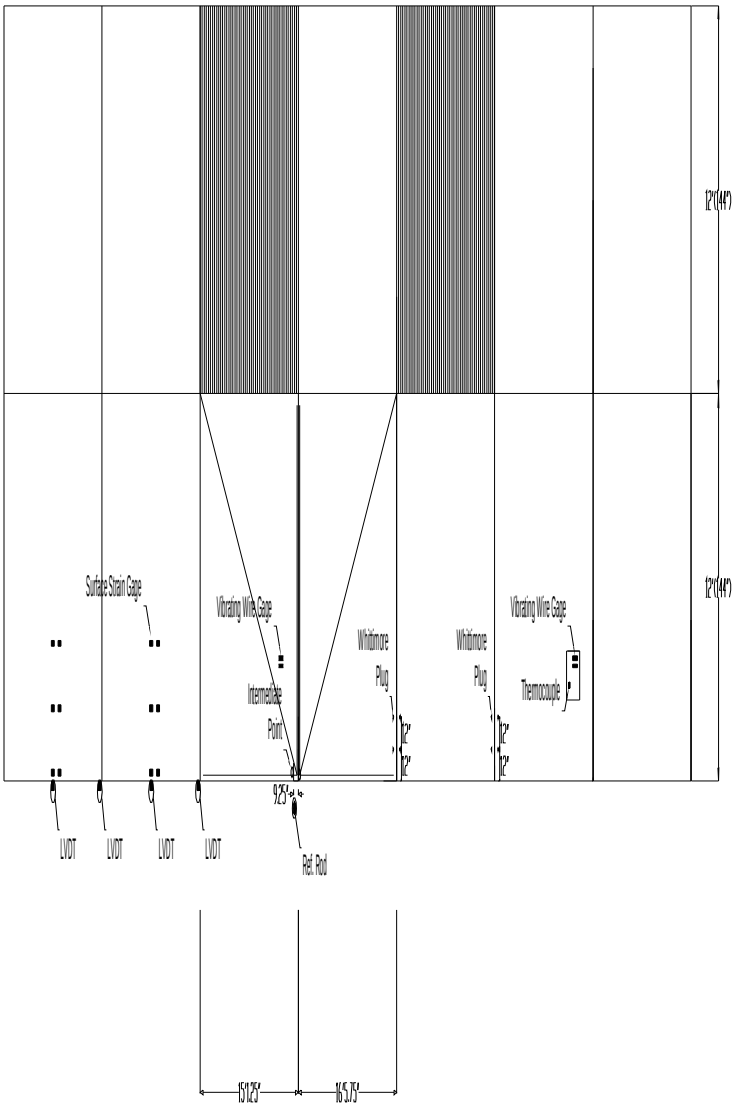

CONCRETE PAVEMENT
#357 SECTION
Low Shrinkage Section

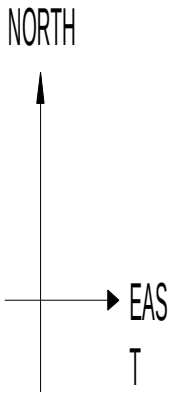

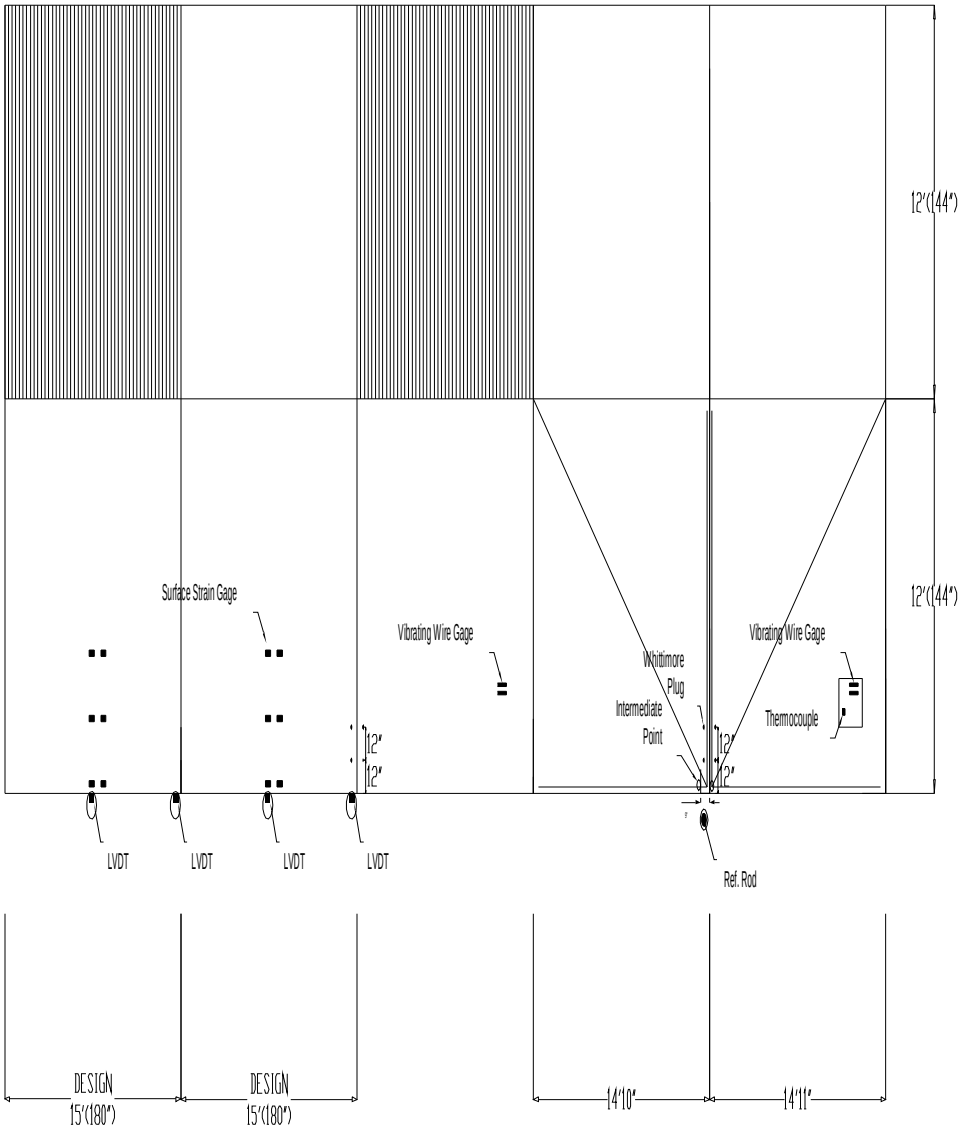

REFERENCES

Bayasi Z., and T. Celik, "Application of Silica Fume in Synthetic Fiber Reinforced Concrete," Transportation Research Record No. 1382, Part 2: Developments in Concrete Technology, National Academy Press, Washington D.C., 1993.

Grzybowski M., and C. Meyer, “Damage Accumulation in Concrete with and without Fiber Reinforcement”, ACI Materials Journal, V. 90, No. 6, November – December 1993.

Grzybowski M., and S. P. Shah, “Shrinkage Cracking of Fiber Reinforced Concrete”, ACI Materials Journal, V. 87, No. 2, March-April 1990.

Johnston C.D., and R. W. Zemp, “Flexural Fatigue Performance of Steel Fiber Reinforced Concrete – Influence of Fiber Content, Aspect Ratio, and Type”, ACI Materials Journal, V. 88, No. 4, July – August 1991.

Malmberg B., and A. Skarendahl, “Method of Studying the cracking of fiber concrete under restrained shrinkage”, Swedish Cement and Concrete Research Institute, 1978.

Nagabhushanam M., V. Ramakrishnan, and G. Vondran, “Fatigue Strength of Fibrillated Polypropylene Fiber Reinforced Concretes”, Transportation Research Record 1226, Washington D.C., 1989.

Ozyildirim C., C. Moen, and S Hladky, “Investigation of Fiber-Reinforced Concrete for Use in Transportation Structures”, Transportation Research Record 1574, Washington D.C., 1997.

Ramakrishanan V., G. Y. Wu, and G. Hosalli, “Flexural Fatigue Strength, Endurance Limit, and Impact Strength of Fiber Reinforced Concretes”, Transportation Research Record 1226, Washington D.C., 1989

Shah, S. P., Weiss, W.J., and Yang, W., "Shrinkage Cracking-Can It Be Prevented?", Concrete International, Vol. 20, No. 4, 51-55, 1998.